

Effect of Woodpecker Damage and Wood Decay on Wood Utility Pole Strength

by

Mark C. Steenhof

A thesis
presented to the University of Waterloo
in fulfillment of the
thesis requirement for the degree of
Master of Applied Science
in
Civil Engineering

Waterloo, Ontario, Canada, 2011

© Mark C. Steenhof 2011

AUTHOR'S DECLARATION

I hereby declare that I am the sole author of this thesis. This is a true copy of the thesis, including any required final revisions, as accepted by my examiners. I understand that my thesis may be made electronically available to the public.

Abstract

In many regions of North America, Europe, and Australia, wood utility poles are used as main and secondary structural members for the support of electrical distribution and transmission lines. In the province of Ontario alone there are over 40000 H-frame, 6000 Gulfport, and thousands of single pole structures constructed of over 2 million wood utility poles (Pandey et al. 2010b). Currently, utility companies report an increasing number of woodpecker damage incidents on in-service utility poles (HONI 2010). In addition, many aging poles have woodpecker damage in combination with wood decay. Both these forms of degradation cause strength reductions in utility poles, making their structural integrity questionable. This has raised concerns regarding the safety of utility maintenance workers and the public, and the dependability of the electrical network.

In response to these concerns, Hydro One Networks Incorporated (HONI) initiated a research project on the effect of woodpecker damage and wood decay on wood utility pole strength. The objective of the research was to develop methods of quantifying the strength reduction caused by woodpecker damage and wood decay. This information was then used to develop in-service assessment methods for determination of whether pole replacement is necessary when specific levels of woodpecker damage and wood decay are present. By developing better assessment methods, in-service utility poles will not be unnecessarily replaced, reducing maintenance costs.

In this study, three analytical models were developed that predicted the theoretical cross-sectional strength reduction caused by the presence of woodpecker damage. A bending failure model was developed since, in the structural design of utility poles, bending moment stresses are known to be the critical design parameter. It was decided that the significance of shear stress in a cross-section should also be considered since the presence of woodpecker damage could cause shear stresses to be a significant parameter. As a result, a shear-bending and a shear failure model was developed to determine the significance of shear stress on cross-section behaviour. These models were developed for analysis purposes and were verified by the subsequent experimental program. A total of 28 new and in-service utility poles were received from HONI for experimental testing. The new poles were received in as-new condition, while the in-service poles received had varying levels of woodpecker damage and wood decay. The poles received were cut into 4.25 m lengths for beam testing. A single new pole and in-service specimen from each pole was tested as a control specimen without woodpecker damage to obtain reference utility pole bending strengths. The remainder of the new pole specimens were mechanically introduced with woodpecker damage, while the remainder of the in-service specimens were tested with natural woodpecker damage. The tested specimens were analyzed and the results were compared with the woodpecker damage analytical model predictions. Results indicated that the effect of woodpecker damage is well modelled by the woodpecker damage analytical models. Overall, the bending failure analytical model was preferable for cross-section analysis due to the accuracy of the model predictions and the simplicity of required calculations. It was evident from the experimental program that the presence of woodpecker damage can severely reduce the strength of utility poles, making replacement necessary according to CSA C22.3 No. 1 Cl. 8.3.1.3 (2006a). In-service specimen experimental results indicated that if wood decay is detected in wood utility poles, severe reduction in wood strength has occurred and the utility pole should be replaced.

Analytical and experimental results were used to develop three application methods for determining whether utility pole replacement is necessary due to the presence of woodpecker damage. These three methods include the simplified method, the chart method, and the case-specific method. The simplified method allows determination of whether a utility pole should be replaced based only on knowledge of the most severe level of woodpecker damage present in a pole. The chart method takes into account additional factors such as the diameter of the pole at the location of the woodpecker damage and the width of the hole opening. The case-specific method is advantageous since it accounts for the parameters used in the chart method and allows the location of woodpecker damage along the length of a pole to be accounted for. The simplified and chart methods are preferable since they are relatively simple and easy to implement in the field. The case-specific method requires a full structural analysis of the utility pole in question to be undertaken and is useful for more accurately assessing whether replacement is necessary. These three methods show how the research completed can be used for improved assessment of in-service utility poles resulting in reduced unnecessary pole replacement and maintenance costs.

Acknowledgements

First of all I am deeply grateful to my advisor, Professor Jeffrey West, for his endless support, guidance, and friendship throughout my research work. I would also like to thank Professor Mahesh Pandey for his advice and guidance.

Special thanks to Richard Morrison, Doug Hirst, and Robert Sluban of the structures lab whose efforts helped the experimental program run successfully.

Many thanks to Hydro One Networks Incorporated for funding the research and providing the test specimens for the experimental program. Thanks to the Canadian Standards Association and the United States Department of Agriculture for use of their design standards. I would also like to acknowledge the Natural Sciences and Engineering Research Council of Canada for providing financial assistance for the project.

Lastly, I would like to express my gratitude to God, my family, and my friends for support when I pursued graduate studies at the University of Waterloo.

Dedication

To God, my family, and my friends.

Table of Contents

AUTHOR'S DECLARATION	ii
Abstract	iii
Acknowledgements	v
Dedication	vi
Table of Contents	vii
List of Figures	xiii
List of Tables	xvii
Chapter 1 Introduction.....	1
1.1 Objectives	2
1.2 Research Approach.....	3
1.3 Organization of Thesis	4
Chapter 2 Literature Review	5
2.1 Structure of Wood	5
2.1.1 Bark, Wood, Branches, and Cambium	5
2.1.2 Sapwood and Heartwood.....	6
2.1.3 Growth Rings.....	6
2.1.4 Wood Cells	7
2.1.5 Chemical Composition	7
2.2 Effect of Natural Characteristics on Mechanical Properties of Wood.....	8
2.2.1 Specific Gravity.....	8
2.2.2 Knots	8
2.2.3 Slope of Grain.....	9
2.2.4 Reaction Wood	10
2.2.5 Juvenile Wood.....	10
2.2.6 Compression Failures	10
2.2.7 Pitch Pockets	10
2.2.8 Extractives	11
2.3 Effect of Manufacturing and Service Environment on Mechanical Properties of Wood.....	11
2.3.1 Moisture Content	11
2.3.2 Reversible Temperature Effects	11
2.3.3 Rate of Loading	12

2.3.4 Duration of Load	12
2.3.5 Aging	12
2.3.6 Waterborne Preservative Treatment	12
2.3.7 Mold and Stain Fungi	13
2.3.8 Decay	13
2.3.9 Insect Damage	14
2.4 Biodeterioration of Wood.....	14
2.4.1 Mold and Fungus Stains	14
2.4.2 Decay	15
2.4.3 Effect of Decay on Wood Strength.....	15
Chapter 3 Characterization of Woodpecker Damage	16
3.1 Woodpecker Damage Levels.....	16
3.2 Effect of Woodpecker Damage on Strength.....	17
3.3 Idealized Woodpecker Damage.....	19
Chapter 4 Woodpecker Damage Analytical Models	22
4.1 Effect of Woodpecker Damage on Cross-section Strength.....	22
4.1.1 Bending Failure Model (BF model)	22
4.1.2 Shear Failure Model (SF model)	23
4.1.3 Shear-Bending Interaction Failure Model (SBIF model)	24
4.2 Shear and Bending Stress Distributions	25
4.2.1 Undamaged Section.....	25
4.2.2 Vertically Oriented Damage.....	26
4.2.3 Horizontally Oriented Damage.....	27
Chapter 5 Utility Pole Structural Analysis Model.....	29
5.1 CSA C22.3 No. 1 Analysis and Design Procedures	29
5.1.1 Vertical load assumptions.....	29
5.1.2 Transverse load assumptions	29
5.1.3 Load Factors	29
5.1.4 Analysis, Failure, and Replacement Requirements	30
5.2 Shear Force and Bending Moment Analysis	30
5.3 Stress Analysis	32
5.3.1 Geometry of Utility Pole	32

5.3.2 Bending Stress Determination	32
5.3.3 Shear Stress Determination	33
5.4 Pre-experimental Analytical Study.....	33
5.4.1 Parameters	33
5.4.2 Wood Mechanical Properties.....	34
5.4.3 Applied Loads	34
5.4.4 Woodpecker Damage	34
5.4.5 Analysis	34
5.4.6 Failure Criteria.....	35
5.4.7 Bending Failure Criteria Analysis Results	35
5.4.8 Shear-Bending Interaction Failure Criteria Analysis Results.....	35
5.4.9 Conclusions from Parametric Study	35
Chapter 6 Experimental Program	36
6.1 Types of Poles	36
6.2 Specimen Analysis Considerations	36
6.3 Targeted Moment-to-Shear Ratio.....	37
6.4 Four-Point Loading	37
6.5 Three-Point Loading.....	37
6.6 Actuator Loading Rate, Force, and Displacement.....	38
6.7 Support Crushing.....	38
6.8 Deflection	39
6.9 Strain	39
6.10 Dissection	39
6.11 Moisture Content.....	39
Chapter 7 New Pole Specimen Analysis, Results, and Discussion	41
7.1 Test Specimens.....	41
7.1.1 Control Specimens.....	42
7.1.2 Specimens Induced with Woodpecker Damage	42
7.2 General Behaviour.....	42
7.3 Influence of Knots, Checks, and Local Wood Properties.....	43
7.4 Control Specimens	45
7.4.1 Bending Failure Analysis	45

7.4.2 Shear-Bending Interaction Failure Analysis.....	46
7.4.3 Experimental Results.....	47
7.5 New Pole Specimens with Woodpecker Damage	48
7.5.1 Bending Failure Analysis	50
7.5.2 Shear-Bending Interaction Failure Analysis.....	51
7.5.3 Shear Failure Analysis.....	52
7.5.4 Experimental Strength Reduction.....	52
7.5.5 Comparison of Analytical Models with Experimental Results	53
7.6 Experimental Strain Data	55
7.6.1 Control Cross-sections.....	55
7.6.2 Cross-sections with Tension and Compression Damage.....	56
7.6.3 Cross-sections with Neutral Axis Damage	60
7.7 Experimentally Determined Modulus of Elasticity	61
7.7.1 Modulus of Elasticity Determined from Deflection	61
7.7.2 Modulus of Elasticity Determined from Strain	62
7.7.3 Relationship of Modulus of Elasticity and Bending Strength	63
7.8 Dissection of Specimen Failure Locations	63
7.8.1 Control Specimens.....	63
7.8.2 Tension Oriented Damage Specimens.....	64
7.8.3 Compression Oriented Damage Specimens	67
7.8.4 Neutral Axis Oriented Damage Specimens	68
7.9 Moisture Content.....	70
7.10 Conclusions	70
Chapter 8 In-service Specimen Analysis, Results, and Discussion.....	72
8.1 In-service Test Specimens.....	72
8.1.1 In-service Control Specimens.....	72
8.1.2 In-service Specimens with Woodpecker Damage	73
8.2 Woodpecker Damage on In-service Poles.....	73
8.3 In-service Specimen Condition Inspection.....	75
8.4 Specimen Condition Inspection.....	77
8.4.1 Cracks and Checks	78
8.4.2 Woodpecker Damage	79

8.4.3 Mechanical Damage	81
8.4.4 Significance of External Indicators	82
8.5 General Behaviour.....	83
8.6 Influence of Knots and Checks.....	84
8.7 In-service Control Specimens.....	85
8.7.1 Bending Failure Analysis Using Gross Cross-section Properties.....	86
8.7.2 Shear Failure Analysis Using Gross Cross-section Properties	86
8.7.3 Bending Failure Analysis Using Effective Cross-section Properties	87
8.7.4 Shear Failure Analysis Using Effective Cross-section Properties.....	87
8.7.5 Experimental Results.....	88
8.8 In-service Specimens with Natural Woodpecker Damage	89
8.8.1 Bending Failure Analysis Using Gross Cross-section Properties.....	91
8.8.2 Experimental Strength Reduction.....	91
8.8.3 Comparison of Analytical Model with Experimental Results	92
8.9 In-service Experimental Strain Data	92
8.9.1 Control Cross-sections.....	93
8.9.2 Cross-sections with Tension Damage.....	93
8.9.3 Cross-sections with Compression Damage	94
8.9.4 Cross-section with Neutral Axis Damage	95
8.10 Experimentally Determined Modulus of Elasticity	96
8.10.1 Modulus of Elasticity Determined from Deflection	96
8.10.2 Relationship of Modulus of Elasticity, Bending Strength, and Age.....	97
8.11 Dissection of Specimen Failure Locations	98
8.11.1 Control Specimens.....	98
8.11.2 Tension Oriented Damage Specimens.....	99
8.11.3 Compression Oriented Damage Specimens	100
8.11.4 Neutral Axis Oriented Damage Specimens	102
8.12 In-service Specimen Moisture Content	103
8.13 Conclusions	103
Chapter 9 Application to Utility Pole Replacement	105
9.1 CSA C22.3 No. 1 Criteria.....	105
9.2 Wood Decay	105

9.3 Woodpecker Damage	105
9.3.1 Simplified Method.....	105
9.3.2 Chart Method.....	106
9.3.3 Case-specific Method	108
Chapter 10 Conclusions and Recommendations	111
10.1 Conclusions	112
10.1.1 New Specimen Experimental Results.....	112
10.1.2 In-service Specimen Experimental Results	112
10.1.3 Comparison of Analytical Model with Experimental Results	113
10.1.4 Application to Utility Pole Replacement.....	113
10.2 Recommendations for Future Research.....	113
References	114
Appendix A : C_b and C_s Constants for Analytical Models.....	117
Appendix B : Pre-experimental Study M/V Ratios	119
Appendix C : Specimen Data	122

List of Figures

Figure 1. - Electrical distribution and transmission structures constructed of wood utility poles.....	1
Figure 2. - Woodpecker damage (left) and decay (right).	2
Figure 3. - Organizational flowchart of thesis.....	4
Figure 4. - Cross-section of tree trunk showing interior structure (USDA 1999f).....	6
Figure 5. - Growth rings in ponderosa pine log (USDA 1999f).....	7
Figure 6. - Encased (A) and intergrown (B) knots (USDA 1999f).	9
Figure 7. - Properties of juvenile wood (USDA 1999f).	10
Figure 8. - Cross-section with fungus stain (USDA 1999f).	14
Figure 9. - Brown rot (left) and soft rot (right) (USDA 1999f).....	15
Figure 10. - In-service exploratory damage (left) and feeding damage (right).	16
Figure 11. - In-service nesting damage and dissection of interior.....	17
Figure 12. - Strength reduction caused by exploratory holes (HONI 2010).	18
Figure 13. - Strength reduction caused by feeding holes (HONI 2010).....	18
Figure 14. - Strength reduction caused by nesting holes (HONI 2010).	19
Figure 15. - Idealized levels of woodpecker damage.	19
Figure 16. - Idealized woodpecker damage orientations.....	20
Figure 17. - New pole specimen idealized exploratory damage.....	20
Figure 18. - New pole specimen idealized feeding damage.....	20
Figure 19. - New pole specimen idealized nesting damage.....	21
Figure 20. - Cross-section depth separated into 21 planes for SBIF analysis.	25
Figure 21. - Stress distributions of an undamaged cross-section.....	25
Figure 22. - Stress distributions of a cross-section with vertical exploratory damage.	26
Figure 23. - Stress distributions of a cross-section with vertical feeding damage.....	26
Figure 24. - Stress distributions of a cross-section with vertical nesting damage.....	27
Figure 25. - Stress distributions of a cross-section with horizontal exploratory damage.....	27
Figure 26. - Stress distributions of a cross-section with horizontal feeding damage.	28
Figure 27. - Stress distributions of a cross-section with horizontal nesting damage.....	28
Figure 28. - CSA C22.3 No. 1 (2006a) loading map of Canada.	30
Figure 29. - Horizontal and vertical spans (USDA 2009c).	31
Figure 30. - Four-point loading test setup ($M/V = 8.72$).....	37
Figure 31. - Three-point loading test setup for control specimens ($M/V = 2.0$).....	38

Figure 32. - Three-point loading test setup for specimens with neutral axis damage ($M/V = 2.0$).....	38
Figure 33. - New pole specimen DCDT configuration.	39
Figure 34. - Typical load-deflection curve for new pole specimen failing in bending (60-2-1).	43
Figure 35. - Typical load-deflection curve for new pole specimen failing in shear (55-2-3).....	43
Figure 36. - New pole specimen with checking at midspan (45-1-3).....	44
Figure 37. - New pole specimen with a large knot at failure location (45-1-2).....	44
Figure 38. - Typical new pole control specimen bending failure (60-2-2).....	45
Figure 39. - SBIF equation iterative solver for new pole control specimens.	47
Figure 40. - Tension fibre rupture of new pole specimen with tension damage (60-2-1).	49
Figure 41. - Compression fibre crushing of new pole specimen with compression damage	49
Figure 42. - Shear failure of new pole specimen with neutral axis nesting damage (55-2-3).	50
Figure 43. - SBIF equation iterative solver for new pole damaged specimens.	52
Figure 44. - New pole control specimen strain profile (45-1-2).....	56
Figure 45. - Strain profile of new pole specimen with tension exploratory damage (45-1-3).....	57
Figure 46. - Strain profile of new pole specimen with tension feeding damage (60-2-1).....	57
Figure 47. - Strain profile of new pole specimen with tension nesting damage (55-1-1).	58
Figure 48. - Strain profile of new pole specimen with compression exploratory damage (60-1-4)....	58
Figure 49. - Strain profile of new pole specimen with compression feeding damage (60-1-1).	59
Figure 50. - Strain profile of new pole specimen with compression nesting damage (50-3-3).....	59
Figure 51. - Strain profile of new pole specimen with neutral axis exploratory damage (50-2-3).....	60
Figure 52. - Strain profile of new pole specimen with neutral axis feeding damage (50-1-1).	60
Figure 53. - Strain profile of new pole specimen with neutral axis nesting damage (55-3-1).	61
Figure 54. - Bending strength vs. modulus of elasticity for new pole specimens.	63
Figure 55. - Cross-section of new control specimen (50-1-2).	64
Figure 56. - Side view of new pole control specimen (50-1-2).	64
Figure 57. - Cross-section of new pole specimen with tension exploratory damage (45-2-3).	65
Figure 58. - Cross-section of new pole specimen with tension feeding damage (60-2-1).	65
Figure 59. - Cross-section of new pole specimen with tension nesting damage (55-1-1).....	66
Figure 60. - Cross-section of new pole specimen with compression exploratory damage (60-2-3). ...	67
Figure 61. - Side view of new pole specimen with compression exploratory damage (60-2-3)	67
Figure 62. - Cross-section of new pole specimen with compression feeding damage (55-1-3).....	68
Figure 63. - Cross-section of new pole specimen with compression nesting damage (45-2-1).	68

Figure 64. - Cross-section of new pole specimen with neutral axis exploratory damage (50-2-3).	69
Figure 65. - Cross-section of new pole specimen with neutral axis feeding damage (60-4-1).	69
Figure 66. - Cross-section of new pole specimen with neutral axis nesting damage (55-2-3).	70
Figure 67. - Group D in-service poles with woodpecker damage locations.	73
Figure 68. - In-service pole C-1 with woodpecker damage locations.	74
Figure 69. - In-service pole 60-3 with woodpecker damage locations.	74
Figure 70. - Group RP in-service poles with woodpecker damage locations.	74
Figure 71. - Group B in-service poles with woodpecker damage locations.	75
Figure 72. - In-service specimen with deep crack and severe decay (D-1-1).	78
Figure 73. - In-service specimen with shallow and high density cracks with no decay (D-2-1).	78
Figure 74. - In-service specimen with nesting level woodpecker damage and decay (D-4-1).	79
Figure 75. - In-service specimen with nesting level woodpecker damage and no decay (RP-3-1).	79
Figure 76. - In-service specimen with intermediate level woodpecker damage and decay (D-3-1). ...	80
Figure 77. - In-service specimens with minor woodpecker damage and no decay (D-4-1).	80
Figure 78. - In-service specimen with severe mechanical damage and decay (D-1-1).	81
Figure 79. - In-service specimen with mechanical damage and crack formation (D-1-1).	81
Figure 80. - In-service specimens with mechanical damage and no decay (60-4-2).	82
Figure 81. - Typical load-deflection curve for in-service specimen failing in bending (D-4-2).	83
Figure 82. - Typical load-deflection curve for in-service specimen failing in shear (D-2-2).	84
Figure 83. - Heavily decayed in-service specimen that failed in shear (D-4-1).	84
Figure 84. - In-service specimen with shear failure plane coinciding with check (D-1-1).	85
Figure 85. - In-service control specimen bending failure (D-3-2).	86
Figure 86. - In-service control specimen shear failure (D-4-1).	86
Figure 87. - Tension fibre rupture of in-service specimen with tension damage (D-3-1).	90
Figure 88. - Tension fibre rupture of in-service specimen with compression damage (D-2-1).	90
Figure 89. - Tension fibre rupture of in-service specimen with neutral axis damage (C-1-2).	90
Figure 90. - In-service control specimen strain profile (D-3-2).	93
Figure 91. - Strain profile of in-service specimen with tension damage (D-3-1).	94
Figure 92. - Strain profile of in-service specimen with tension damage (D-4-3).	94
Figure 93. - Strain profile of in-service specimen with compression damage (D-2-1).	95
Figure 94. - Strain profile of in-service specimen with compression damage (C-1-1).	95
Figure 95. - Strain profile of in-service specimen with neutral axis damage (C-1-2).	96

Figure 96. - Bending strength vs. modulus of elasticity for in-service specimens.....	97
Figure 97. - Modulus of elasticity vs. age for in-service specimens.	97
Figure 98. - Cross-section of in-service control specimen (D-3-2).	98
Figure 99. - Cross-section of in-service control specimen (D-2-2).	99
Figure 100. - Cross-section of in-service specimen with tension damage (D-3-1).	99
Figure 101. - Cross-section of in-service specimen with tension damage (60-3-1).	100
Figure 102. - Cross-section of in-service specimen with compression damage (D-2-1).....	101
Figure 103. - Cross-section of in-service specimen with compression damage (C-1-1).....	101
Figure 104. - Cross-section of in-service specimen with compression damage (RP-3-1).....	102
Figure 105. - Cross-section of in-service specimen with neutral axis exploratory damage (C-1-2). .	102
Figure 106. - Remaining strength due to exploratory level woodpecker damage.	107
Figure 107. - Remaining strength due to feeding level woodpecker damage.	107
Figure 108. - Remaining strength due to nesting level woodpecker damage.	108
Figure 109. - New pole design.	109
Figure 110. - Analysis of pole with woodpecker damage.	109

List of Tables

Table 1. - HONI historical woodpecker damage levels (HONI 2010).	16
Table 2. - I and Z factors for cross-sections with woodpecker damage.	23
Table 3. - Q/It factor for cross-section with woodpecker damage	23
Table 4. - CSA C22.3 No. 1 (2006a) deterministic weather loads.	29
Table 5. - CSA C22.3 No. 1 (2006a) wood pole load factors for non-linear analysis.	30
Table 6. - Pre-experimental study assumed wood mechanical properties.	34
Table 7. - Pre-experimental parametric study ice, wind, and wire dead loads.	34
Table 8. - Received new pole details and specimens.	41
Table 9. - New pole specimen experimental matrix.	42
Table 10. - New pole control specimen bending strengths.	48
Table 11. - New pole control specimen average bending strengths and COV's.	48
Table 12. - Published bending and shear strengths and COV's (USDA 1999f).	48
Table 13. - New pole specimen strength reductions caused by woodpecker damage.	53
Table 14. - New pole specimen I_e/I_t values for bending failure criteria.	54
Table 15. - New pole specimen I_e/I_t values for shear-bending interaction failure criteria.	54
Table 16. - New pole specimen I_e/I_t values for shear failure criteria.	54
Table 17. - New pole control specimen modulus of elasticity values.	62
Table 18. - Average new pole moisture contents.	70
Table 19. - Received in-service pole details and specimens.	72
Table 20. - In-service specimen condition rating criteria.	76
Table 21. - In-service specimen condition ratings.	77
Table 22. - In-service control specimen bending and shear strengths.	88
Table 23. - In-service control specimen average bending and shear strengths and COV's.	88
Table 24. - Published bending strengths, shear strengths, and COV's (USDA 1999f).	88
Table 25. - Relationship between decay level and in-service bending and shear strength.	89
Table 26. - Strength reductions caused by decay.	89
Table 27. - In-service specimen strength reductions caused by woodpecker damage.	91
Table 28. - In-service specimen I_e/I_t values for bending failure criteria.	92
Table 29. - In-service control specimen average modulus of elasticity values.	96
Table 30. - Average in-service pole moisture contents.	103
Table 31. - Strength reduction caused by woodpecker damage.	106

Table 32. - Analytical model C_b and C_s constants for vertically oriented damage.....	117
Table 33. - Analytical model C_b and C_s constants for horizontally oriented damage.	118
Table 34. - 13.72 m pole M/V ratios (bending failure).	119
Table 35. - 15.24 m pole M/V ratios (bending failure).	119
Table 36. - 16.76 m pole M/V ratios (bending failure).	119
Table 37. - 18.29 m pole M/V ratios (bending failure).	120
Table 38. - 13.72 m pole M/V ratios (shear-bending interaction failure).....	120
Table 39. - 15.24 m pole M/V ratios (shear-bending interaction failure).....	120
Table 40. - 16.76 m pole M/V ratios (shear-bending interaction failure).....	121
Table 41. - 18.29 m pole M/V ratios (shear-bending interaction failure).....	121
Table 42. - New specimen failure data.	122
Table 43. - New specimen failure data (cont.).	123
Table 44. - In-service specimen failure data.....	123
Table 45. - In-service specimen failure data (cont.).	124
Table 46. - In-service pole woodpecker damage dimensions.....	124
Table 47. - In-service pole woodpecker damage dimensions (cont.).	125

Chapter 1 Introduction

In many regions of North America, Europe, and Australia, wood utility poles are used as main and secondary structural members for the support of electrical distribution and transmission lines, as shown in Figure 1 (Grigsby 2001). In the province of Ontario alone there are over 40,000 H-frame, 6000 Gulfport, and thousands of single pole structures constructed of over 2 million wood utility poles (Pandey et al. 2010b).



Figure 1. - Electrical distribution and transmission structures constructed of wood utility poles.

Currently, utility companies report an increasing number of woodpecker damage incidents on in-service utility poles (HONI 2010). In addition, many aging poles have woodpecker damage in combination with wood decay. Both these forms of degradation cause strength reductions in utility poles, making their structural integrity questionable. This has raised concerns regarding the safety of utility maintenance workers and the public, and the dependability of the electrical network.

It is generally accepted that the presence of woodpecker damage and wood decay causes reduced strength of wood utility poles, although quantification of this strength reduction has not been determined. The majority of literature investigating wood utility pole woodpecker damage focuses on woodpecker behaviour, preventative methods, and repair techniques (Harness and Walters 2005). Most commonly, woodpeckers target wood utility poles for nesting, food, and food storage as shown in Figure 2. All of these uses involve woodpeckers carving out volumes of wood, reducing the pole cross-sectional strength. Several preventative methods include lethal removal, scare tactics, artificial nests, barriers, and repellents. Common repair techniques include replacement, void fillers, bulking agents, splints, and wraps.

Rumsey and Woodson (1973) conducted a study on the effect of woodpecker damage on 50 ft southern pine utility poles. In this study, 18 full size poles were tested to failure in a field test setup modeling in-service conditions. The strength of specimens with woodpecker damage was compared to the strength of undamaged control specimens. Predicted strengths were estimated based on reduced section modulus due to woodpecker damage. In this study, pole specimens did not necessarily fail at

locations of damage and the combinations of damage level and orientation tested were not extensive. A highly conservative analytical model was proposed based on a 95% exclusion limit (Rumsey and Woodson 1973). This study was found to be informative, although the results and conclusions were not extensive enough to be of any practical use.

Wood decay has been extensively researched in the past (USDA 1999f). Results indicate that internal decay (Figure 2) is the most significant type of decay in terms of strength reduction. A major difficulty in diagnosing and quantifying internal decay strength reduction in utility poles is the lack of external indicators. In many cases by the time internal decay has been identified in a wood pole, the majority of the pole strength has been already been lost.

Based on current literature, there is an insufficient dataset available to enable quantification of the strength reducing effect of woodpecker damage and wood decay. This data is essential as a first step in developing condition rating criteria to assess wood utility pole structural integrity and transmission line reliability when woodpecker damage and wood decay are present.



Figure 2. - Woodpecker damage (left) and decay (right).

1.1 Objectives

The main objective of this thesis was to determine the effect of woodpecker damage and wood decay on the strength of wood utility poles. This was achieved by:

1. Performing a literature review on the structure of wood and determining the significant factors that affect its mechanical properties.
2. Developing analytical models to predict the strength reducing effect of woodpecker damage and to analyze in-service utility poles.
3. Performing experimental beam testing of new and in-service wood utility pole specimens with varying levels of woodpecker damage and wood decay.
4. Analyzing new pole and in-service specimen experimental results to better understand the effect of woodpecker damage and wood decay on the strength of wood utility poles.
5. Using analytical and experimental results to develop application methods for determining if utility poles should be replaced due to woodpecker damage and decay.

1.2 Research Approach

In order to determine the effect of woodpecker damage and wood decay on the strength of wood utility poles, background literature review and analytical work was performed. The literature review involved reviewing current design standards for wood utility poles, the mechanical properties of wood, the effect of decay on wood strength, and the effect of woodpecker damage on wood utility pole strength. The Hydro One Networks Incorporated (HONI) current approach to determining the effects of woodpecker damage and wood decay on wood utility pole strength was reviewed. Based on the HONI classification of woodpecker damage, woodpecker damage levels were organized into three levels of severity for research purposes.

Three analytical models were developed that predicted the theoretical strength reduction caused by the presence of woodpecker damage in a cross-section. The models developed were based on mechanics of materials principles using modified cross-section geometry due to woodpecker damage. A bending failure model was developed since, in the structural design of utility poles, bending moment stresses are known to be the critical design parameter. It was decided that the significance of shear stress in a cross-section should also be considered since the presence of woodpecker damage could cause shear stresses to be a significant parameter. As a result, a shear-bending and a shear failure model was developed to determine the significance of shear stress on cross-section behaviour. These models were developed for analysis purposes and were verified by the subsequent experimental program. In order to develop an experimental beam test setup that simulated the load effects representative of in-service utility poles, a utility pole structural analytical model was developed. This analytical model incorporated the theoretical effect of woodpecker damage using the previously developed woodpecker damage analytical models. Using the utility pole structural analytical model, a parametric study was performed with varying levels and orientation of woodpecker damage. Based on this study, two experimental beam test setups were developed for use in the experimental program for testing of new and in-service utility poles.

A total of 28 new and in-service utility poles were received from HONI for experimental testing. The poles received were cut into 4.25 m for beam testing. A single new pole and in-service specimen from each pole was tested as a control specimen without woodpecker damage for reference wood strength. The remainder of the new pole specimens were mechanically introduced with woodpecker damage. The remainder of the in-service specimens were tested with natural woodpecker damage. Tested specimens were analyzed and results were compared with the woodpecker damage analytical model predictions. Results indicated that the effect of woodpecker damage is well modelled by the woodpecker damage analytical models. Overall, the BF analytical model was preferable for cross-section analysis due to the accuracy of the model predictions and the simplicity of required calculations. The effect of decay on wood strength was also determined from experimental in-service specimen results. Results indicated that by the time wood decay can be detected in wood utility poles, severe reduction in wood strength has occurred.

Analytical and experimental results were used to develop three application methods for determining whether utility pole replacement is necessary due to the presence of woodpecker damage. These three methods include the simplified method, the chart method, and the case-specific method. The simplified method allows determination of whether a utility pole should be replaced based only on knowledge of the most severe level of woodpecker damage present in a pole. The chart method

takes into account additional factors such as the diameter of the pole at the location of the woodpecker damage and the width of the hole opening. The case-specific method is advantageous since it accounts for the parameters used in the chart method and allows the location of woodpecker damage along the length of a pole to be accounted for. The simplified and chart methods are preferable since they are relatively simple and easy to implement in the field. The case-specific method requires a full structural analysis of the utility pole in question to be undertaken and is useful for more accurately assessing whether replacement is necessary.

1.3 Organization of Thesis

Chapter 2 presents a literature review on the structure, mechanical properties, and decay of wood. Chapter 3 focuses on the characterization of woodpecker damage from HONI and introduces the categorization of woodpecker damage developed for research purposes. Using the woodpecker damage categories previously developed, three woodpecker damage analytical models for predicting strength reduction were developed and are presented in Chapter 4. In Chapter 5, a utility pole structural analysis model is presented that incorporates the effect of woodpecker damage. A parametric study using this model was performed to aid in developing experimental beam test setups representative of in-service conditions. The experimental program for new pole and in-service beam specimens is reviewed in Chapter 6, followed by the new pole and in-service beam specimen results, analysis, and discussion in Chapter 7 and Chapter 8, respectively. Application of analytical and experimental results to utility pole replacement is presented in Chapter 9. Overall conclusions and recommendations are presented in Chapter 10.

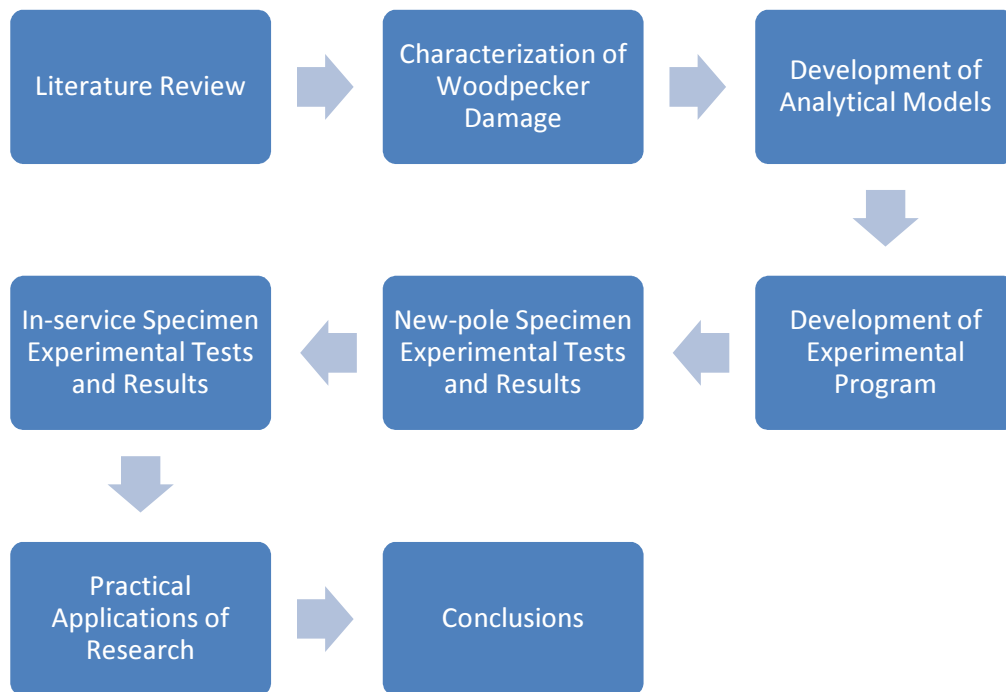


Figure 3. - Organizational flowchart of thesis.

Chapter 2 Literature Review

A literature review was performed to gain background knowledge on factors that affect the structural behaviour of wood. Topics including the structure of wood, the effect of natural characteristics on the mechanical properties of wood, the effect of manufacturing and service environment on the mechanical properties of wood, and biodeterioration of wood were investigated. These topics were informative and gave the author a better understanding of wood used as a structural material.

2.1 Structure of Wood

All information described in this section was obtained from the Wood Handbook (USDA 1999f).

2.1.1 Bark, Wood, Branches, and Cambium

Figure 4 shows a cross-section of a tree with labels A – G.

1. Bark
 - a. The outer corky dead part (A) with varying thickness depending on species and age of tree.
 - b. The inner thin living part (B) carries food from leaves to growing parts of the tree.
2. The cambium layer (C) is a microscopic layer that is inside the inner bark and forms wood and bark cells.
3. Growing parts of the tree
 - a. The sapwood (D) contains dead tissue as well as living tissue that carries sap from the roots to the leaves.
 - b. The heartwood (E) is formed of sapwood that has gradually changed and is inactive.
 - c. The pith (F) is a small core of tissue located at the center of tree stems, branches, and twigs about which initial wood growth takes place.
4. Wood rays (G) are tissues that are horizontally oriented through the radial plane of the tree. Rays vary in size and connect various layers from pith to bark for storage and transfer of food.

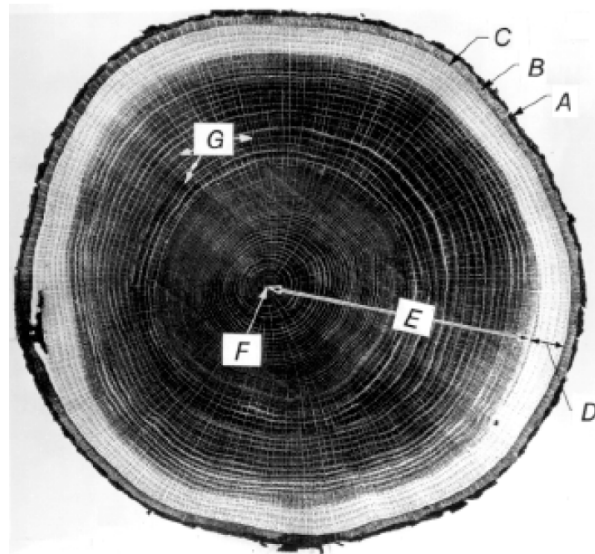


Figure 4. - Cross-section of tree trunk showing interior structure (USDA 1999f).

2.1.2 Sapwood and Heartwood

Sapwood is located between the cambium and heartwood and contains both living and dead cells. Sapwood functions mainly for the storage of food, although it also transports water and sap. Typically sapwood is 4-6 cm in radial thickness.

Heartwood consists of inactive cells that do not function for water conduction or food storage and have a high extractive content. Heartwood extractives affect wood by reducing permeability, increasing stability in changing moisture conditions, and slightly increasing weight. The basic strength of the wood is essentially not affected by the transition from sapwood cells to heartwood cells.

2.1.3 Growth Rings

Wood species in temperate climates form annual growth rings due to the difference in wood formed in the early and late growing seasons. The inner part of the growth ring formed in the early season is called the early wood and the outer part is called latewood. Earlywood is characterized by cells with relatively large cavities and thin walls. Latewood cells have smaller cavities and thicker walls. Growth rings are prominent in most softwood where earlywood physical properties differ significantly compared to latewood. Earlywood is lighter in weight, softer, and weaker than latewood. Because of the greater density of latewood, the proportion of latewood is sometimes used to judge the strength of the wood.



Figure 5. - Growth rings in ponderosa pine log (USDA 1999f).

2.1.4 Wood Cells

Wood cells of various size and shape form the structure of wood and are firmly cemented together forming the structure of wood. Most wood cells, or fibres, are elongated and pointed at the ends and range in length from 3-8 mm in softwoods. Wood rays are a type of cell that conduct sap radially across the grain in the direction from the pith to the bark. Another cell type is longitudinal parenchyma which is used for storage of food.

2.1.5 Chemical Composition

Dry wood is composed of cellulose, lignin, hemicelluloses, and minor amounts of extraneous materials.

Cellulose is the major component and constitutes approximately 50% of wood substance by weight. It is a high-molecular-weight linear polymer consisting of chains of glucose monomers. During tree growth, cellulose molecules are arranged into ordered strands called fibrils that are organized into the larger structural elements that make up the cell wall of wood fibres. Most of the cell wall cellulose is crystalline.

Lignin constitutes 23% to 33% of the wood substance in softwoods. Lignin occurs in wood throughout the cell wall although it is concentrated toward the outside of the cells and between cells. Lignin is often called the cementing agent that binds individual cells together. Lignin is a three-dimensional phenylpropanol polymer, and its structure and distribution in wood are still not fully understood.

The hemicelluloses are associated with cellulose and are branched, low-molecular-weight polymers composed of several different kinds of sugar monomers.

Unlike the major constituents of wood, extraneous materials are not structural components. Both organic and inorganic extraneous materials are found in wood. The organic component takes the form of extractives, which contribute to such wood properties as color, odor, taste, decay resistance,

density, hygroscopicity, and flammability. Extractives include tannins and other polyphenolics, coloring matter, essential oils, fats, resins, waxes, gum starch, and simple metabolic intermediates. This component is termed extractives because it can be removed from wood by extraction with solvents, such as water, alcohol, acetone, benzene, or ether. Extractives may constitute roughly 5% to 30% of the wood substance, depending on such factors as species, growth conditions, and time of year when the tree is cut.

2.2 Effect of Natural Characteristics on Mechanical Properties of Wood

Clear straight-grained wood is used for determining fundamental mechanical properties of wood. Due to natural growth characteristics of trees, wood products vary in specific gravity, may contain cross grain, or may have knots and localized slope of grain. Natural defects such as pitch pockets may occur as a result of biological or climatic elements influencing the living tree. These wood characteristics must be taken into account in assessing actual properties or estimating the actual performance of wood products. All information described in this section was obtained from the Wood Handbook (USDA 1999f).

2.2.1 Specific Gravity

The substance that wood is composed of is heavier than water with a specific gravity of 1.5 for all species. Due to cell cavities and pores most species of wood have a specific gravity of less than 1.0. Variations in the size of cell openings and thickness of cell walls cause different species to have different specific gravities. As a result, specific gravity is a good index of the amount of wood substance in a piece of wood. Specific gravity can also be a good index of mechanical properties if the wood is clear, straight-grained, and free of defects. Mechanical properties within a species have been found to be linearly related to specific gravity. The presence of gums, resins, and extractives also contribute to increased specific gravity with little contribution to mechanical properties.

2.2.2 Knots

A knot is the portion of a branch that intersects with the trunk of a tree. Knots interrupt continuity and change direction of the wood fibres, changing mechanical properties in these locations. The influence of a knot depends on their size, location, shape, and soundness. Knots are classified as intergrown (A) or encased (B) as shown in Figure 6. When a limb remains alive there is continuous growth at the limb-trunk interface and the knot formed is intergrown. Once a limb has died wood growth covers the dead limb and the knot formed is encased. Encased knots tend to have less effect on wood mechanical properties since they produce less cross-grain.

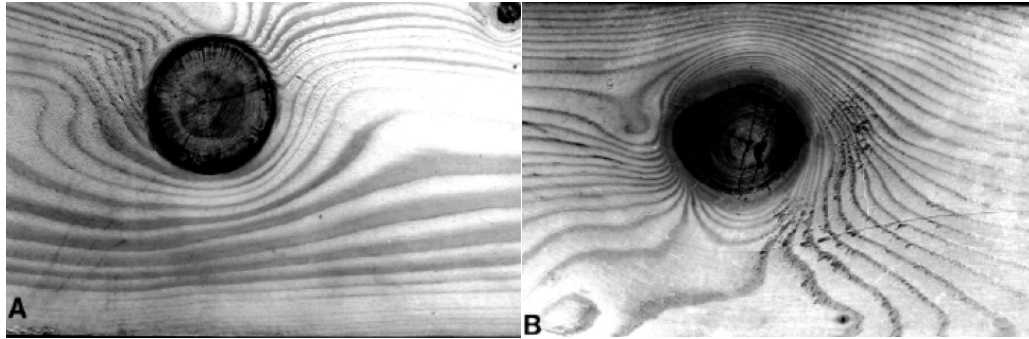


Figure 6. - Encased (A) and intergrown (B) knots (USDA 1999f).

Mechanical properties are lower in sections containing knots since (a) the clear wood is displaced by the knot, (b) the fibres around the knot are distorted, resulting in cross grain, (c) the discontinuity of wood fibre leads to stress concentrations, and (d) checking often occurs around the knots during drying. Hardness and strength in compression perpendicular to the grain are exceptions to this rule. Knots have a much greater effect in axial tension than in axial short-column compressions. The effects in bending are somewhat less than those in axial tension.

Knots in round timbers, such as poles, have less effect on strength than in sawn timbers. Although the grain is irregular around knots in both forms of timber, the angle of the grain to the surface is smaller in naturally round timber. In addition, in round timbers there is no discontinuity in wood fibres due to sawing.

2.2.3 Slope of Grain

In some wood product applications the directions of important stresses may not coincide with the natural axes of fibre orientation in the wood. Elastic properties in directions other than along the natural axes can be obtained from elastic theory. Strength properties and modulus of elasticity in directions ranging from parallel to perpendicular to the fibres can be approximated using a Hankinson-type formula:

$$N = \frac{PQ}{P \sin^n \Theta + Q \cos^n \Theta} \quad \text{Equation 1}$$

where N is strength at angle Θ from fibre direction, Q is strength perpendicular to the grain, P is strength parallel to the grain, and n is an empirically determined constant. Values of n have been developed for different properties including tensile, compression, and bending strengths as well as modulus of elasticity and toughness.

In wood there are several types of cross grains including spiral, wavy, dipped, interlocked, and curly. Spiral grain is caused by winding growth of wood fibres around the trunk of the tree instead of vertical growth. The direction of checks in a log is an indicator of grain direction.

2.2.4 Reaction Wood

Reaction wood is abnormally woody tissue that is associated with leaning trunks and crooked limbs. It is believed that reaction wood is formed as a natural response of a tree to return its trunk and limbs into a more normal position. In softwood reaction wood is called compression wood since it found on the lower sides of limbs and inclined trunks. Common traits of compression wood are a dark appearance and density that is 30-40% greater than normal wood. In general, compression wood of equal density to normal wood has lower strength than the normal density wood. A common property of compression wood is that it undergoes extensive longitudinal shrinkage (5-10 times normal wood) when subjected to moisture loss.

2.2.5 Juvenile Wood

Juvenile wood in softwoods is produced near the pith of the tree with different physical and anatomical properties. Juvenile wood has a high fibril angle (angle between axis of wood cell and cellulose fibres) that causes longitudinal shrinkage up to 10 times that of mature wood. Compression wood and spiral grain are also more common in juvenile wood in comparison to mature wood. In general, juvenile wood has reduced mechanical properties in comparison to mature wood.

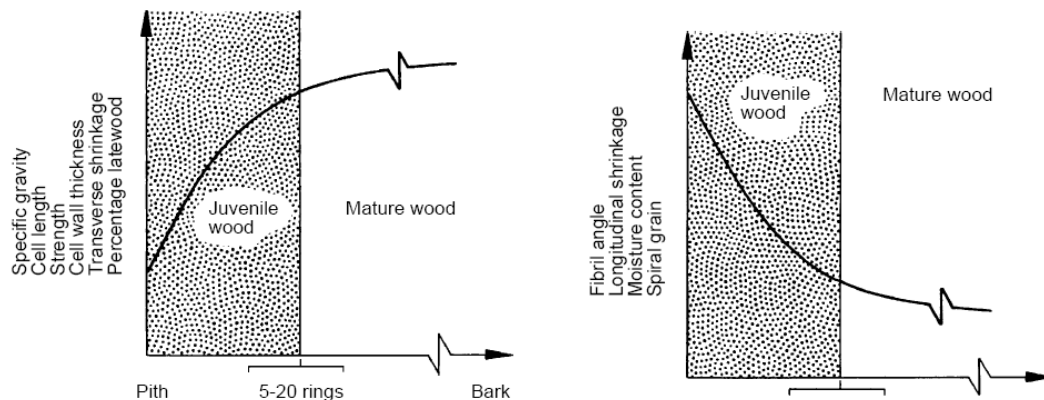


Figure 7. - Properties of juvenile wood (USDA 1999f).

2.2.6 Compression Failures

Compression failures can be caused by excessive compressive stresses along the grain from excessive bending of standing trees, felling of trees on rough surfaces, and rough handling of logs. Compression failures are difficult to see with the naked eye although they may be indicated by fibre breakage on the end grain. The main effect of compression failures is a reduction in tensile strength and shock resistance.

2.2.7 Pitch Pockets

A pitch pocket is an opening parallel to annual rings that contains free resin. This opening is curved on the bark side and almost flat on the pith side. The effect of pitch pockets depends on their location,

size, and number. Excessive pitch pockets indicate lack of bond between annual growth layers and could result in shakes or separation along the grain.

2.2.8 Extractives

Many wood species contain removable extraneous materials or extractives that do not degrade the structure of the wood. Modulus of rupture and strength in compression parallel to grain are slightly reduced for some species after extractives have been removed. The extent to which extractives influence strength is a function of the amount of extractives, the moisture content of the piece, and the mechanical property under consideration.

2.3 Effect of Manufacturing and Service Environment on Mechanical Properties of Wood

Due to manufacturing and service environments factors such as moisture content, temperature, rate and duration of load, aging, water borne preservative treatment, decay, and insect damage may affect wood mechanical properties. All information described in this section was obtained from the Wood Handbook (USDA 1999f).

2.3.1 Moisture Content

The mechanical properties of wood are affected by reduction in moisture content below fibre saturation point. The relationship that describes moisture content is represented in the following equation.

$$P = P_{12} \left(\frac{P_{12}}{P_g} \right)^{\frac{12-M}{M_p-12}} \quad \text{Equation 2}$$

where P_{12} is the property at 12% moisture content, P_g is the property for green wood, P is property at moisture content M , and M_p is a moisture content value dependent on species. This equation can be used to estimate properties at any moisture content below M_p . Care must be taken since below 12% moisture content some species do not follow this relationship. Specimens with large numbers of knots can be insensitive to changes in moisture content due to the low percentage of clear wood in the specimen.

2.3.2 Reversible Temperature Effects

The mechanical properties of wood decrease when heated and increase when cooled. At constant moisture content and temperature below 150°C mechanical properties are approximately linearly related to temperature. When wood is quickly heated or cooled the change in properties is called an immediate effect. Immediate effects are generally reversible below 100°C.

2.3.3 Rate of Loading

Mechanical property values of wood recorded in tables are referred to as static strength values. Static strength tests are conducted at rates that cause failure within five minutes. Higher and lower values of strength are obtained for wood loaded at faster and slower rates, respectively.

2.3.4 Duration of Load

The duration of load acting on a wood member is a factor in determining the load a member can withstand. A member that carries a load continuously for a long period of time has a lower load capacity than tabulated strength properties predict. Similarly, a member that carries a load continuously for a short period of time has a higher load capacity than tabulated strength properties predict. Intermittent loads have been found to have a cumulative effect that is equal to a continuous load of equivalent cumulative time.

2.3.5 Aging

In dry and moderate temperature conditions where wood is protected from decay the mechanical properties of wood show little change over time. Very old timbers have shown significant loss in wood strength only after centuries of aging. In general wood is very durable and maintains mechanical properties over time.

2.3.6 Waterborne Preservative Treatment

Preservative treatments generally reduce the mechanical properties of wood although initial loss in strength from treatment must be balanced against loss of strength from decay when untreated wood is placed in wet conditions. Waterborne preservative treatment has negligible effects on modulus of elasticity and compressive strength, while it causes a reduction from 0-20% in tensile strength and modulus of rupture. The effects of waterborne preservative treatment on mechanical properties are related to preservative retention, post-treatment drying temperature, size and grade of material, initial kiln-drying temperature, incising, and both temperature and moisture in service.

2.3.6.1 Preservative Retention

Retention levels lower than 16 kg/m^3 have no effect on modulus of elasticity and compressive strength and a slight negative effect on tensile strength and modulus of rupture. A retention level of 40 kg/m^3 further reduces modulus of rupture.

2.3.6.2 Post-treatment Drying Temperature

Air drying after treatment causes no significant reduction in static strength of wood treated at a level of 16 kg/m^3 . The post-treatment redrying temperature has been found to be critical when temperatures exceed 75°C . The limit for redrying temperature has been set to 74°C .

2.3.6.3 Size of Material

Larger material has been found to undergo less reduction in strength than smaller material. This relationship appears to be a function of surface-to-volume ratio, which controls the amount of preservative retention.

2.3.6.4 Material Grade

The effect of preservative treatment is a quality dependent phenomenon. The trend is that higher grades of wood have larger reductions in mechanical properties than lower grades.

2.3.6.5 Initial Kiln-Drying Temperature

Kiln-drying at 100-116°C results in more hydrolytic degradation of cell walls than drying at lower temperatures. This results in greater reduction in bending and tensile strength of the wood.

2.3.6.6 Incising

Incising is a pre-treatment mechanical process that punches small slits into the surface of a wood product to increase preservative penetration and distribution in difficult to treat species. Incising does cause strength reduction although its effects have to be balanced against increase in performance over time. Incising and treating timbers at a density of 1500 incisions/m², 19 mm deep reduces strength by 5-10%.

2.3.6.7 In-service Temperature

Preservative treatments accelerate the thermal degradation of bending strength at temperatures above 54°C.

2.3.6.8 In-service Moisture Content

No differences in strength have been found between treated and untreated wood at moisture contents above 12%. It was found that treated wood at a moisture content of 10% had a lower bending strength than untreated wood.

2.3.7 Mold and Stain Fungi

Low levels of mold and stain fungi do not have a major affect on wood mechanical properties since these organisms feed on cell cavities rather than the cell wall structure. Heavy staining can cause a reduction of 1-2% in specific gravity, 2-10% in surface hardness, 1-5% in bending and crushing strength, and 15-30% in toughness or shock resistance.

2.3.8 Decay

Wood destroying fungi seriously reduce wood strength by metabolizing the cellulose fraction of wood that gives wood its strength. Early stages of decay are hard to detect. Brown-rot fungi may reduce mechanical properties over 10% before considerable weight loss and visible deterioration occur. When weight loss reaches 5-10%, mechanical properties are reduced from 20-80%. Decay has

considerable effect on toughness, impact bending, and work to maximum load in bending, little effect on shear and hardness, and intermediate effect on other properties. Decay can be prevented from starting by keeping wood at a moisture content less than 20%. There are currently no methods for predicting strength reduction from the appearance of decayed wood. A safe method of dealing with decayed wood is to simply discard it.

2.3.9 Insect Damage

Insect damage may occur in all forms of wood are classified as pinholes, grub holes, and powderpost holes. Powderpost larvae create irregular burrows that can destroy a wood piece's interior while leaving very little surface indication. This can result in a severe reduction in wood strength with little warning. Currently there are no reliable methods of visually estimating strength reduction of insect-damaged wood.

2.4 Biodeterioration of Wood

All information described in this section was obtained from the Wood Handbook (USDA 1999f).

2.4.1 Mold and Fungus Stains

Mold and fungus stains generally affect only sapwood and appear in a variety of colors. Fungus stains penetrate into sapwood and cannot be removed by surfacing. On a tree cross-section stains appear as radially oriented pie-shaped discoloration as shown in Figure 8. Discoloration may completely cover the sapwood or may occur in streaks and patches. Fungus stain colors include black, grey, blue, brown, yellow, orange, purple, and red.

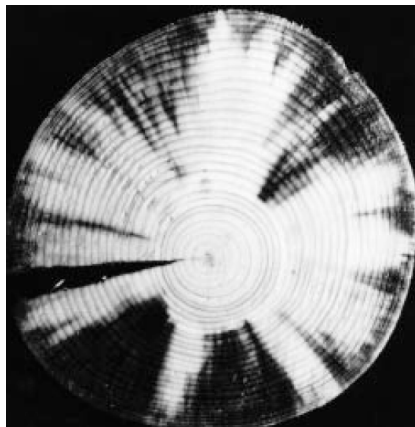


Figure 8. - Cross-section with fungus stain (USDA 1999f).

Mold discolorations appear as fuzzy or powdery surface growths in a wide range of colors. On softwoods the fungus may penetrate deeply and the discoloured surface can be easily brushed or surfaced off. Mold and fungus stains develop rapidly in conditions that are humid and warm and discoloration can be visible in as little as five days. Side effects are increased water absorbance and reduced shock resistance and toughness. In terms of strength there is only a slight reduction caused by these growths.

2.4.2 Decay

Decay producing fungi may attack either heartwood or sapwood depending on the conditions. Fungi appear as white or brown fan-shaped patches, strands, or root like structures. Sometimes fungi produce fruiting bodies such as mushrooms, crusts, and crusts. Certain fungi colonize the heartwood of living trees while others confine their activities to manufactured products such as utility poles.

Decay progress rapidly at temperatures that favour plant growth (10-35°C). Serious decay will only occur when wood is at its fibre saturation moisture content which is around 30%. This high of a moisture content is not attainable from humid air, rather the wood must come into contact with water and become saturated. When wood is water soaked, decay will cease since air can no longer reach the interior of the piece of wood.

The two main types of decay are brown rot and white rot. Brown-rot fungi remove large amounts of cellulose causing the wood to take on a browner color as shown in Figure 9. The result of brown-rot is wood cracking across grain, shrinkage, and collapse. White-rot fungi remove cellulose and lignin causing the wood to lose its color and appear white and spongy. Both types of fungi colonize hardwoods and softwoods although brown rot is present more often in softwoods and white rot in hardwoods.

A third less severe type of decay is soft rot. Soft rot is relatively shallow causing wood to be greatly degraded and soft when wet. Immediately beneath the zone of rot the wood is typically firm as shown in Figure 9.

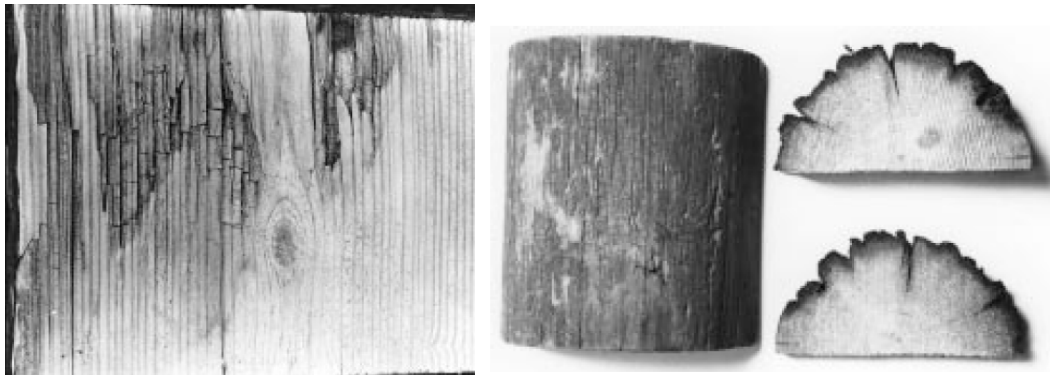


Figure 9. - Brown rot (left) and soft rot (right) (USDA 1999f).

2.4.3 Effect of Decay on Wood Strength

The initial effect of decay is on toughness and the ability of the wood to withstand impact. Following this, strength reduction in static bending occurs and eventually all strength properties are reduced. It has been found that strength loss depends mainly on the type of fungi present rather than on the species of wood being decayed. At a 1% weight loss from fungal attack toughness can be reduced from 6% to over 50%. Once weight loss reaches 10% strength losses generally exceed 50%. At 10% weight loss, decay is only detectable microscopically. Once wood has visibly detectable decay it can be assumed to cause a large reduction in strength properties.

Chapter 3 Characterization of Woodpecker Damage

The Hydro One Networks Incorporated (HONI) has used field observations of woodpecker damage on utility poles to categorize woodpecker damage into levels and to understand the strength reduction caused by woodpecker damage (HONI 2010). Based on this information, idealized woodpecker damage levels were developed for research purposes.

3.1 Woodpecker Damage Levels

Woodpecker damage has been observed in a large variety of levels and orientations on in-service utility poles. HONI currently categorizes woodpecker damage into exploratory, feeding, and nesting levels, in order of increasing severity as shown in Table 1. Examples of the three different woodpecker damage levels on in-service poles are shown in Figure 10 and Figure 11. These photos were taken from in-service utility poles received from HONI.

Table 1. - HONI historical woodpecker damage levels (HONI 2010).

Damage Level	Description
Exploratory	< 3" (75 mm) Ø opening and 3" (75 mm) deep
Feeding	< 3" (75 mm) x 7" (175 mm) opening and 6" (150 mm) deep
Nesting	3" (75 mm) Ø opening, 2' (600 mm) long with 1-3" (25-75 mm) shell thickness



Figure 10. - In-service exploratory damage (left) and feeding damage (right).



Figure 11. - In-service nesting damage and dissection of interior.

3.2 Effect of Woodpecker Damage on Strength

The effect of woodpecker damage on strength was characterized by HONI using the woodpecker damage levels defined in the previous section. Three different graphs were developed as shown in Figure 12, Figure 13, and Figure 14. In these graphs, strength reduction levels are a function of the width of the hole opening and circumference of the subject utility pole. As expected, increased hole opening widths cause increased strength reductions. While keeping the hole width constant, increasing the circumference of a utility pole will result in decreased strength reduction. The graphs developed are simple and easy to implement in the field when a replacement level of remaining strength is chosen. A drawback of these graphs is that they do not account for the effect of the location of the hole along the utility pole length. This is an important consideration since it affects whether a utility pole should remain in-service or be replaced.

EXPLORATORY HOLES

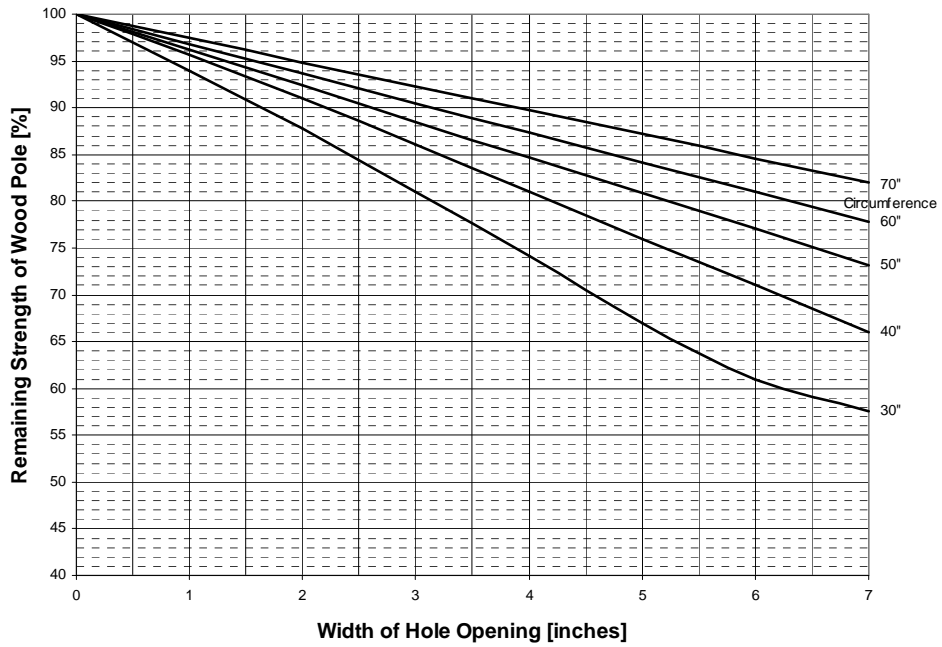


Figure 12. - Strength reduction caused by exploratory holes (HONI 2010).

FEEDING HOLES

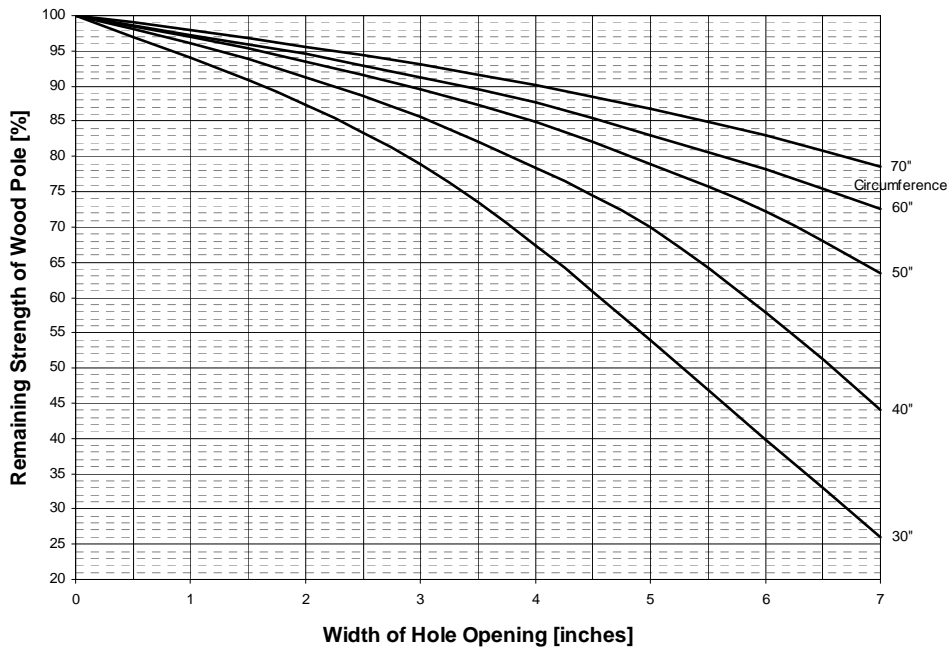


Figure 13. - Strength reduction caused by feeding holes (HONI 2010).

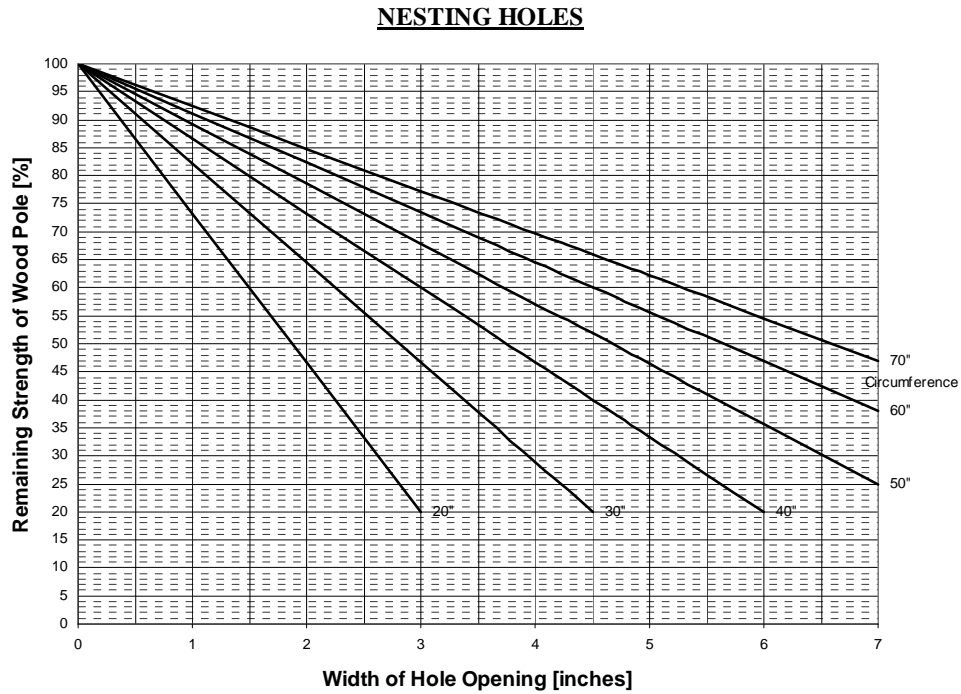


Figure 14. - Strength reduction caused by nesting holes (HONI 2010).

3.3 Idealized Woodpecker Damage

For research purposes, the three levels of woodpecker damage defined by HONI were idealized non-dimensionally as shown in Figure 15 in the current study. These levels of damage are a function of cross-section diameter and represent the range of woodpecker damage severity typically observed in-service. Woodpecker damage can be present in an infinite number of orientations around the circumference of the section. For experimental purposes, three orientations were considered that cover the extreme ranges of cross-sectional behaviour: tension, compression, and neutral axis locations, as displayed in Figure 16.

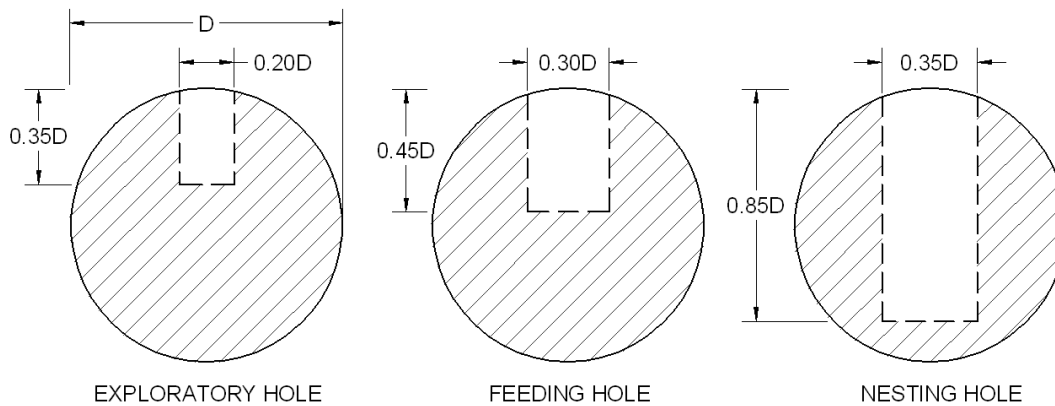


Figure 15. - Idealized levels of woodpecker damage.

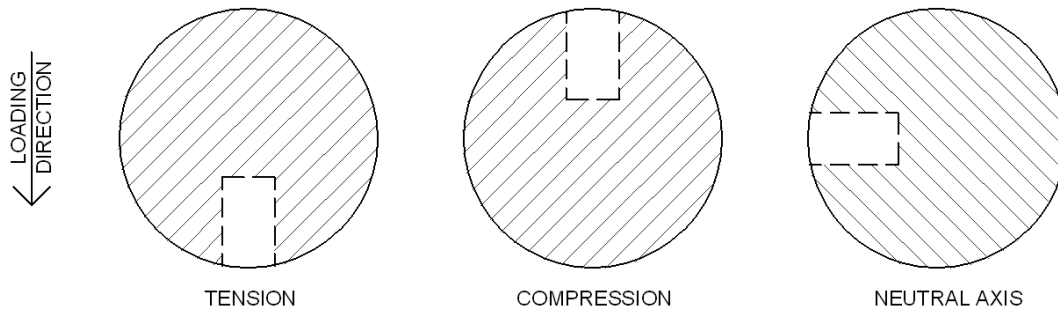


Figure 16. - Idealized woodpecker damage orientations.

The idealized damage levels were used to categorize damage for the experimental portion of this research. As is discussed in Chapter 6, damage was mechanically introduced in some pole specimens. Figure 17, Figure 18, and Figure 19 show examples of idealized exploratory, feeding, and nesting holes introduced into test specimens using saw-tooth bits and an electric drill.



Figure 17. - New pole specimen idealized exploratory damage.



Figure 18. - New pole specimen idealized feeding damage.



Figure 19. - New pole specimen idealized nesting damage.

Chapter 4 Woodpecker Damage Analytical Models

Three analytical models based on bending, shear, and shear-bending interaction were developed to determine the theoretical effect of woodpecker damage on cross-section strength. It was decided that reduced geometric section properties would be used to demonstrate strength reduction, rather than reduced wood bending and shear strengths. This approach was chosen since woodpecker damage modifies cross-section geometry while wood strength remains essentially unaffected. Required section properties, dependent on the model, were calculated using geometric properties and mechanics of materials principles (Mikhelson 2004). Based on the moments and shears present at a section, the models can be used to determine the stresses present at a cross-section for comparison with failure criteria. The ultimate moment and shear capacities of a cross-section with woodpecker damage present can also be determined using these models. The accuracy of the models will be verified by experimental results. Shear and bending stress distributions were also determined for the different levels and orientations of woodpecker damage to gain a better understanding of cross-sectional behaviour.

4.1 Effect of Woodpecker Damage on Cross-section Strength

4.1.1 Bending Failure Model (BF model)

The most common definition of failure for wood utility poles, as specified by CSA C22.3 No. 1 (2006a) and the USDA (1965a; 2001b; 2009c; 2005d), states that failure occurs when the bending strength of a wood pole has been reached at a critical section. The bending strength of wood, or modulus of rupture, is governed by the tensile strength of wood fibres. This definition of failure assumes that bending effects are dominant and neglects the effects of shear. The bending failure criteria is given by the following equation:

$$\sigma = \frac{My}{I} = \frac{M}{Z} \leq f_b \quad \text{Equation 3}$$

where σ is bending stress, M is applied moment at the section, y is distance from neutral axis to the extreme tension fibre, I is moment-of-inertia, Z is elastic section modulus, and f_b is wood bending strength. Theoretical expressions for section properties I and Z were derived for use in the bending model. Using mechanics of materials principles, reduced section properties, I_{red} and Z_{red} , were computed for all combinations of woodpecker damage levels and orientation. Values of Z were derived for critical locations of maximum stress. Theoretical section properties are presented as ratios of undamaged section properties in Table 2. The following equations for section properties of undamaged circular cross-sections are given as a function of cross-section diameter:

$$I = \frac{\pi D^4}{64} \quad \text{Equation 4}$$

$$Z = \frac{\pi D^3}{32} \quad \text{Equation 5}$$

Table 2. - I and Z factors for cross-sections with woodpecker damage.

Damage Level	Damage Orientation			
	Tension or Compression		Neutral Axis	
	I_{red}/I	Z_{red}/Z	I_{red}/I	Z_{red}/Z
Exploratory	0.82	0.79	0.99	0.99
Feeding	0.72	0.67	0.98	0.98
Nesting	0.60	0.59	0.94	0.94

A theoretical analysis of wood poles with woodpecker damage can be performed using the bending failure criteria equation presented, the I and Z factors in Table 2, and the following equations:

$$I_{red} = \frac{I_{red}}{I} \left(\frac{\pi D^4}{64} \right) \quad \text{Equation 6}$$

$$Z_{red} = \frac{Z_{red}}{Z} \left(\frac{\pi D^3}{32} \right) \quad \text{Equation 7}$$

4.1.2 Shear Failure Model (SF model)

Shear failure is rarely observed in wood utility poles that are undamaged. Despite this, the shear failure mode needs to be considered as a possible failure mode due to the presence of woodpecker damage. This failure mode is based on the assumption that shear effects are dominant and bending effects can be neglected. This assumption was only found to be applicable for nesting level woodpecker damage oriented in the neutral axis during experimental testing. As a result, the SF model was only applied for this woodpecker damage case. The shear failure criteria is given by the following equation:

$$\tau = \frac{vQ}{It} \leq f_v \quad \text{Equation 8}$$

where τ is shear stress, V is applied shear force at the section, Q is moment of the area between the plane being analyzed and the extreme cross-section fibres about the neutral axis, t is shear plane thickness, and f_v is wood shear strength. A theoretical expression for the term Q/It at the critical location was derived for nesting level neutral axis damage based on mechanics of materials principles (Mikhelson 2004). The Q/It value accounting for section loss due to woodpecker damage is presented as a ratio of the equivalent undamaged section property in Table 3. The following equation for Q/It of an undamaged circular cross-section is given as a function of diameter:

$$\frac{Q}{It} = 1.70D^{-2} \quad \text{Equation 9}$$

Table 3. - Q/It factor for cross-section with woodpecker damage

Damage Level	Orientation
	Neutral Axis
	$(Q/It)_{red}/(Q/It)$
Nesting	7.38

A theoretical analysis of wood poles with nesting level woodpecker damage in the neutral axis can be performed based on the shear failure criteria equation presented in conjunction with:

$$\left(\frac{Q}{It}\right)_{red} = 12.55D^{-2} \quad \text{Equation 10}$$

4.1.3 Shear-Bending Interaction Failure Model (SBIF model)

Failure occurring as a result of bending strength being exceeded is a simplification for utility pole design. In structures where shear forces are significant, failure could occur due to the interaction of shear and bending stresses (Yoshihara and Kawasaki 2006; van der Put, T. A. C. M. 2010; USDA 1962e). As a result, shear-bending stress interaction is a more general failure criteria that could result in an improved analysis method. The Goldenblat-Kopnov shear-bending interaction equation calibrated for wood failure is given as (Yoshihara and Kawasaki 2006):

$$1 = \left(\frac{\sigma}{f_b}\right)^{4.36} + \left(\frac{\tau}{f_v}\right)^{0.21} \quad \text{Equation 11}$$

Since maximum shear and bending stresses do not typically occur at the same plane, shear-bending interaction checks must be conducted at multiple planes throughout the cross-section. In addition, the section properties Z , y , Q and t vary depending on the plane being analyzed. Expressions for theoretical geometric sections properties Z and Q/It were derived as a function of diameter for all combinations of woodpecker damage levels and orientations, and are presented in the following form:

$$Z = C_b D^3 \quad \text{Equation 12}$$

$$\frac{Q}{It} = C_s D^{-2} \quad \text{Equation 13}$$

Constants C_b and C_s have been tabulated in Appendix A for 21 evenly spaced shear planes throughout a cross-section's depth for all combinations of woodpecker damage levels and orientations. Using these expressions, in conjunction with the shear-bending interaction equation, a cross-section can be analyzed at 21 planes over the cross-section depth by varying the constants C_b and C_s appropriately. The bending and shear stresses are computed at each potential failure plane and the interaction equation is evaluated. If the interaction equation exceeds 1, failure will occur theoretically. Figure 20 graphically shows how a cross-section is divided into 21 planes for analysis.

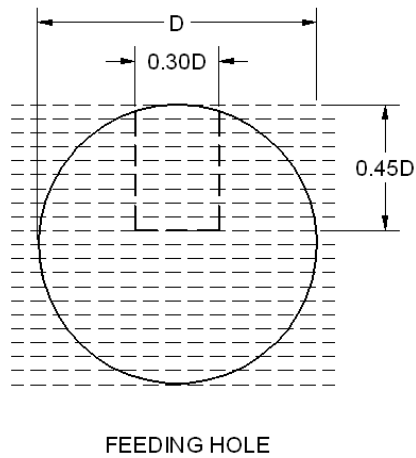


Figure 20. - Cross-section depth separated into 21 planes for SBIF analysis.

4.2 Shear and Bending Stress Distributions

Based on the previously derived analytical models, normalized bending and shear stress distributions for cross-sections with varying levels and orientations of woodpecker damage were computed.

4.2.1 Undamaged Section

For comparison purposes, normalized shear and bending stress distributions for an undamaged circular cross-section are provided in Figure 21. Peak stress locations are indicated by a normalized stress of 1.00.

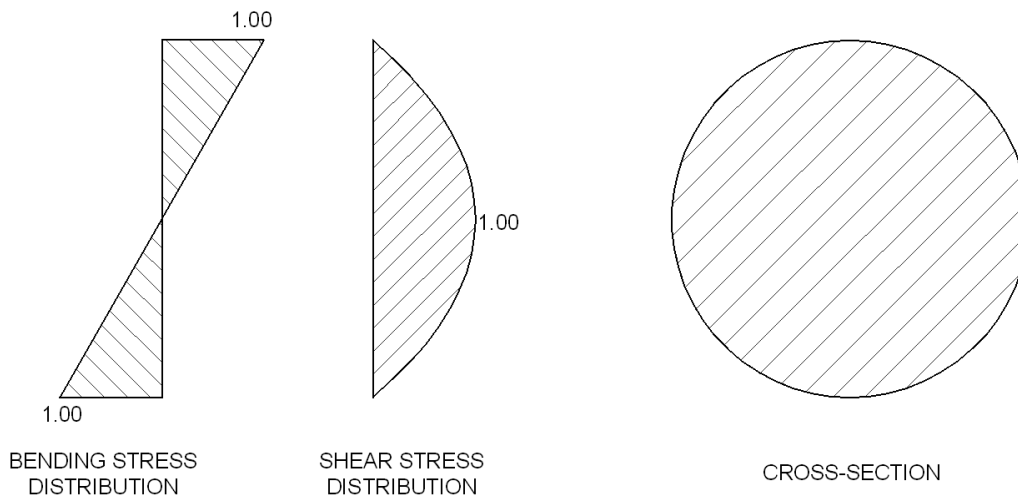


Figure 21. - Stress distributions of an undamaged cross-section.

4.2.2 Vertically Oriented Damage

Vertically oriented damage caused a large decrease in section modulus due to the large areas of extreme fibres being removed. As a result, significant increases in bending stresses were observed. In addition, shear stress distributions formed local peaks on shear planes located at the base of damage locations due to reduced shear plane thicknesses. Normalized shear and bending stress distributions for cross-sections with different levels of vertically oriented damage are given in Figure 22, Figure 23, and Figure 24. Damage levels were defined previously in Figure 15.

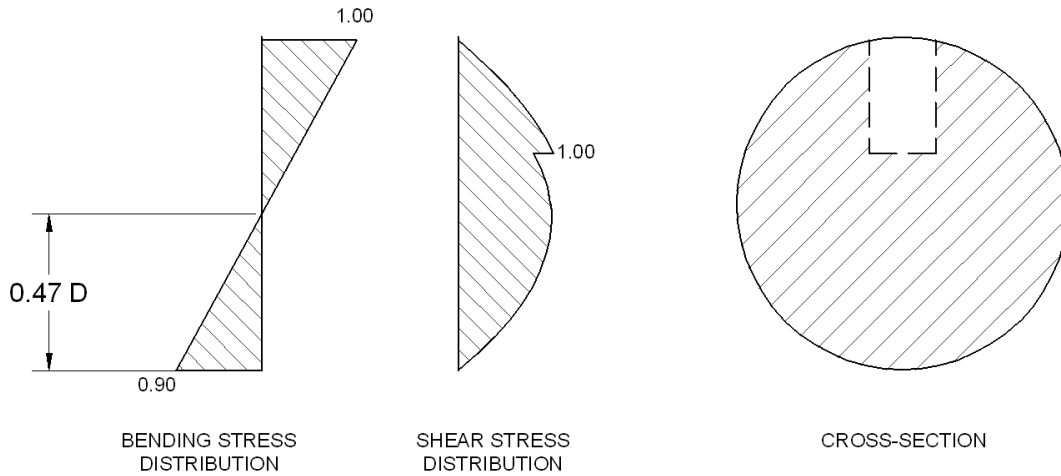


Figure 22. - Stress distributions of a cross-section with vertical exploratory damage.

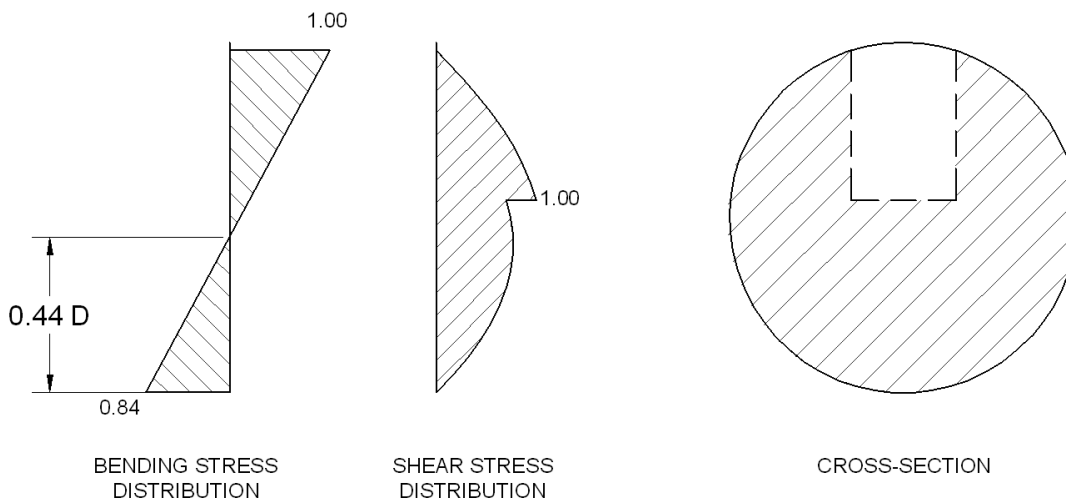


Figure 23. - Stress distributions of a cross-section with vertical feeding damage.

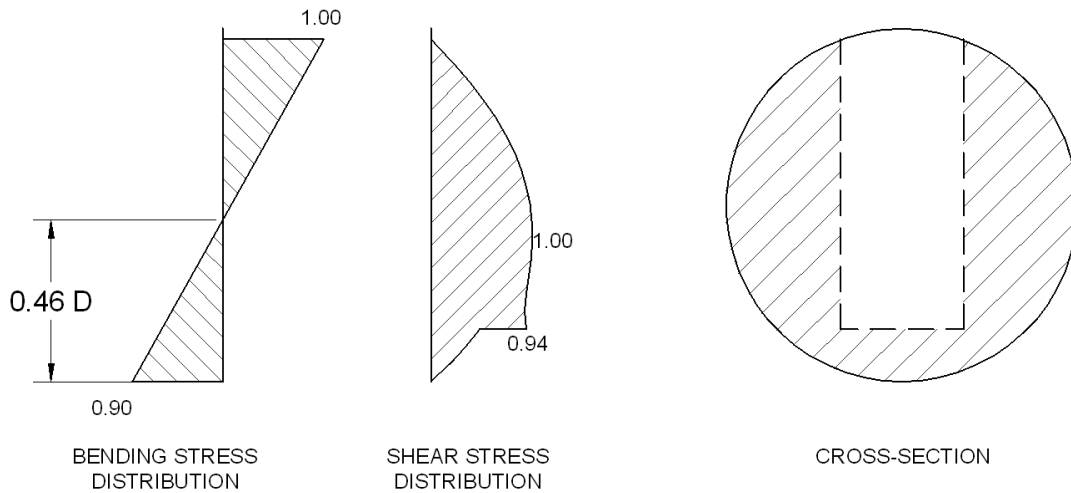


Figure 24. - Stress distributions of a cross-section with vertical nesting damage.

4.2.3 Horizontally Oriented Damage

Horizontally oriented damage was observed to cause large shear stress increases due to a significant reduction in shear plane thicknesses at hole locations. Section moduli were minimally reduced since horizontal damage locations were located close to the neutral axis. As a result, bending stress increases were observed to be minimal. Normalized shear and bending stress distributions for cross-sections with different damage levels are given in Figure 25, Figure 26, and Figure 27.

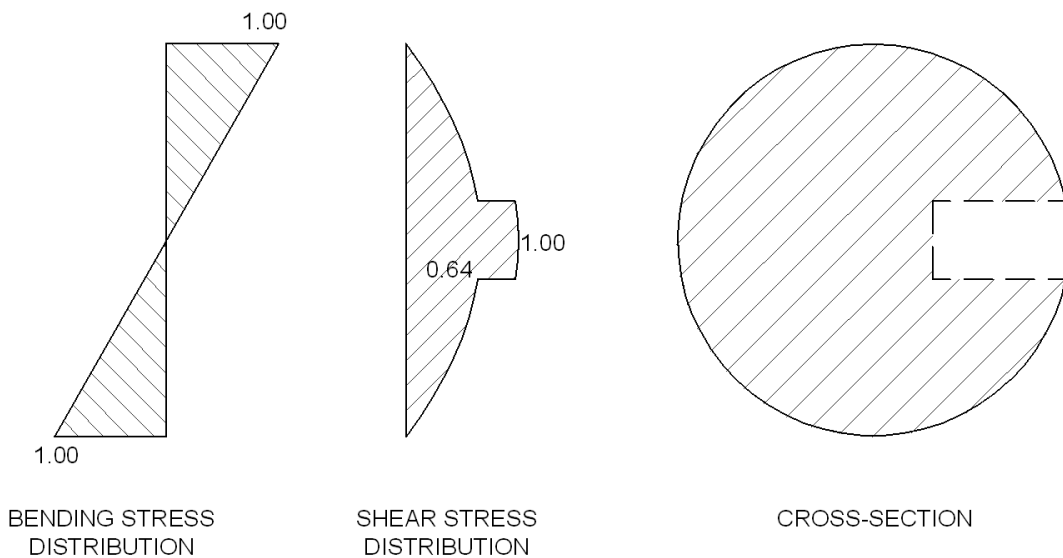


Figure 25. - Stress distributions of a cross-section with horizontal exploratory damage.

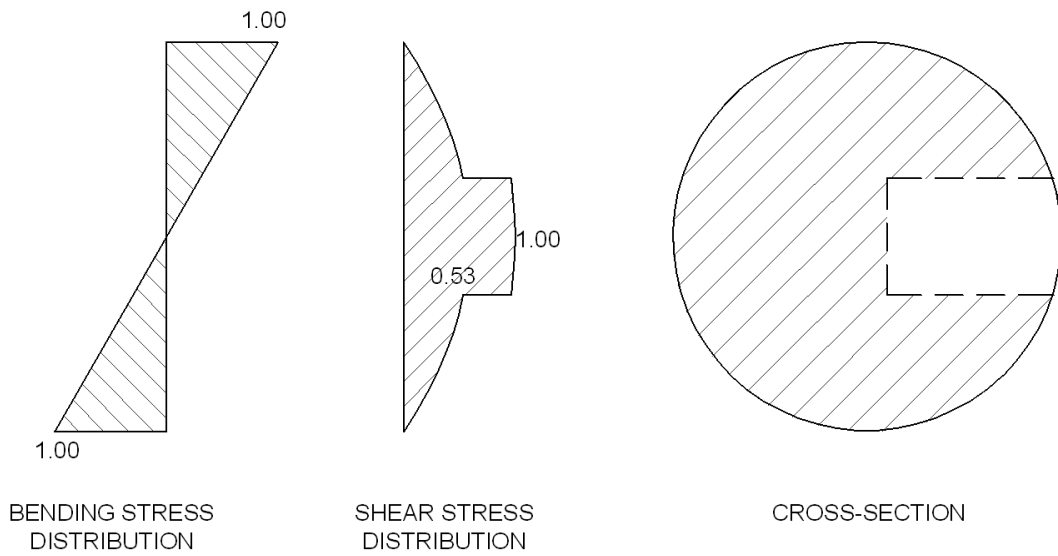


Figure 26. - Stress distributions of a cross-section with horizontal feeding damage.

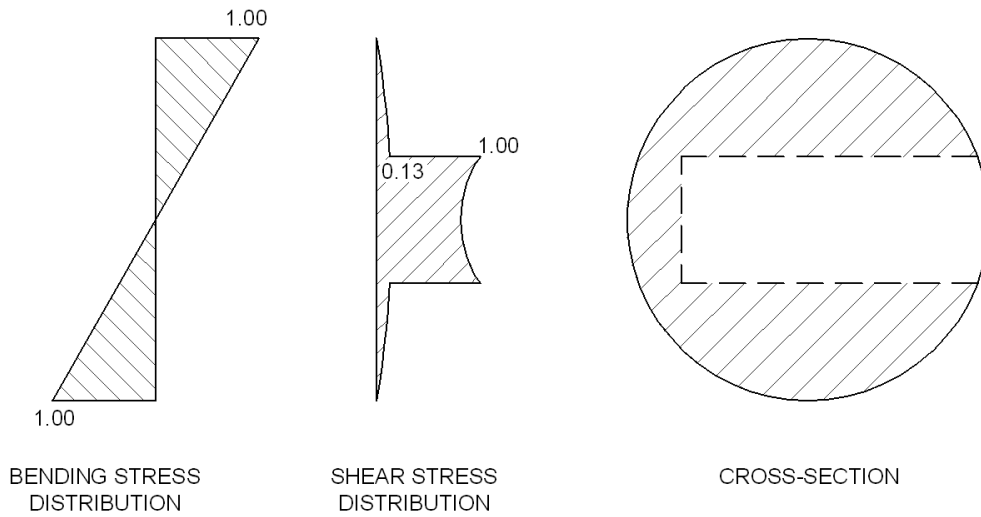


Figure 27. - Stress distributions of a cross-section with horizontal nesting damage.

Chapter 5 Utility Pole Structural Analysis Model

A utility pole structural analysis model was developed to gain a better understanding of wood utility pole behaviour under imposed loads. The model allowed the strength reducing effect of woodpecker damage to be simulated in different cross-sections along the length of a utility pole. A parametric study that incorporated different woodpecker damage levels was performed using the analysis model. This study aided in developing an experimental beam test setup that simulated load effects representative of field conditions.

5.1 CSA C22.3 No. 1 Analysis and Design Procedures

According to CSA C22.3 No.1 (2006a), supply and communication lines should be designed using either deterministic design methods or reliability-based design methods. Reliability-based design methods are recommended for supply lines greater than 70 kV in locations where meteorological data is available. Typically, low voltage distribution lines are designed using the deterministic approach (Li, Zhang and Bhuyan 2006) so this approach was adopted in the current study. The deterministic design method categorizes loads into the following four conditions: severe, heavy, medium loading A, and medium loading B, as shown in Table 4. Annex C of CSA C22.3 No. 1 (2006a) provides a map for determination of what load condition should be used in specific geographic locations as shown in Figure 28.

Table 4. - CSA C22.3 No. 1 (2006a) deterministic weather loads.

Loading Category				
Loading Conditions	Severe	Heavy	Medium	
			A	B
Radial thickness of ice (mm)	19	12.5	6.5	12.5
Horizontal wind loading (N/m ²)	400	400	400	400

5.1.1 Vertical load assumptions

According to CSA C22.3 No. 1 (2006a), the vertical load upon poles shall be the vertical force produced by their own mass plus ice-coated wire and cable attachments in the parts of adjacent spans carried by the support. The radial thickness of ice only needs to be applied to wire and cable attachments. The density of ice is to be assumed as 900 kg/m³.

5.1.2 Transverse load assumptions

According to CSA C22.3 No. 1 (2006a), the assumed transverse load on supports due to wind pressure on the wire and cable attachments shall be the load created by the wind acting horizontally on ice-covered wires and cable attachments. The span length used in calculations should be one-half the sum of adjacent span lengths. The load created by wind pressure on the surfaces of the structure without an ice covering shall also be included.

5.1.3 Load Factors

Load factors for wood pole non-linear analysis from CSA C22.3 No. 1 (2006a) are provided in Table 5. These factors are based on the wood strength having a coefficient-of-variation of over 20%.



Figure 28. - CSA C22.3 No. 1 (2006a) loading map of Canada.

Table 5. - CSA C22.3 No. 1 (2006a) wood pole load factors for non-linear analysis.

Type of Load	Construction Grade	Minimum Load Factor
Vertical	1	2.00
	2	1.50
	3	1.20
Transverse	1	1.90
	2	1.30
	3	1.10

5.1.4 Analysis, Failure, and Replacement Requirements

According to CSA C22.3 No. 1 (2006a), a non-linear analysis including a stability check is the preferred method for analysis of structures. Two failure limits are specified for wood poles in CSA C22.3 No. 1 (2006a). The first limit is when the ultimate tensile stress of the wood has been reached due to bending moment. The second limit is when collapse due to instability occurs, caused by excessive axial loads on the pole. CSA C22.3 No. 1 (2006a) also requires that a support structure be reinforced or replaced when its strength has deteriorated to 60% or less of the required capacity.

5.2 Shear Force and Bending Moment Analysis

The following equations were used for single wood pole structural analysis and are based on equations used in the Department of Agriculture Bulletin 1724E-200 (USDA 2009c). These equations were

extended so shear and bending moments could be determined along the length of the pole. Second order effects were also accounted for based on well established equations (USDA 2009c; Gaiotti and Smith 1989).

Uniformly distributed transverse load on multiple wires:

$$p_t = \sum(q(d_w + 2t_{ice})) \tag{Equation 14}$$

where d_w is diameter of wire and t_{ice} is radial thickness of ice.

Uniformly distributed vertical load on multiple wires:

$$w_t = \sum(w_w + \gamma_{ice} \frac{\pi}{4} [(d_w + 2t_{ice})^2 - d_w^2]) \tag{Equation 15}$$

where w_w is wire weight and γ_{ice} is ice unit weight. Vertical and horizontal spans were important factors in determining transverse and vertical resultant loads. Both spans are geometrical dimensions of the hydro line being analyzed, as shown in Figure 29. The vertical span, or weight span, is the horizontal distance between the lowest points on the sag curve of two adjacent spans. The horizontal span, or wind span, is the horizontal distance between the mid-span points of adjacent spans. Horizontal span is equal to half the sum of adjacent span lengths.

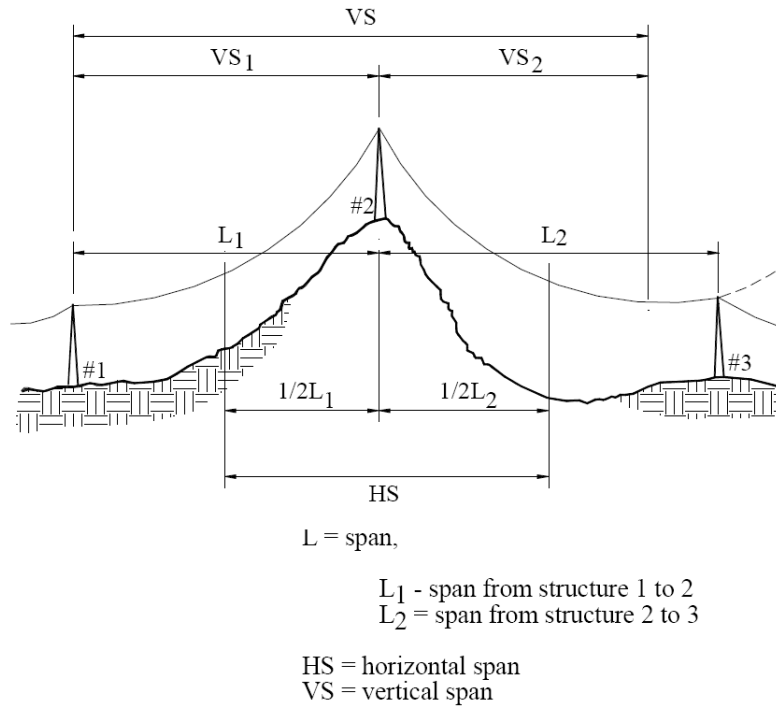


Figure 29. - Horizontal and vertical spans (USDA 2009c).

Shear and moment due to wind on face of pole:

$$V_{wp}(x) = q(d_t x + \frac{(d_g - d_t)x^2}{2h}) \tag{Equation 16}$$

$$M_{wp}(x) = q(d_t \frac{x^2}{2} + \frac{(d_g - d_t)x^3}{6h}) \quad \text{Equation 17}$$

for $0 < x < h$ where q is wind pressure, d_g and d_t are groundline and top of pole diameter, respectively, h is the height of pole above ground, and x is the distance from the top of the pole.

Shear and moment due to wire load:

$$V_{wc} = p_t HS \quad \text{Equation 18}$$

$$M_{wc} = p_t(x + h_r - h)HS$$

for $h - h_r < x < h$ where p_t is the sum of transverse wire loads and h_r is the resultant height of transverse loads. The resultant height of transverse loads can be calculated based on the location and number of wires present on a given utility pole.

Second order moment (p-delta) due to pole deflection:

$$M_{p\delta} = VSw_t \delta_{imp} \quad \text{Equation 19}$$

$$\delta_{mag} = \frac{1}{1 - VSw_t / P_{cr}} \quad \text{Equation 20}$$

$$\delta_{imp} = \frac{6.78 p_t HS (x + h_r - h)^3}{E(d_g)^3 d_r} \delta_{mag} \quad \text{Equation 21}$$

$$P_{cr} = \frac{\pi^2 E I_t}{4h^2} \left(\frac{d_g}{d_t}\right)^{2.7} \quad \text{Equation 22}$$

for $h - h_r < x < h$ where E is modulus of elasticity, d_r is pole diameter at resultant location, I_t is moment of inertia at the top of the pole, w_t is the sum of vertical wire loads, P_{cr} is critical buckling load taking into account taper of pole, and $M_{p\delta}$ is p-delta moment .

5.3 Stress Analysis

5.3.1 Geometry of Utility Pole

In order to obtain shear force, bending moment, and section properties along a utility pole's length, an analysis program was developed to section the subject pole every 100 mm along its length. Knowing the end diameters of the pole, a linear taper was assumed along the pole length. By interpolation, the pole diameter, and therefore section properties, could be determined at every 100 mm section location. From the shear and bending analysis described earlier, shear force and bending moment values were calculated at each section location.

5.3.2 Bending Stress Determination

The bending stress at each section location along the pole length was calculated using the following equation:

$$\sigma = \frac{M}{Z} \quad \text{Equation 23}$$

where M is bending moment at the section being analyzed and Z is section modulus of the section being analyzed at a specified distance from the neutral axis at which the bending stress is being calculated. Experimental or theoretical values of section modulus for undamaged and damaged sections were used in this equation.

5.3.3 Shear Stress Determination

The shear stress at any location along the pole length was calculated using the following equation:

$$\tau = \frac{vQ}{It} \quad \text{Equation 24}$$

where V is shear force at the section being analyzed, Q is moment of area dependent on the plane at which shear is being determined, I is moment of inertia of the section being analyzed, and t is thickness of the plane at which shear is being determined. Experimental and theoretical values of Q/It for undamaged and damaged sections were used in this equation.

5.4 Pre-experimental Analytical Study

The purpose of the parametric study was to determine what shear and bending conditions to simulate in the experimental beam test setup in order to best represent in-service conditions. This was achieved by determining failure locations of in-service models under different parameter combinations and recording moment-to-shear (M/V) ratios at these locations. The study incorporated the previously described woodpecker damage analytical model and utility pole structural analysis model. Several typical in-service utility poles were modeled with input including wood mechanical properties, pole geometry, environmental and dead loads, and section properties.

5.4.1 Parameters

The following parameters were considered in the parametric study:

1. Level of woodpecker damage
 - a. Undamaged, exploratory, feeding, and nesting
2. Orientation of woodpecker damage
 - a. Vertical and horizontal
3. Location of damage along pole length
 - a. Move each damage level in 100 mm increments along the entire length of pole
4. Geometry of pole
 - a. 13.72, 15.42, 16.76, and 18.29 m pole lengths
 - b. Butt and end diameters corresponding to pole length and class
5. Location of horizontal resultant as a function of height above ground (HAG)
 - a. Assume resultant acts at 0.80HAG and 0.90HAG

6. Horizontal and vertical spans
 - a. Assume equal horizontal and vertical spans
 - b. Increase span length until first failure occurs

5.4.2 Wood Mechanical Properties

In order to determine representative values of utility pole mechanical properties, several sources were researched (ANSI 2008; CSA 2008c; CSA 2005d; CSA 2009e; ASTM 2009b; 2006c; ASTM 2006d; ASTM 2005f; USDA 1999f). The ANSI O5.1 (2008) method was focused on since it allows incorporation of specific factors in determining wood pole mechanical properties. Nominal bending strength, shear strength, and modulus of elasticity were calculated, as shown in Table 6, assuming the utility poles were jack pine at a moisture content of 20%.

Table 6. - Pre-experimental study assumed wood mechanical properties.

Property	Value
Nominal Bending Strength (MPa)	45
Nominal Shear Strength (MPa)	5
Nominal Modulus of Elasticity (MPa)	7590

5.4.3 Applied Loads

Utility poles are subjected to a variety of loads including ice, wind, and wire loads (CSA 2006a; CSA 2006b). Ice and wind loads were calculated according to the deterministic design method of CSA C22.3 No. 1 (2006a) assuming heavy loading. The ice, wind, and wire loads used are given in Table 7.

Table 7. - Pre-experimental parametric study ice, wind, and wire dead loads.

Factor	Value
Radial Ice Thickness (mm)	12.5
Horizontal Wind Pressure (N/mm ²)	400
Ice Density (kg/m ³)	900
Conductor wire (kg/m/wire)	0.52
Ground wire (kg/m/wire)	0.38

5.4.4 Woodpecker Damage

The theoretical strength reducing effects of exploratory, feeding, and nesting levels of woodpecker damage at different orientations were accounted for in the pre-experimental study. The previously developed BF and SIBF analytical models were used to determine theoretical strength reduction caused by the woodpecker damage.

5.4.5 Analysis

According to CSA C22.3 No. 1 (2006a), the preferred method of analysis is non-linear. The structural model previously discussed in Section 5.2 was used in the pre-experimental study and incorporates second order effects through a p-delta analysis.

5.4.6 Failure Criteria

In the pre-experimental parametric study, bending and shear-bending interaction failure criteria were both considered through the use of BF and SBIF analytical models.

5.4.7 Bending Failure Criteria Analysis Results

The first stage of the parametric study was performed assuming failure occurred when the utility pole's bending strength was reached. Once first failure occurred, the location of failure was determined and the M/V ratio at this location was recorded. As the level of damage was increased, lower M/V ratios were observed at failure locations. This was expected since failures occurred higher in the utility pole where M/V ratios were lower, due to increased cross-section strength reductions. Varying other parameters, such as resultant height and pole length, had insignificant effects on M/V ratios observed. Detailed tables are provided in Appendix B that show M/V ratios for varying parameter values. M/V ratios at failure locations ranged from 2.19 – 16.27.

5.4.8 Shear-Bending Interaction Failure Criteria Analysis Results

The second stage of the parametric study was performed assuming failure occurred in the utility pole due to shear-bending interaction. Once failure occurred, the location of failure was determined and the M/V ratio at this location was recorded. Very similar M/V trends were observed as when bending failure criteria was implemented. In comparison to when bending failure criteria was implemented, lower M/V ratios were observed at failure locations since the shear-bending interaction failure criteria resulted in failures higher in the utility pole. Detailed tables are provided in Appendix B that show M/V ratios for varying parameter values. M/V ratios at failure locations ranged from 2.13 – 13.00. It was observed that failure loads were reduced based on SBIF analysis in comparison to BF analysis.

5.4.9 Conclusions from Parametric Study

It was concluded that the M/V ratios from the parametric study based on SBIF failure criteria were the most appropriate for designing the experimental program. This was based on the assumption that SBIF criteria better predicts utility pole failure than BF criteria. A weighted average of the M/V ratios from the shear-bending failure results was calculated to be 8.72 and was the target M/V ratio in the experimental program.

Chapter 6 Experimental Program

The experimental program was focused on determining the effect of woodpecker damage and wood decay on the strength of new and in-service utility poles. Several testing methods were considered including testing full sized wood utility poles (ASTM 2005a). It was determined that beam testing would be the most appropriate method of testing since it allowed multiple specimens to be tested from a single utility pole, making optimal use of the utility poles received. Beam testing methods were developed that simulated M/V ratios at failure locations that are representative of field conditions as determined during the parametric analysis described in Chapter 5. Load, deflection, and strain profiles at locations of woodpecker damage were acquired during beam testing. After beams were tested to failure they were dissected to confirm failure mode and moisture content samples were taken.

6.1 Types of Poles

A variety of new and in-service poles were received from HONI. The new poles received were red pine and western red cedar, and were free of decay and mechanical damage. The in-service poles received were red pine, western red cedar, and lodgepole pine and had ages of manufacture from 1979 to 2009. Older in-service poles typically had combinations of decay and woodpecker damage, while newer in-service poles had only woodpecker damage. When new and in-service poles were received they were cut into 4.25 m beam specimens. A new pole specimen from each new pole was tested as a control specimen without damage. The remainder of the new pole specimens were introduced with varying levels and orientations of simulated woodpecker damage using a drill and sawtooth bit. In-service specimens had varying levels of woodpecker damage and decay and were cut as seen appropriate for determining the effects of woodpecker damage and decay.

6.2 Specimen Analysis Considerations

Literature review indicated that bending effects are typically dominant in utility pole design (CSA 2006a; USDA 2009c). Despite this, it was determined that shear effects could be significant due to the presence of woodpecker damage. As a result, the experimental program was developed based on BF, SF, and SBIF for new pole specimens. Only BF and SF criteria was considered for analysis of in-service specimens since in-service shear strengths could not be assumed for SBIF analysis. In order to perform an analysis of experimental results based on SBIF criteria, specimen shear strength, bending strength, and damaged section properties were required. The number of new pole specimens available for testing made it impractical to experimentally determine all these factors. As a result, shear strengths were assumed based on published values (USDA 1999f) and bending strengths were obtained from the control specimens tested. Geometric section properties affecting shear stress distribution (Q/It) were calculated based on the previously developed SBIF model. Using this approach, the interaction effects due to shear could be accounted for with a combination of theoretical and experimental input. The approach of assuming shear geometric and strength properties for analysis was practical since it was anticipated that shear effects would contribute significantly less to failure than bending effects, allowing them to be approximated.

6.3 Targeted Moment-to-Shear Ratio

Based on the pre-experimental parametric analysis, it was concluded that the M/V ratios obtained based on SBIF failure criteria were the most appropriate for designing the experimental program. This was based on the assumption that SBIF criteria better predicts utility pole failure than BF criteria. The range of M/V ratios obtained from the analysis was 2.13 – 13.00. A weighted average of the M/V ratios was calculated to be 8.72 and was selected as the target M/V ratio in the experimental program.

6.4 Four-Point Loading

Four-point loading was used for specimens with woodpecker damage in tension and compression orientations (Figure 30). This setup allowed the M/V ratio to be held constant at 8.72 at the midspan cross-section where damage was introduced. The M/V ratio of 8.72 was attained by applying the actuator load point onto the spreader beam off-center a specified distance. Based on preliminary calculations, the damage introduced reduced the specimen strength enough to cause failure to occur at the midspan location.

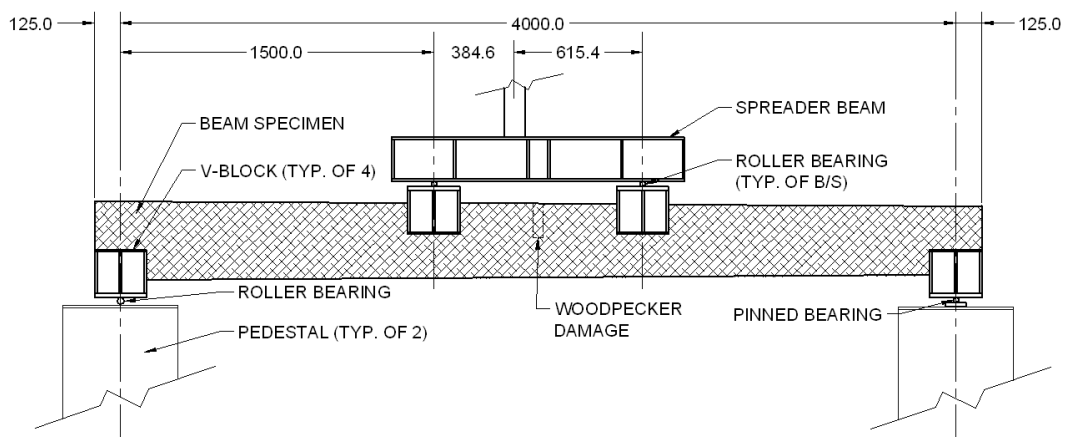


Figure 30. - Four-point loading test setup ($M/V = 8.72$).

6.5 Three-Point Loading

The remainder of specimens included control specimens and specimens with woodpecker damage in the neutral axis orientation. These specimens differed from the specimens being tested in four-point loading due to either a lower severity of damage being introduced, or no damage being introduced. As a result, if these specimens were tested under four-point loading, failure would likely occur under a load point rather than at midspan. Failure under a load point was undesirable in damaged specimens since failure would not occur where the damage was introduced. In addition, the M/V ratio at load points would be 1.50, which is lower than what an in-service utility pole is typically subjected to. Thus, it was decided that three-point loading would be the most practical test setup for control specimens and specimens with neutral axis damage as shown in Figure 31 and Figure 32, respectively. Three-point loading of specimens resulted in midspan failures at an M/V ratio of 2.00. This setup was advantageous since damage could be introduced at midspan where failure was most

likely to occur. In addition, failure at an M/V ratio of 2.00 versus 1.50 better represents in-service loading conditions.

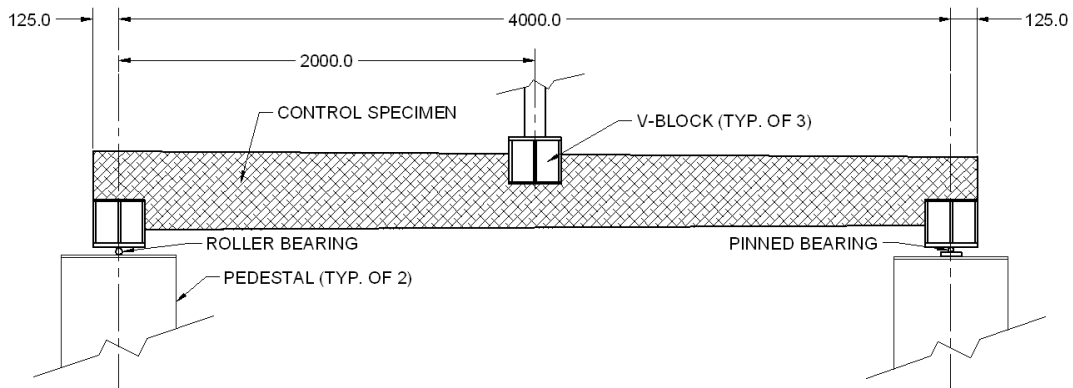


Figure 31. - Three-point loading test setup for control specimens (M/V = 2.0).

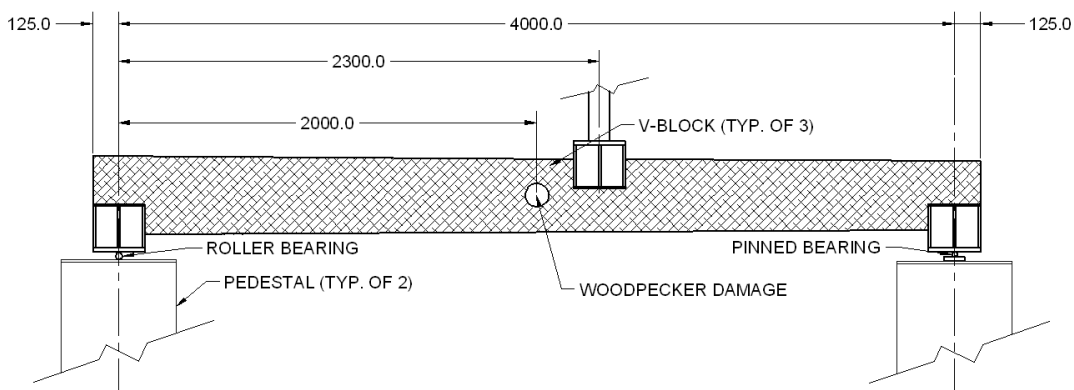


Figure 32. - Three-point loading test setup for specimens with neutral axis damage (M/V = 2.0).

6.6 Actuator Loading Rate, Force, and Displacement

Load was applied to specimens using stroke control at a rate of 7.5 mm/min. This resulted in beam failures occurring within 10-20 minutes of the start of loading. Actuator load and deflection were continuously recorded during the experiment.

6.7 Support Crushing

Prior to testing it was speculated that wood crushing might occur due to the large point loads and relatively small bearing areas. In order to measure crushing, deflection dial gauges were used at the support points of bearing. After the first specimen was tested, it was observed that wood crushing was not significant and measurement was discontinued.

6.8 Deflection

Deflections at points of load application were recorded using retractable wire string potentiometers. When testing control specimens, two string potentiometers were attached at the midspan. Specimens with neutral axis damage had single string potentiometers attached at the load point and at the location of woodpecker damage. The remaining specimens were tested in four-point loading and had single string potentiometers attached at the load points.

6.9 Strain

In order to better understand cross-sectional behaviour in flexure at the damaged locations, longitudinal strain was measured at the hole locations using displacement transducers (DCDTs). The DCDTs provided measurement of the average strain within gauge lengths varying from 50 to 100 mm. The DCDTs used had a range of ± 1.27 mm and a sensitivity of ± 0.001 mm. Strain was measured at four locations evenly spaced around the cross-section circumference as shown in Figure 33 so that the strain profile could be determined over the cross-section depth.

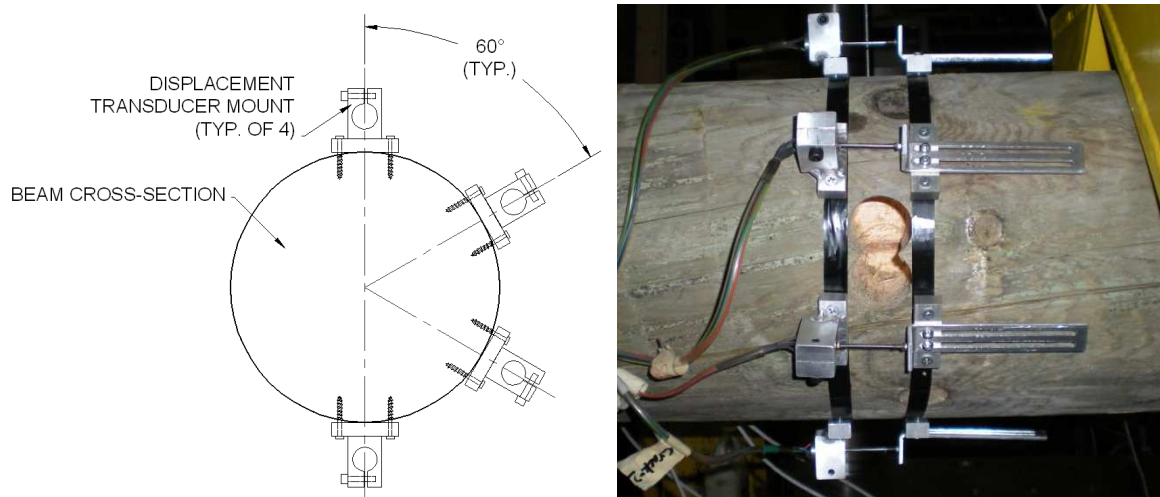


Figure 33. - New pole specimen DCDT configuration.

6.10 Dissection

After specimens were tested for strength, failure regions were dissected and photo documented for a better understanding of the failure mechanism. Failure regions were mapped into several 150 mm long divisions with the number of divisions depending on the length of the failure region. Failure regions were then sectioned at division lines with a chainsaw to inspect the specimen internal condition.

6.11 Moisture Content

The moisture content of specimens is a potentially important factor since it has an effect on the mechanical properties of wood. ASTM D 4933 (2004h) and D 4442 (2007g) provide guidelines for

testing the moisture content of wood and wood-based materials. Method B of ASTM D 4442 (2007g) was followed and required samples to be oven dried at $103 \pm 2^{\circ}\text{C}$ until the change in sample weight did not appreciably change over a four hour period. Moisture content samples for each specimen were taken near the locations of failure during dissection.

Chapter 7 New Pole Specimen Analysis, Results, and Discussion

Twenty new utility poles of varying length, class, and species were provided by HONI for experimental beam testing. The purpose of the test program was to determine the effect of woodpecker damage on utility pole cross-sectional strength. This was achieved by testing a single specimen from each utility pole as a control specimen without woodpecker damage. Control specimens were useful in obtaining reference utility pole bending strengths. The remainder of the new pole specimens were introduced with varying levels and orientations of woodpecker damage. The effect of woodpecker damage on cross-sectional strength was then determined based on reference control specimen bending strengths.

7.1 Test Specimens

The utility poles received were cut into 4.25 m segments for beam testing. The following naming system was developed for beam specimens: length of pole – pole number – segment number. For example, 45-2-1 is segment number 1 from the 2nd 45 ft long pole. In order for a utility pole of specified length to fall within a certain class it must meet minimum end circumference measurements as specified by CSA O15 (2005d). In the beam naming system, RP and B stand for Red Pine and Beam, respectively. A summary of the beam test specimens is given in Table 8.

Table 8. - Received new pole details and specimens.

Pole	Species	Class	Specimens
45-1	Red pine	3	45-1-1, 45-1-2, 45-1-3
45-2	Red pine	3	45-2-1, 45-2-2, 45-2-3
50-1	Red pine	3	50-1-1, 50-1-2, 50-1-3
50-2	Red pine	3	50-2-1, 50-2-2, 50-2-3
50-3	Red pine	3	50-3-1, 50-3-2, 50-3-3
55-1	Red pine	2	55-1-1, 55-1-2, 55-1-3
55-2	Western red cedar	2	55-2-1, 55-2-2, 55-2-3
55-3	Red pine	2	55-3-1, 55-3-2, 55-3-3
60-1	Red pine	2	60-1-1, 60-1-2, 60-1-3, 60-1-4
60-2	Red pine	2	60-2-1, 60-2-2, 60-2-3, 60-2-4
60-3	Red pine	2	60-3-2, 60-3-3, 60-3-extra
60-4	Red pine	2	60-4-1, 60-4-2, 60-4-3, 60-4-4
RP-4	Red pine	4	RP-4-1, RP-4-2
RP-5	Red pine	3	RP-5-1, RP-5-2
RP-6	Red pine	3	RP-6-1, RP-6-2, RP-6-3
RP-7	Red pine	4	RP-7-1, RP-7-2
RP-8	Red pine	3	RP-8-1, RP-8-2, RP-8-3
RP-9	Red pine	3	RP-9-1, RP-9-2, RP-9-3
B-1	Red pine	2	B-1-2, B-1-3
B-2	Red pine	2	B-1-2, B-1-3

7.1.1 Control Specimens

In order to determine a representative value of bending strength for each utility pole, one segment of each new pole was assigned as a control specimen to be tested without woodpecker damage. Due to utility pole taper, the cross-section along the length of a pole varies. Based on background literature review of CSA 086 (2009e) and ASTM D 245 (2006d), it was evident that change in cross-section depth and width affects bending strength. This phenomenon is known as size effect, and the trend is that larger cross-sections have reduced bending strength in comparison to smaller cross-sections. It was determined that the change in cross-section size within a single utility pole was not large enough to cause significant bending strength variation due to size effect. Despite this, control specimens were taken from middle segments of each pole to obtain an average value of bending strength from each pole.

7.1.2 Specimens Induced with Woodpecker Damage

Based on the pre-experimental parametric analysis it was determined that the main experimental factors in damaged beams were level and orientation of woodpecker damage. The number of test specimens available allowed for a factorial design to be undertaken with a minimum of two repetitions of each combination as shown in Table 9. The number of control specimens (24) is greater than the number of new pole specimens (20) since four extra control specimens were obtained from the new poles. The different combinations of factors were assigned randomly to the available test segments to prevent bias from entering the test specimens. Woodpecker damage was introduced into new pole specimens in the lab using a drill and sawtooth bits of varying diameter.

Table 9. - New pole specimen experimental matrix.

Number of Tests			
Level	Orientation		
	Tension	Compression	Neutral Axis
Exploratory	3	3	3
Feeding	5	2	4
Nesting	6	4	4
Total Specimens	= 34 + 24 controls = 58 specimens		

7.2 General Behaviour

Typical load-deflection curves for new pole specimens are shown in Figure 34 and Figure 35 for bending and shear failure, respectively. Below the proportional limit, the load-deflection behaviour was linear. Beyond the proportional limit, the specimens behaved non-linearly with deflection increasing more rapidly. Specimens reached their ultimate load with only limited non-linear response. After specimens reached their ultimate load, further deformation resulted in decreased load capacity. The vast majority of control and woodpecker damaged specimens failed in bending and had a relatively gradual stepped decrease in load capacity as shown in Figure 34. Specimens with neutral axis nesting damage failed in shear and underwent a more sudden significant decrease in load capacity as shown in Figure 35.

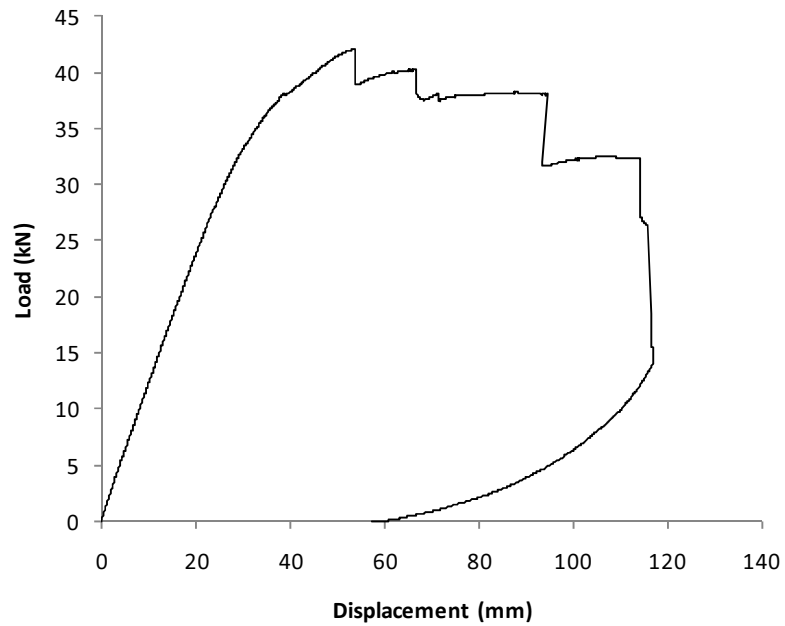


Figure 34. - Typical load-deflection curve for new pole specimen failing in bending (60-2-1).

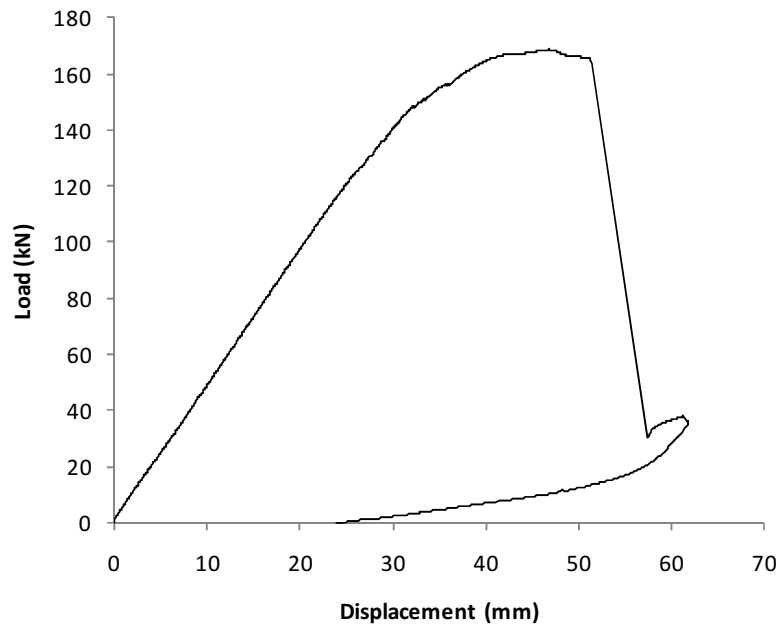


Figure 35. - Typical load-deflection curve for new pole specimen failing in shear (55-2-3).

7.3 Influence of Knots, Checks, and Local Wood Properties

The influence of knots and checks was closely monitored during beam testing and dissection of failure locations. Western red cedar specimens typically had very clear wood and specimen strength was minimally influenced by knots and checks. In contrast to this, red pine specimens often had

checking and large amounts of knots. Checks, as shown in Figure 36, were observed to have minimal impact on wood strength and did not influence failure locations. Red pine specimens typically had rings of knots located at close intervals along specimen lengths. Many failures occurred at cross-sections with knot rings, indicating they cause strength reduction in red pine specimens. Large knots, such as the one shown in Figure 37, were found to be more significant than knot rings, and caused severely reduced bending strength. It was observed that some specimens within red pine poles had unusually clear wood at failure locations. Typically the larger the diameter of the specimen the clearer the wood became and higher bending strengths were observed.

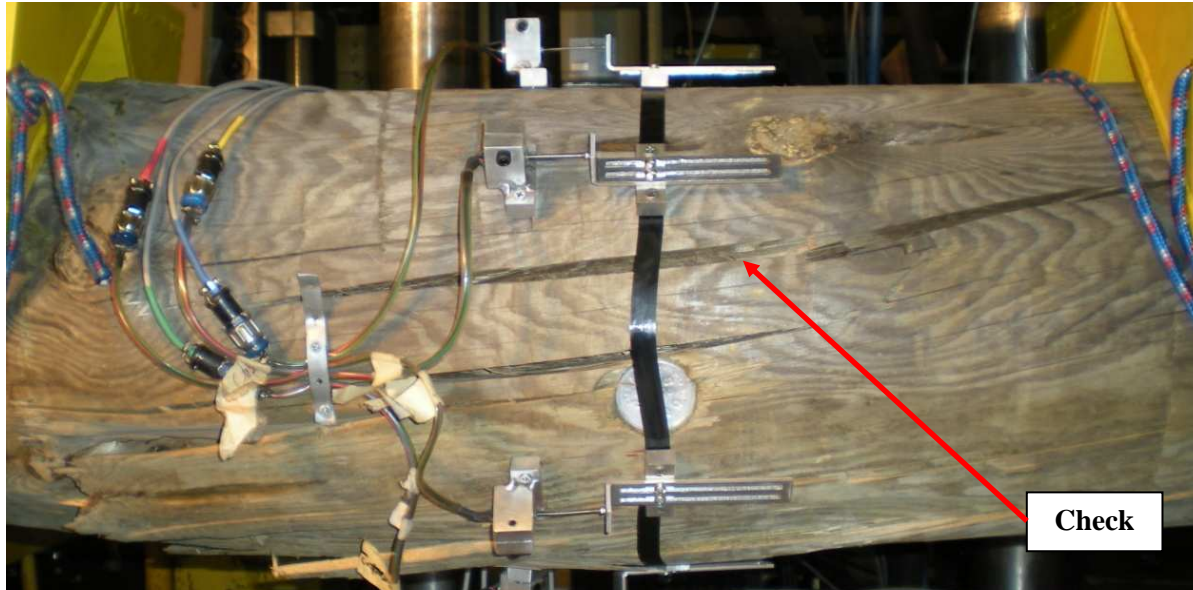


Figure 36. - New pole specimen with checking at midspan (45-1-3).



Figure 37. - New pole specimen with a large knot at failure location (45-1-2).

7.4 Control Specimens

Control specimens were tested in three-point bending in order to obtain reference bending strengths for analysis of woodpecker damaged specimens. All control specimens failed in bending as shown in Figure 38. Several specimens had minor compression fibre crushing and ultimately all specimens failed due to tension fibre rupture. Control beam bending strengths were calculated using both the BF and SBIF analytical models. Shear strengths were assumed based on values from published literature for specific species and moisture content (USDA 1999f). Geometric section properties were determined using mechanics of materials principles (Mikhelson 2004).

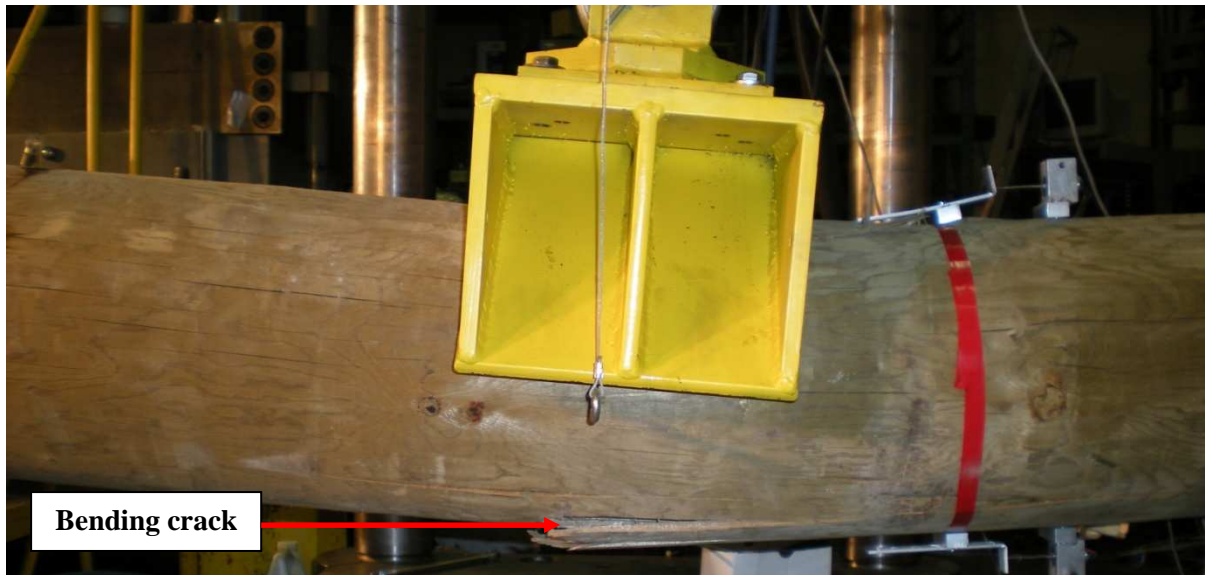


Figure 38. - Typical new pole control specimen bending failure (60-2-2).

7.4.1 Bending Failure Analysis

Bending failure analysis for the control specimens was performed based on the assumption that specimen section moduli at failure locations were accurately represented by theoretically calculated section moduli using the following equation:

$$Z = \frac{\pi D^3}{32} \quad \text{Equation 25}$$

where D is cross-section diameter at failure location. Based on the ultimate failure load recorded during testing, the ultimate moment at the midspan failure location was determined using the following equation:

$$M = \frac{PL}{4} \quad \text{Equation 26}$$

where P is the ultimate failure load and L is the beam span of 4 m.

The bending strengths of the control specimens were computed directly using the following equation:

$$f_b = \frac{M}{Z} \quad \text{Equation 27}$$

7.4.2 Shear-Bending Interaction Failure Analysis

Shear-bending interaction failure analysis for the control specimens was performed based on geometric and strength assumptions. The first assumption was that specimen shear strengths were accurately represented by values from published values for the specific species and moisture content (USDA 1999f). The second assumption was that the moment of inertia and moment of area values were accurately represented by the following theoretical equations, respectively:

$$I = \frac{\pi D^4}{64} \quad \text{Equation 28}$$

$$Q = Ax \quad \text{Equation 29}$$

where A is the area of cross-section enclosed by the failure plane and extreme fibres and x is the distance from the neutral axis to centroid of area A. Based on the ultimate failure loads recorded during testing, the ultimate moment and shear values at the midspan failure location were determined using the previously defined moment equation and the following shear equation:

$$V = \frac{P}{2} \quad \text{Equation 30}$$

where P is the ultimate failure load. The bending and shear stresses at a specified plane of a cross-section at the failure locations were calculated using the following equations:

$$\sigma = \frac{My}{I} \quad \text{Equation 31}$$

$$\tau = \frac{VQ}{It} \quad \text{Equation 32}$$

where y is the distance from neutral axis to the plane being analyzed and t is the thickness of the plane being analyzed. The control specimen bending strengths, accounting for the influence of shear, were computed using the iterative process provided in Figure 39 with the following shear-bending interaction equation (Yoshihara and Kawasaki 2006):

$$1 = \left(\frac{\sigma}{f_b}\right)^{4.36} + \left(\frac{\tau}{f_v}\right)^{0.21} \quad \text{Equation 33}$$

where f_v is shear strength from published data (USDA 1999f).

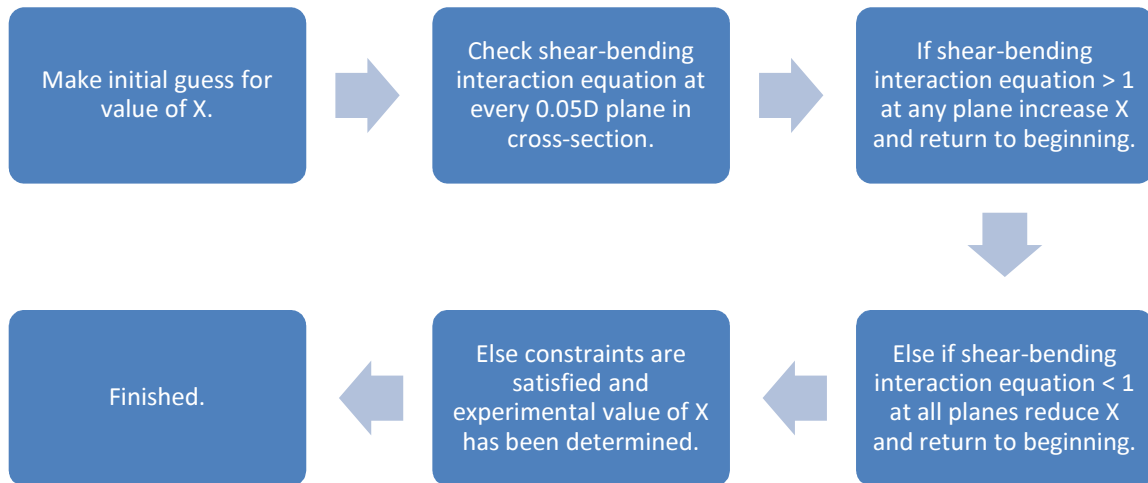


Figure 39. - SBIF equation iterative solver for new pole control specimens.

7.4.3 Experimental Results

The control specimens were analyzed as explained using the previously developed BF and SBIF analytical models. A summary of the test data is provided in Appendix C, which includes ultimate bending moment and shear force values at failure locations. Analytical models were assumed to be valid for control specimen analysis since the unknown effects of woodpecker damage were not a factor. Based on the measured ultimate failure loads, the bending strengths of the control specimens were determined and are summarized in Table 10 for both the BF and SBIF models. For comparison purposes, average and coefficient-of-variation (COV) values of bending strength from experimental data and published data have been provided in Table 11 and Table 12, respectively (USDA 1999f). These values were determined using 23 red pine control specimens and 1 western red cedar control specimen. The average and COV values of experimental bending strength agree well with the published values, with slightly better agreement being achieved when the BF model was used.

Table 10. - New pole control specimen bending strengths.

Pole	f_b (MPa)	
	BF	SBIF
45-1	29.06	30.45
45-2	38.97	41.34
50-1	40.77	43.17
50-2	27.75	28.92
50-3	34.29	36.17
55-1	34.83	36.79
55-2 (cedar)	45.56	48.53
55-3	34.13	36.13
60-1	35.58	37.61
60-2	33.23	34.91
60-3	35.02	37.19
60-4	35.99	37.89
RP-4	31.40	33.13
RP-5	47.12	50.77
RP-6	54.96	59.27
RP-7	51.97	56.07
RP-8	32.45	34.08
RP-9	35.17	37.17
B-1	34.87	37.01
B-2	28.58	29.88

Table 11. - New pole control specimen average bending strengths and COV's.

Species	Red pine		Western red cedar	
Failure Criteria	$f_{b\text{ avg}}$ (MPa)	COV (%)	$f_{b\text{ avg}}$ (MPa)	COV (%)
BF	36.64	20.20	45.56	-
SBIF	38.84	21.29	48.53	-

Table 12. - Published bending and shear strengths and COV's (USDA 1999f).

Species	$f_{b\text{ avg}}$ (MPa)	COV (%)	$f_{v\text{ avg}}$ (MPa)	COV (%)
Red pine	30.60	16.00	4.41	14.06
Western red cedar	43.11	16.01	5.14	13.94

7.5 New Pole Specimens with Woodpecker Damage

The failure modes exhibited by the tested specimens varied depending primarily on the woodpecker damage orientation. The most common form of failure observed was tension fibre rupture (Figure 40). This failure mode occurred in control specimens and specimens with tension and neutral axis oriented woodpecker damage. The second most common failure mode was compression fibre crushing (Figure 41) which occurred in specimens with compression oriented woodpecker damage. Compression fibre crushing was initiated by local buckling of wood fibres at the hole locations, and was consistently followed by tension fibre rupture. Shear failure was rare, only being observed in specimens with nesting level damage oriented in the neutral axis (Figure 42). This failure mode was

sudden and resulted in cross-section separation along the longitudinal axis of the beam at the failure plane. The moment of inertia of the specimens with woodpecker damage was calculated using the BF, SF, and SBIF analytical models. Shear strengths were assumed to follow values from published literature (USDA 1999f) while geometric section properties were determined using mechanics of materials (Mikhelson 2004). It was assumed that the damaged specimen bending strengths were equivalent to the control specimen bending strengths taken from the corresponding poles.

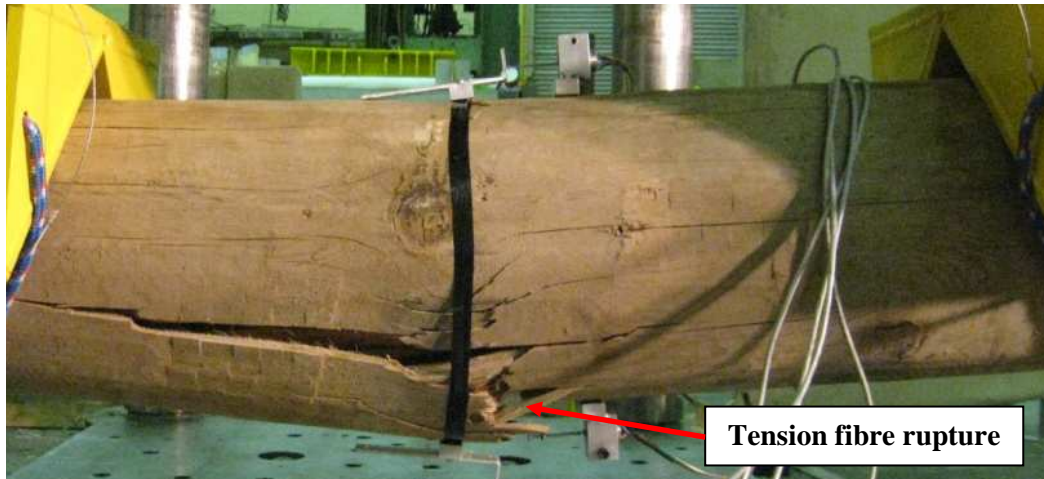


Figure 40. - Tension fibre rupture of new pole specimen with tension damage (60-2-1).

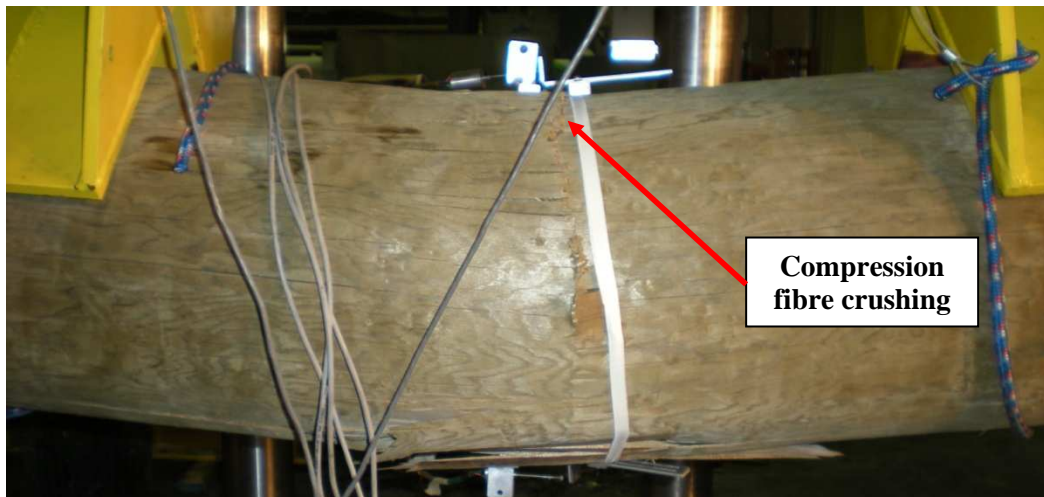


Figure 41. - Compression fibre crushing of new pole specimen with compression damage (60-2-4).

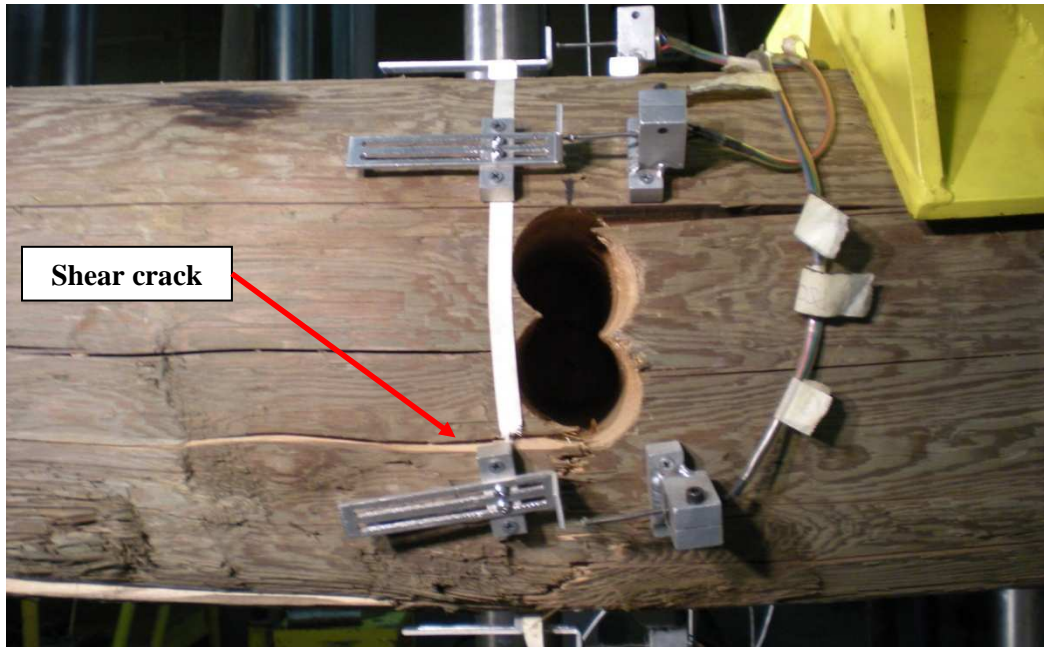


Figure 42. - Shear failure of new pole specimen with neutral axis nesting damage (55-2-3).

7.5.1 Bending Failure Analysis

Bending failure analysis for the damaged specimens was performed assuming that a damaged specimen's bending strength was equivalent to the control specimen bending strength taken from corresponding pole. Based on the ultimate failure load recorded during testing, the ultimate moment at the midspan failure location for four-point loading ($M/V = 8.72$) was determined using the following equation:

$$M = \frac{3PL}{16} \quad \text{Equation 34}$$

where P is the ultimate failure load and L is the beam span of 4 m. Ultimate moments at the midspan failure locations of neutral axis damaged specimens in three-point bending were determined using the following equation:

$$M = \frac{17PL}{80} \quad \text{Equation 35}$$

Damaged specimens section moduli were then computed directly using the following equation:

$$Z_e = \frac{M}{f_b} \quad \text{Equation 36}$$

where M is the ultimate moment at failure and f_b is the bending strength determined from the control specimen test. The ratio of experimental-to-theoretical moment of inertia (I_e/I_t) for specimens were then determined by calculating the values of Z_t based on the BF analytical model for section modulus

developed earlier. Based on the assumption that the neutral axis was located in the same location experimentally as it is theoretically, the following equation was used to obtain I_e/I_t :

$$\frac{I_e}{I_t} = \frac{Z_e}{Z_t} \quad \text{Equation 37}$$

7.5.2 Shear-Bending Interaction Failure Analysis

Shear-bending interaction failure analysis was performed based on several geometric and strength assumptions. The first assumption was that the shear strengths of specimens were accurately represented by published values for specific species and moisture content (USDA 1999f). The second assumption was that a damaged specimen's bending strength is equivalent to the control specimen bending strength taken from corresponding pole. The final assumption made was that the moment of area values were accurately represented by the following theoretical equation:

$$Q = Ax \quad \text{Equation 38}$$

where A is area of cross-section enclosed by failure plane and closest extreme fibres and x is the distance from neutral axis to centroid of area A. Based on the ultimate failure loads recorded during testing, the ultimate moment and shear values at the midspan failure locations for four-point bending were determined using the previously defined moment equation and the following shear equation:

$$V = \frac{43P}{500} \quad \text{Equation 39}$$

Ultimate moment and shear values at the midspan failure locations of neutral axis specimens in three-point bending were determined using the previously defined moment equation and the following shear equation:

$$V = \frac{17P}{40} \quad \text{Equation 40}$$

It can be verified, using the following equations, that the only unknown that was required for determination of bending stresses and shear stresses at a specified plane in the cross-section was moment of inertia.

$$\sigma = \frac{My}{I} \quad \text{Equation 41}$$

$$\tau = \frac{VQ}{It} \quad \text{Equation 42}$$

where y is the distance from neutral axis to the plane being analyzed and t is the thickness of the plane being analyzed. The experimental moment of inertia was then computed using the iterative process shown in Figure 43 with the following shear-bending interaction equation (Yoshihara and Kawasaki 2006):

$$1 = \left(\frac{\sigma}{f_b}\right)^{4.36} + \left(\frac{\tau}{f_v}\right)^{0.21} \quad \text{Equation 43}$$

where f_b is bending strength from control specimens and f_v is shear strength from published data (USDA 1999f).

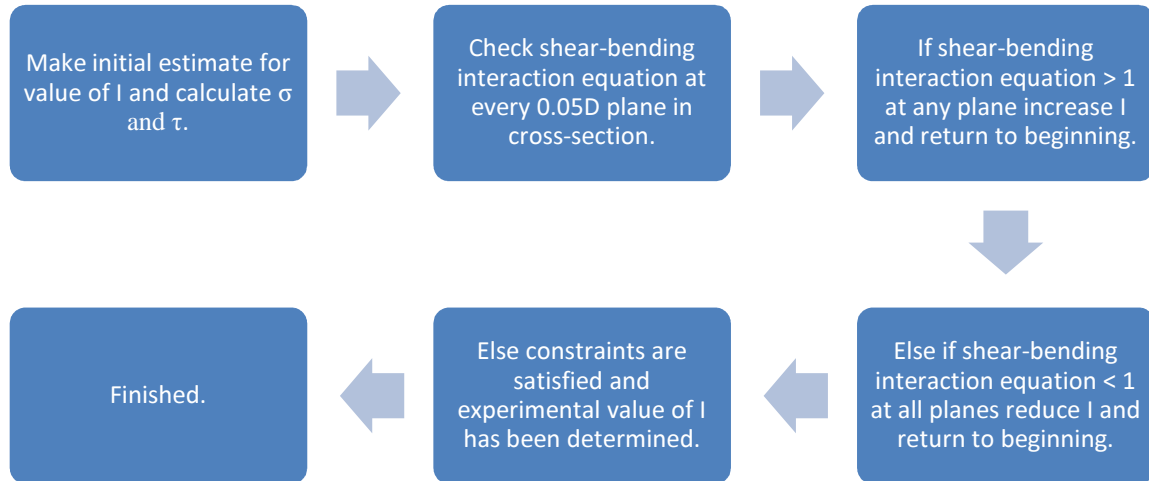


Figure 43. - SBIF equation iterative solver for new pole damaged specimens.

The I_e/I_t ratio for a specimen was then determined by calculating I_t based on geometry for the corresponding damage level and orientation.

7.5.3 Shear Failure Analysis

The shear failure analysis was performed based on the same assumptions as for the shear-bending interaction failure criteria. Specimen shear strengths were assumed to be accurately represented by published values for the specific species and moisture content (USDA 1999f). The following equation was used in calculation of experimental moment of inertia:

$$I_e = \frac{vQ}{f_v t} \quad \text{Equation 44}$$

The I_e/I_t ratio for a specimen was then determined by calculating I_t based on geometry for the corresponding damage level and orientation.

7.5.4 Experimental Strength Reduction

It was assumed that the bending strength of a control specimen was representative of the bending strength of the utility pole it was obtained from. As a result, the bending and shear strengths of specimens with woodpecker damage were known prior to analysis. This enabled the strength reduction (SR) caused by the presence of woodpecker damage to be determined from the experimental failure loads using the following equation.

$$SR = \frac{P_t - P_{max}}{P_t} \cdot 100\% \quad \text{Equation 45}$$

where P_{max} is the experimental failure load and P_t is the theoretical failure load assuming an undamaged cross-section. Strength reductions with coefficient-of-variation (COV) are given in Table 13 for different levels and orientations of woodpecker damage.

Table 13. - New pole specimen strength reductions caused by woodpecker damage.

Damage Type	SR (%)	COV (%)	Failure Mode
Neutral Axis Exploratory	2	5.60	Bending
Neutral Axis Feeding	19	9.84	Bending
Neutral Axis Nesting	24	6.50	Shear
Tension Exploratory	28	8.42	Bending
Tension Feeding	25	17.94	Bending
Tension Nesting	47	7.06	Bending
Compression Exploratory	8	8.67	Bending
Compression Feeding	31	2.77	Bending
Compression Nesting	42	19.23	Bending

As expected, the values of strength reduction indicate that as the level of woodpecker damage becomes more severe, the loss in cross-section strength increases. In addition, damage oriented in the neutral axis caused smaller reductions in strength in comparison to tension or compression orientations. This was expected since neutral axis damage removes wood fibres at the neutral axis, which causes less reduction in section modulus compared to removing extreme tension or compression fibres. Nesting level damage oriented in tension and compression locations caused severe strength reductions of over 40%. As a result, woodpecker damage was observed to cause significant strength reductions that would require replacement according to CSA C22.3 No. 1 Cl. 8.3.1.3 (2006a) since the in-service strength was reduced by more than 40%.

7.5.5 Comparison of Analytical Models with Experimental Results

Direct comparison and averaging of results in terms of failure load or moment was not possible since the diameter of the poles varied from specimen to specimen. Thus, it was decided to compare experimental results with the analytical model predictions in terms of member section properties (moment of inertia, I) calculated using the measured failure loads and material properties through back-calculation of the analytical models. As described previously, the wood bending strength was established by testing the control specimens, and the shear strength was assumed based on published values (USDA 1999f). Results were expressed as the ratio of experimental to theoretical moment of inertia (I_e/I_t), and are listed in Table 14, Table 15, and Table 16. Note that the theoretical moments of inertia account for the section reduction due to the presence of the woodpecker damage. Thus, differences between the values calculated using experimental data (failure load and material strength) and the theoretical values must result from assumptions in the analytical models and other factors as discussed below.

Table 14. - New pole specimen I_c/I_t values for bending failure criteria.

Damage Type	I_c/I_t	COV (%)
Neutral Axis Exploratory	0.98	5.60
Neutral Axis Feeding	0.83	9.84
Neutral Axis Nesting	0.81	6.50
Tension Exploratory	0.91	8.42
Tension Feeding	1.12	17.94
Tension Nesting	0.90	17.06
Compression Exploratory	1.17	8.67
Compression Feeding	1.02	2.77
Compression Nesting	0.98	19.23
All Tension and Compression	1.01	16.99

Table 15. - New pole specimen I_c/I_t values for shear-bending interaction failure criteria.

Damage Type	I_c/I_t	COV (%)
Neutral Axis Exploratory	0.98	6.21
Neutral Axis Feeding	0.83	10.40
Neutral Axis Nesting	1.16	31.40
Tension Exploratory	0.88	9.50
Tension Feeding	1.13	18.35
Tension Nesting	0.94	17.57
Compression Exploratory	1.14	8.90
Compression Feeding	1.04	2.05
Compression Nesting	1.03	19.58
All Tension and Compression	1.02	17.01

Table 16. - New pole specimen I_c/I_t values for shear failure criteria.

Damage Type	I_c/I_t	COV (%)
Neutral Axis Nesting	1.01	26.67

Results indicated that the I_c values for all levels of tension and compression damage were predicted well using the BF and SBIF models. In addition, damage oriented in the neutral axis at the exploratory and feeding levels were also well predicted by these models. Overall, experimental behaviour was modeled slightly better by the BF model than by the SBIF model. This is likely due to assumed values of shear strength used in the SBIF model that do not exactly represent true values. In addition, the exponents of the SBIF model were not specifically calibrated for use with circular cross-sections. Another advantage of the BF model was its ease of use in comparison to the SBIF model which required considerably more involved calculations. Due to the small number of specimens tested at each woodpecker damage level and orientation, trends in data in Table 14 and Table 15 cannot be interpreted.

During experimental lab testing, it was observed that shear failure occurred when nesting level damage was oriented in the neutral axis of specimens. Analysis results using the SF model showed good correlation with experimental results for this type of damage, indicating that shear effects were dominant in these specimens. As a result, the SF model should be used for analysis when nesting level damage oriented in the neutral axis is present.

A major assumption in calculating I_e was that the control specimen bending strength from a specific utility pole has the same bending strength as other specimens from the same pole. This is a practical assumption for research purposes, although it is not strictly correct. Due to the highly variable nature of wood from checks, knots, and local cellular structure, bending strength within a wood pole has some unknown variation. Furthermore, the specimen shear strength values used in analysis also introduced unknown variation since they were assumed based on published data (USDA 1999f). These assumptions, with unknown errors, contributed to the differences between the theoretical predictions and experimental results.

A one-way analysis of variance was conducted on the experimental data gathered from woodpecker damaged specimens (Jones 2010). According to this analysis, mean values of I_e/I_t for different levels of woodpecker damage in tension and compression specimens are the same at the 5% confidence interval. This indicates that the analytical model predictions were equally valid for different levels of woodpecker damage in tension and compression specimens. As a result, this data was grouped and analyzed together as shown in the last row of Table 14 and Table 15.

Comparison of experimental and analytical results indicated that bending effects were dominant in specimens with woodpecker damage. The exception to this was for nesting level damage oriented in the neutral axis, where shear effects dominated due to the significant reduction in shear plane thickness and resulting increased shear stresses.

7.6 Experimental Strain Data

Strain profiles at cross-sections of interest were acquired using displacement transducers. The measured strain profiles were found to be informative of cross-sectional behaviour before roughly two-thirds of the ultimate load of the specimen was reached. Beyond this level of load, and up to the ultimate load, compression fibre crushing and tension fibre rupture caused DCDT apparatus to disconnect from the specimens. As a result, strain profiles analyzed in this section were obtained when specimens were loaded to one-third of their ultimate load.

7.6.1 Control Cross-sections

The control specimens exhibited a linear strain profile as shown in Figure 44. The predicted strain profile is also included for comparison. Minor differences were observed between the theoretical and experimental strain magnitudes, likely due the difference between the assumed and actual modulus of elasticity at the cross-section location. In addition, the slight non-linearity of the theoretical strain profile can be attributed to an imperfect circular cross-section and the non-homogenous nature of wood due to knots and local wood properties.

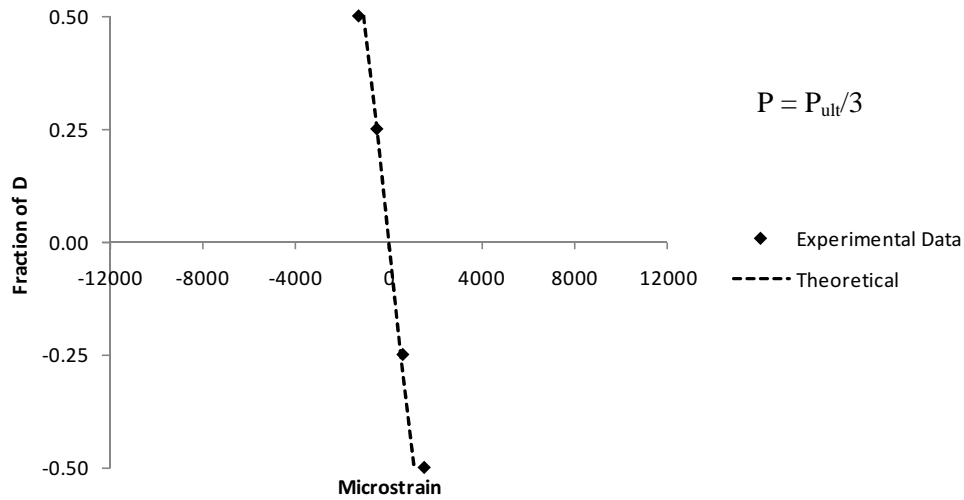


Figure 44. - New pole control specimen strain profile (45-1-2).

7.6.2 Cross-sections with Tension and Compression Damage

Specimens with woodpecker damage oriented in the tension and compression positions exhibited similar, but inverted, strain profiles (Figure 45 to Figure 50). Strain profiles were linear over the majority of the cross-section and rapidly increased near the surface where woodpecker damage is present. Theoretical analysis predicts a linear strain profile for specimens with tension and compression oriented damage (Figure 45 to Figure 50). The experimental profiles did not match theoretical strain profiles very well at the surface where woodpecker damage was present. Experimental strain magnitudes for tension and compression damage at surface locations ranged from 2 to 7 and 4 to 9 times higher, respectively than those predicted theoretically. The low ends of these ranges corresponded to low level damage while the upper end represents high level damage. Increased strain magnitudes at damage locations are attributed to stress concentrations that arise due to the discontinuity between damaged and undamaged cross-sections. At a localized area in the cross-section where damage is introduced, the presence of the hole caused an abrupt redistribution of the bending stress field, resulting in a local increase in stress around the hole or damage location. This increased stress was reflected in the increased measured strains at the damage locations.

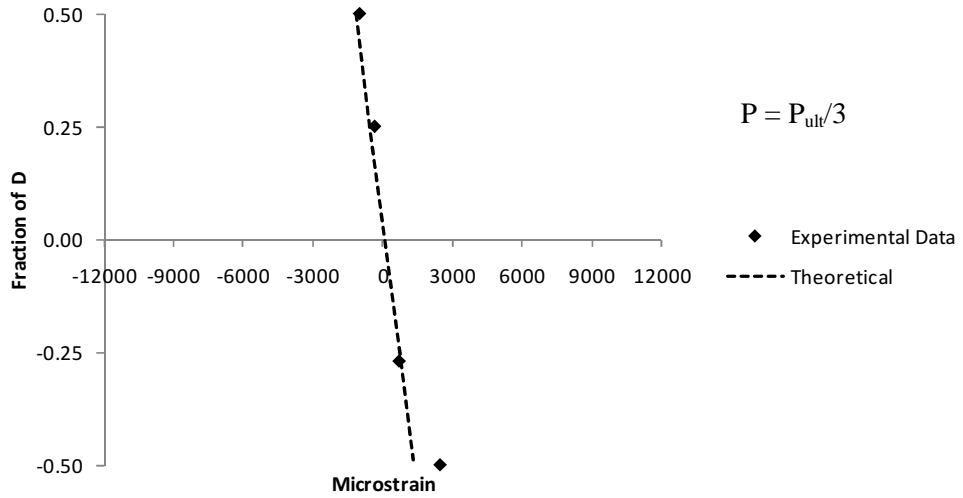


Figure 45. - Strain profile of new pole specimen with tension exploratory damage (45-1-3).

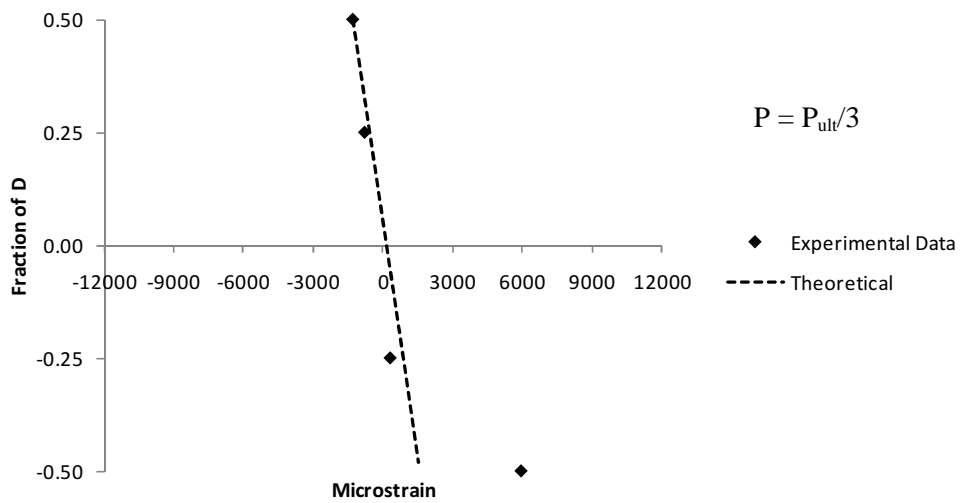


Figure 46. - Strain profile of new pole specimen with tension feeding damage (60-2-1).

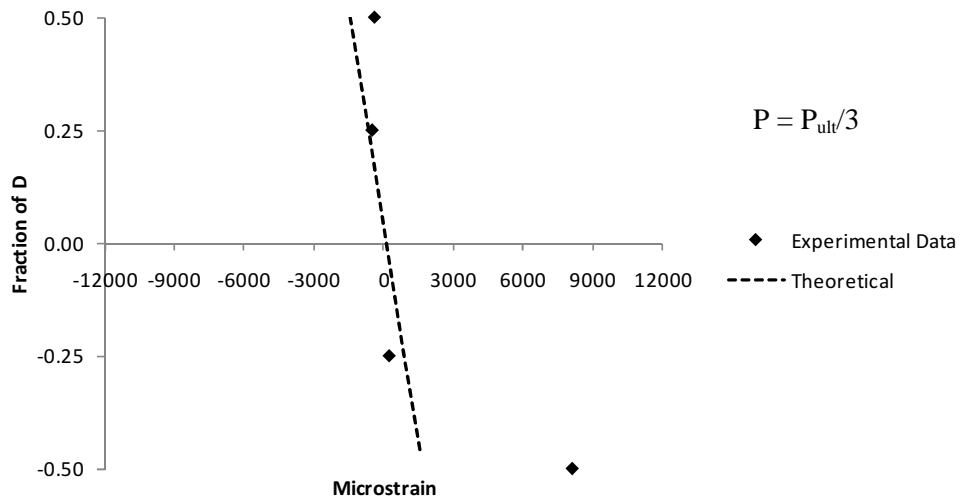


Figure 47. - Strain profile of new pole specimen with tension nesting damage (55-1-1).

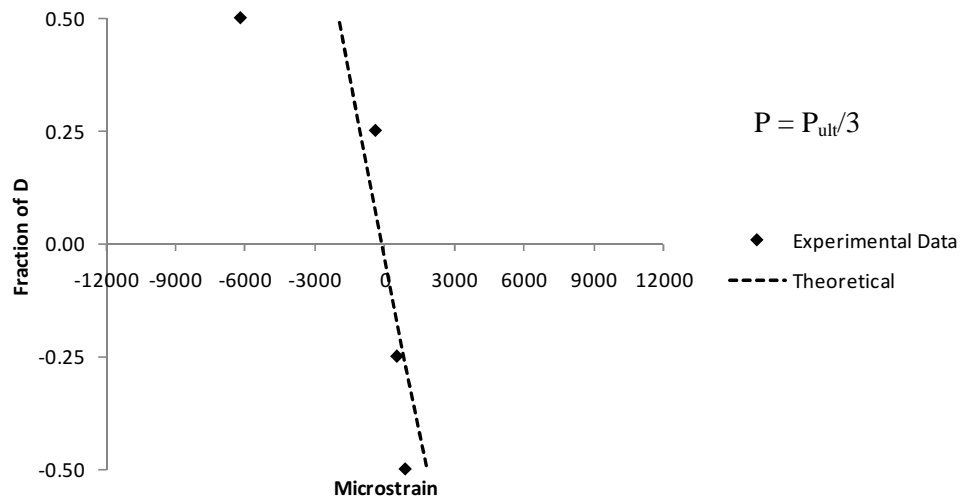


Figure 48. - Strain profile of new pole specimen with compression exploratory damage (60-1-4).

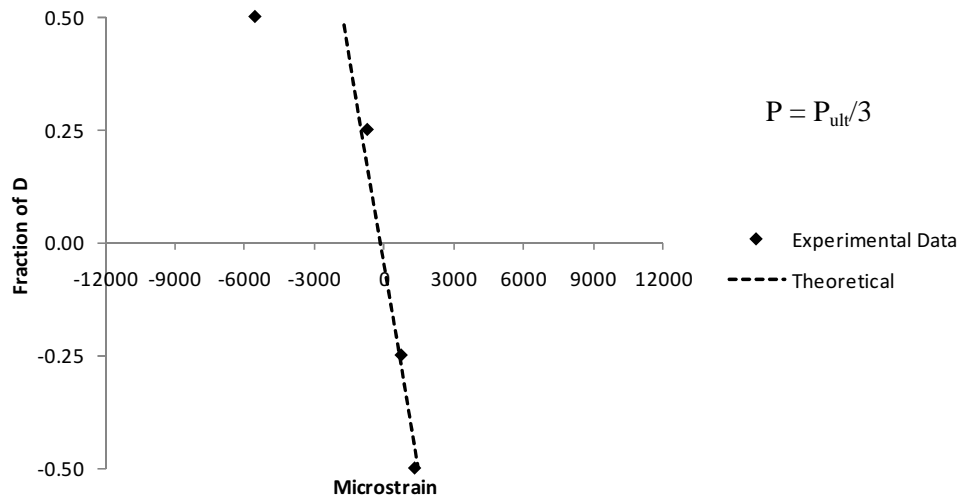


Figure 49. - Strain profile of new pole specimen with compression feeding damage (60-1-1).

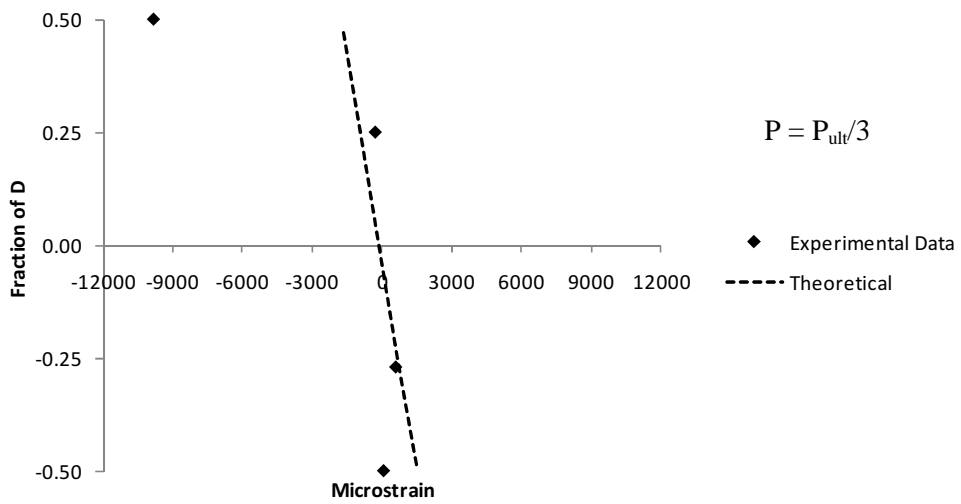


Figure 50. - Strain profile of new pole specimen with compression nesting damage (50-3-3).

7.6.3 Cross-sections with Neutral Axis Damage

Specimens with neutral axis damage behaved in a similar manner to the control specimens. This was due to symmetry of damage about the horizontal axis that resulted in similar magnitudes of strain in tension and compression. Typical strain profiles for different levels of neutral axis woodpecker damage are given in Figure 51 to Figure 53. The experimental strain profiles were modeled well by the theoretical strain profiles that incorporated modified moments of inertia due to damage.

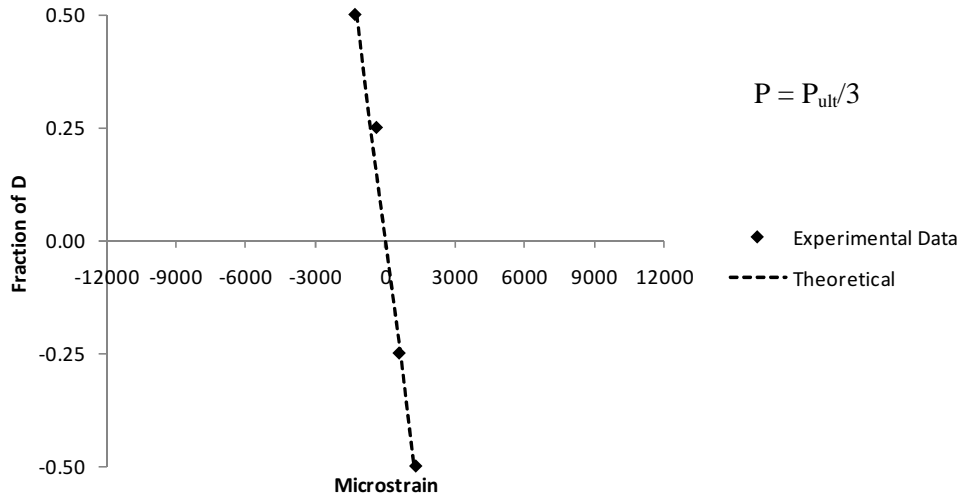


Figure 51. - Strain profile of new pole specimen with neutral axis exploratory damage (50-2-3).

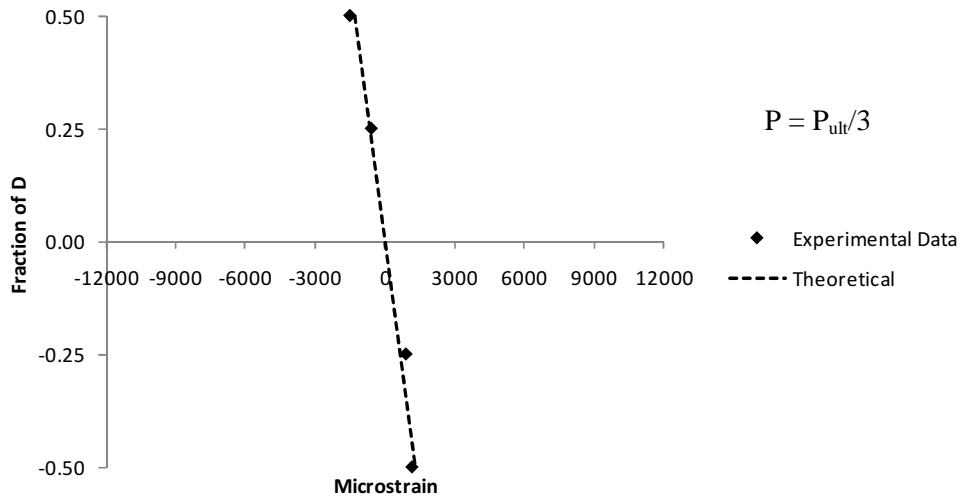


Figure 52. - Strain profile of new pole specimen with neutral axis feeding damage (50-1-1).

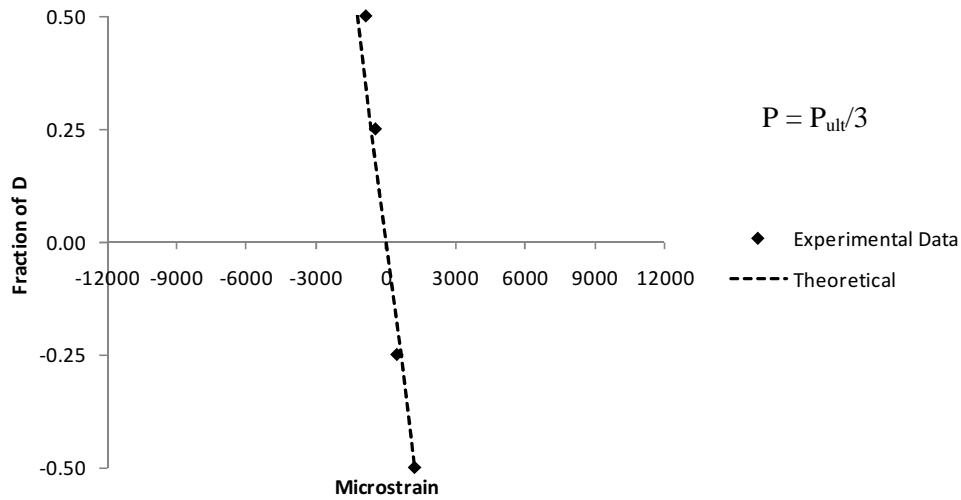


Figure 53. - Strain profile of new pole specimen with neutral axis nesting damage (55-3-1).

7.7 Experimentally Determined Modulus of Elasticity

7.7.1 Modulus of Elasticity Determined from Deflection

Deflection measurements were used to calculate the average modulus of elasticity values of control specimens using the double-integration method. Since the specimens were tapered, the equation of radius of curvature is difficult to integrate in equation form. As a result, numerical integration was used to determine beam curvature (ρ), slope (θ), and deflection (Δ) using the following equations (Mikhelson 2004).

$$\rho = \frac{M}{EI} \quad \text{Equation 46}$$

$$\theta = \int \frac{M}{EI} dx \quad \text{Equation 47}$$

$$\Delta = \int \int \frac{M}{EI} dx dx \quad \text{Equation 48}$$

It was found that shear deflection accounted for roughly 5% of total deflection in the control specimens. As a result, shear deflection was accounted for using the following formula suggested in the Wood Handbook for tapered beams (USDA 1999f).

$$\Delta_{\text{shear}} = \frac{0.3Pl}{AG} \quad \text{Equation 49}$$

where G is the wood shear modulus (0.081E for red pine and 0.086E for western red cedar), E is modulus of elasticity, and A is cross-sectional area (USDA 1999f). The modulus of elasticity was

back calculated using deflection and load data from specimen testing. The boundary conditions used in numerical integration were zero deflection at supports and compatibility of deflection and slope at midspan. The average modulus of elasticity values (E_{avg}) calculated for control specimens are provided in Table 17. The average modulus of elasticity of red pine and western red cedar specimens were 8215 MPa with COV of 12% and 8704 MPa with COV of 5%, respectively.

Table 17. - New pole control specimen modulus of elasticity values.

Specimen	Species	Deflection Based	Strain Based	% difference from E_{avg}
		E_{avg} (MPa)	E_{local} (MPa)	
45-1-1	Red pine	6855	6520	-4.89
45-1-2	Red pine	7485	5820	-22.24
45-2-2	Red pine	9763	9599	-1.68
50-1-1	Red pine	7649	6084	-20.47
50-1-2	Red pine	8017	8815	9.95
50-2-2	Red pine	7485	6436	-14.01
50-2-3	Red pine	8415	7391	-12.17
55-1-2	Red pine	7387	8569	15.99
55-3-2	Red pine	8800	8264	-6.09
55-3-3	Red pine	8132	7513	-7.61
60-1-2	Red pine	9417	11117	18.06
60-2-2	Red pine	8676	8743	0.77
60-3-2	Red pine	9138	7942	-13.09
60-4-2	Red pine	9449	8500	-10.04
50-3-2	Red pine	6549	7896	20.57
55-2-1	Western red cedar	9021	8541	-5.32
55-2-2	Western red cedar	8388	8902	6.13

7.7.2 Modulus of Elasticity Determined from Strain

Strain magnitudes determined from DCDDT measurements were used to calculate the local modulus of elasticity values of control specimens. Modulus of elasticity values determined using this method represent the local modulus of elasticity of the cross-section where strain is being measured. This contrasts the modulus of elasticity determined from deflection, which is the average modulus of elasticity of the entire specimen. Strain based modulus of elasticity values were determined using the following equation.

$$E = \frac{\sigma}{\epsilon} = \frac{M}{\epsilon Z} \quad \text{Equation 50}$$

where M is the moment at the cross-section where strain is being measured, ϵ is the strain measurement at the extreme cross-section fibres, and Z is the cross-section elastic section modulus. Local modulus of elasticity values (E_{local}) for control specimens are provided in Table 17. The average modulus of elasticity of red pine and western red cedar specimens were 7947 MPa with COV of 18% and 8722 MPa with COV of 3%, respectively. These values are very similar to those determined based on deflection measurements. It can be seen that, within a single specimen, the average and local values of modulus of elasticity measured vary by up to 22% from each other due to the varying

properties of wood along a specimen's length. The Wood Handbook (USDA 1999f) predicts a modulus of elasticity value of 7400 MPa with 22% COV and 7200 MPa with 22% COV for red pine and western red cedar, respectively. These values are both considerably lower than what was calculated from experimental data and is likely due to the small experimental sample size which does not represent the population.

7.7.3 Relationship of Modulus of Elasticity and Bending Strength

Modulus of elasticity and bending strength are graphed in Figure 54. It is evident that as the modulus of elasticity of a specimen increases, the bending strength also increases. This trend is apparent, although there is weak correlation.

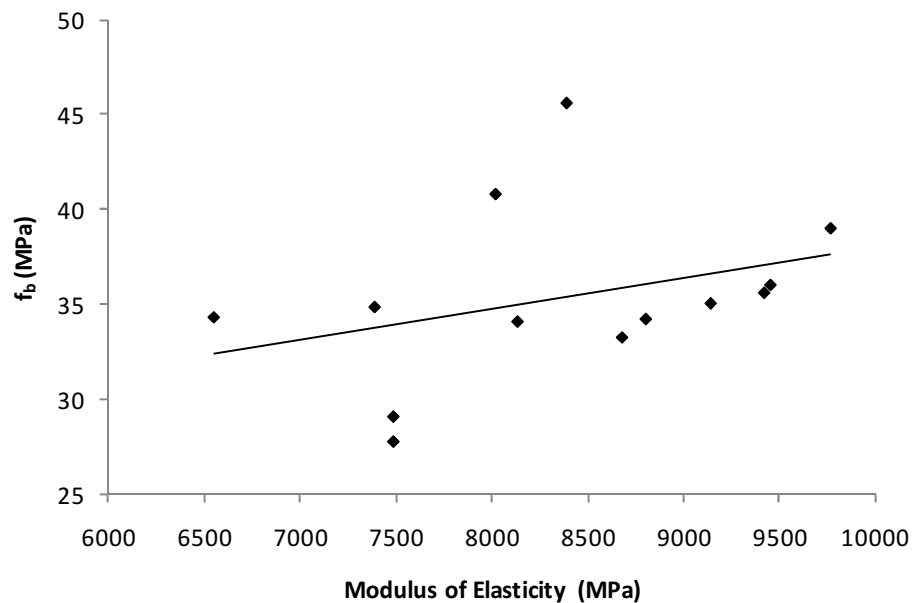


Figure 54. - Bending strength vs. modulus of elasticity for new pole specimens.

7.8 Dissection of Specimen Failure Locations

In order to better understand cross-section behaviour of control and woodpecker damaged cross-section at failure, specimens were dissected after beam testing. Dissection consisted of cross-sectioning failure locations in 150 mm long segments along a specimen's length.

7.8.1 Control Specimens

Dissection of control specimens at failure locations indicated tension fibre rupture was the primary cause of failure, as shown in Figure 55 and Figure 56.

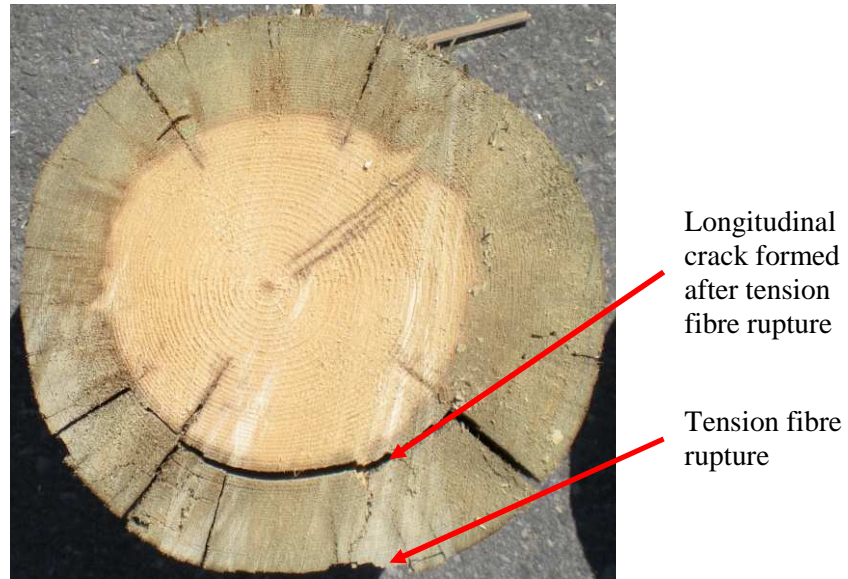


Figure 55. - Cross-section of new control specimen (50-1-2).

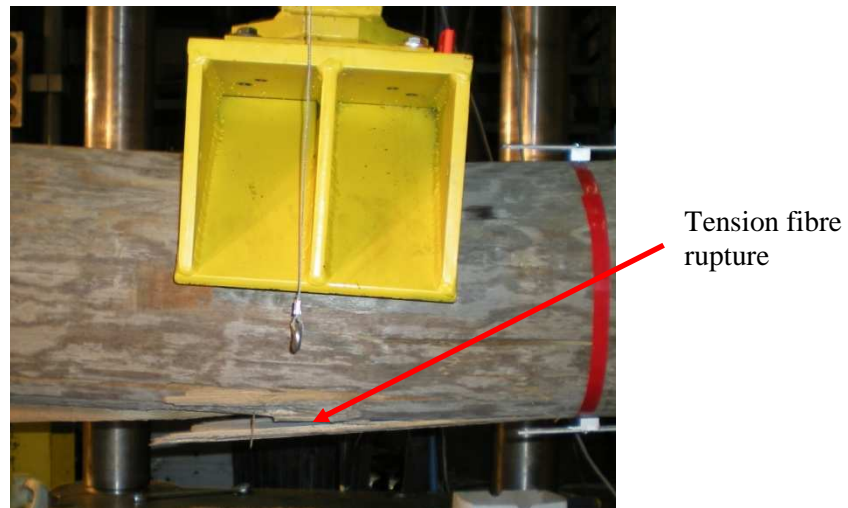


Figure 56. - Side view of new pole control specimen (50-1-2).

7.8.2 Tension Oriented Damage Specimens

Specimens with tension oriented damage typically failed due to tension fibre rupture. Similar to the control specimens, tension fibre rupture initiated at the extreme tension fibres of specimens and caused fracture of the cross-section. Typically, prior to tension fibre rupture, longitudinal cracks would form along specimen lengths. Examples of failure cross-sections of tension specimens with varying levels of damage are shown in Figure 57 to Figure 59.

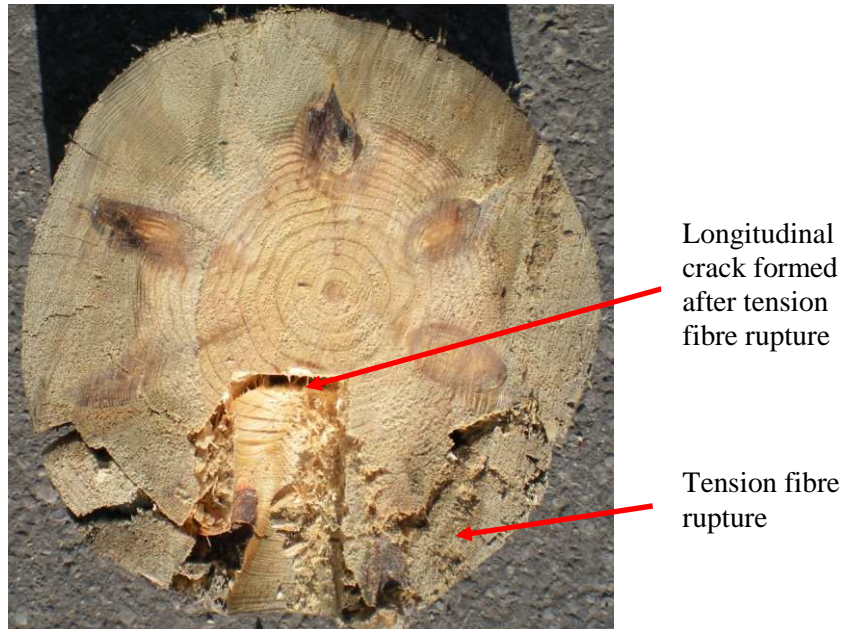


Figure 57. - Cross-section of new pole specimen with tension exploratory damage (45-2-3).

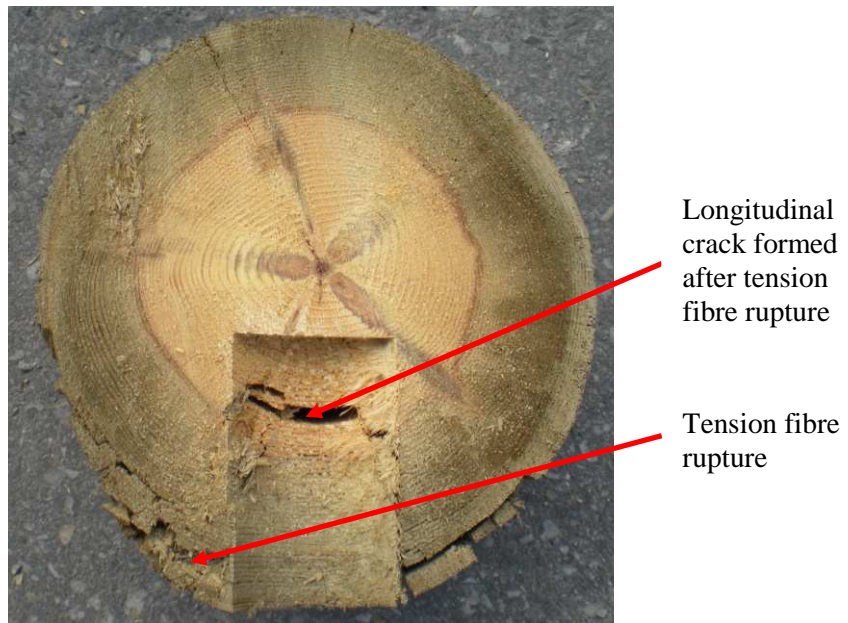


Figure 58. - Cross-section of new pole specimen with tension feeding damage (60-2-1).

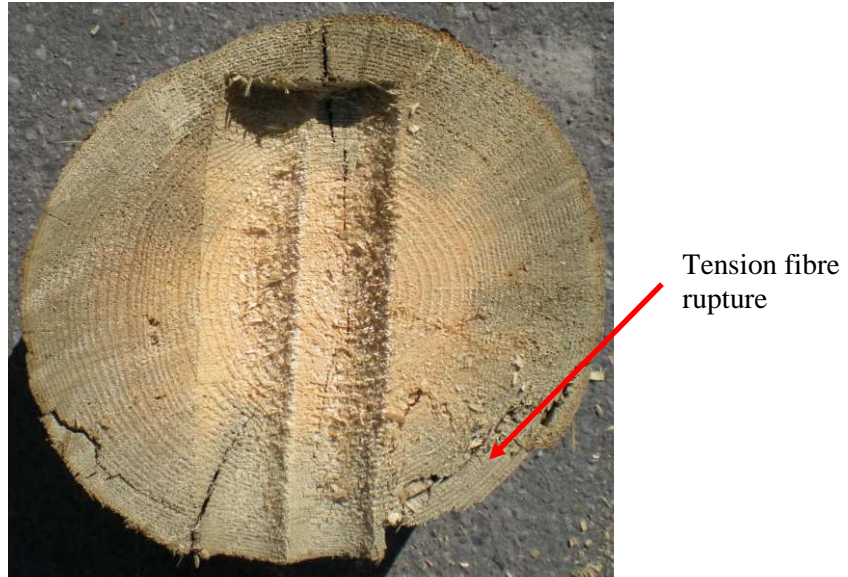


Figure 59. - Cross-section of new pole specimen with tension nesting damage (55-1-1).

7.8.3 Compression Oriented Damage Specimens

Specimens with compression oriented damage failed due to a combination of compression fibre crushing and tension fibre rupture. Typically, as loading commenced, specimens underwent compression fibre crushing at the extreme compression fibres around locations of woodpecker damage. The effect of compression fibre crushing in an extreme case can be seen in Figure 62. As loading progressed, tension fibre rupture occurred at extreme tension fibre locations as shown in Figure 60 to Figure 63.

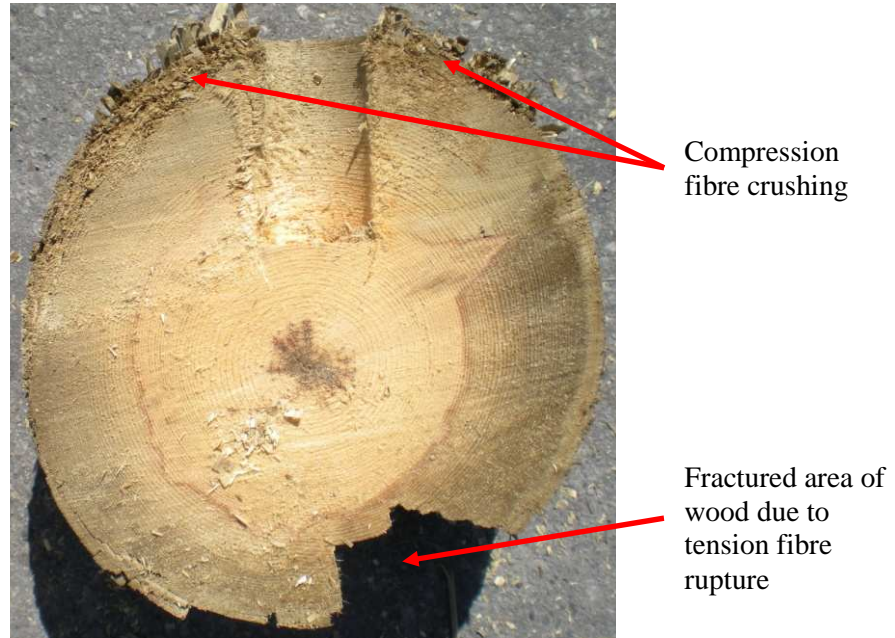


Figure 60. - Cross-section of new pole specimen with compression exploratory damage (60-2-3).

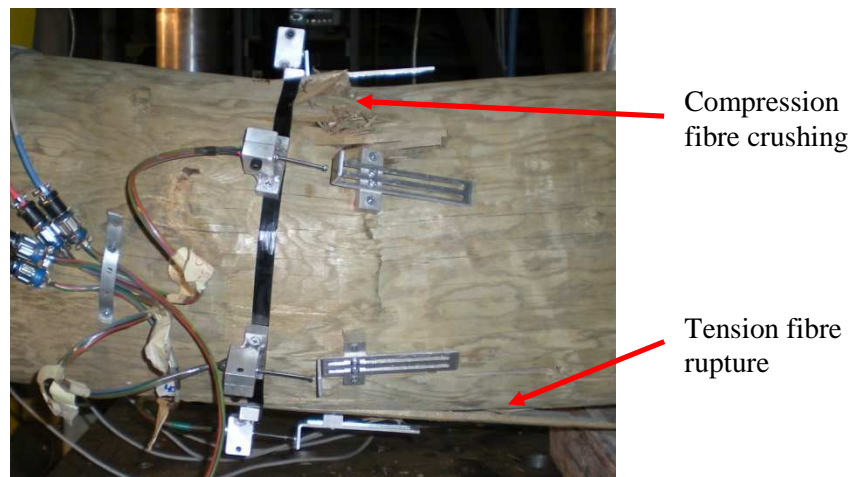


Figure 61. - Side view of new pole specimen with compression exploratory damage (60-2-3)

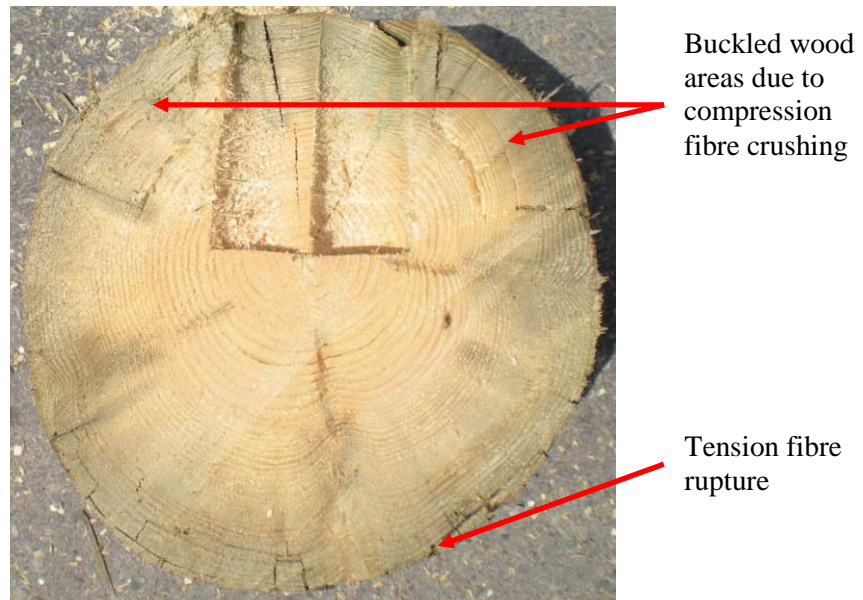


Figure 62. - Cross-section of new pole specimen with compression feeding damage (55-1-3).

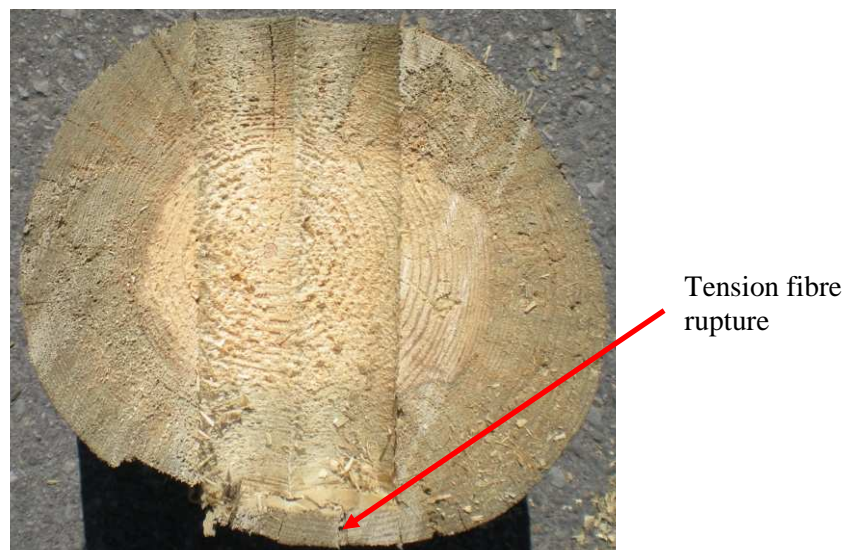


Figure 63. - Cross-section of new pole specimen with compression nesting damage (45-2-1).

7.8.4 Neutral Axis Oriented Damage Specimens

Specimens with neutral axis oriented damage were observed to fail in two different modes. Specimens with exploratory and feeding level damage (Figure 64 and Figure 65) failed due to tension fibre rupture in the same manner as the control specimens. Specimens with nesting level damage typically failed due to shear crack formation as shown in Figure 66. The shear cracks typically formed at the edges of the holes in the horizontal plane as predicted by SF analysis.

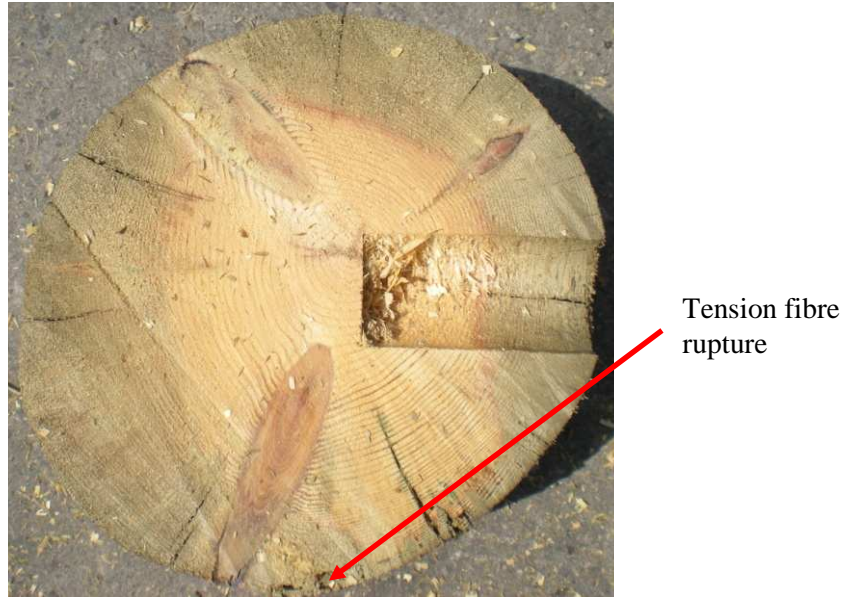


Figure 64. - Cross-section of new pole specimen with neutral axis exploratory damage (50-2-3).

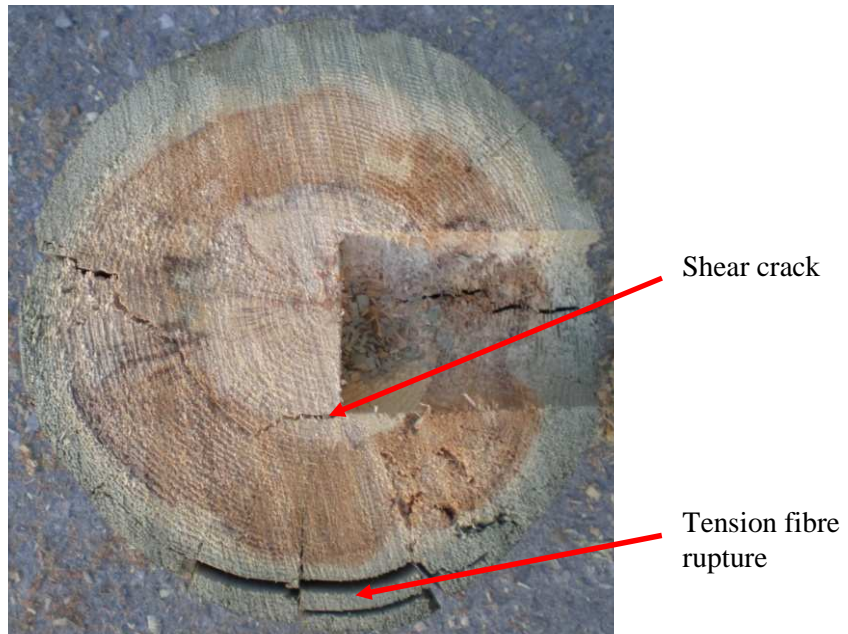


Figure 65. - Cross-section of new pole specimen with neutral axis feeding damage (60-4-1).

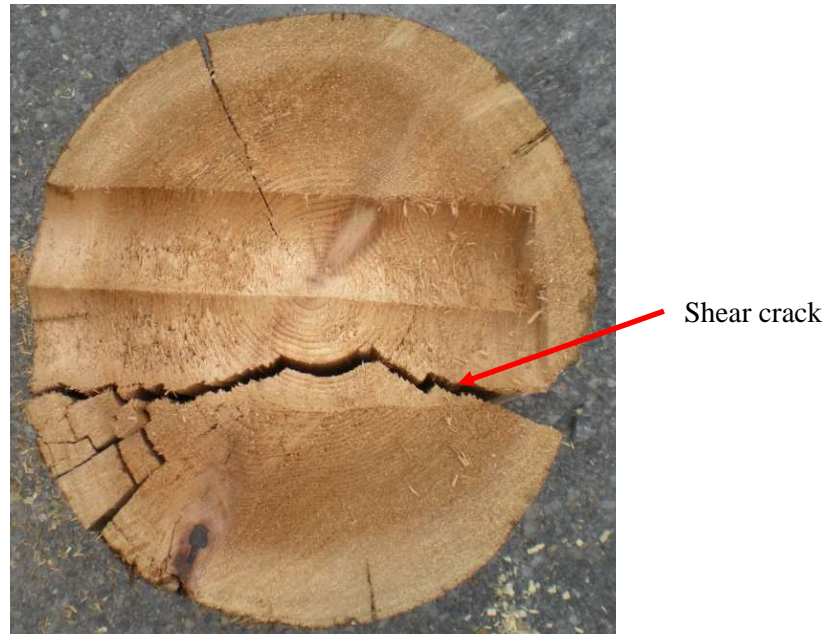


Figure 66. - Cross-section of new pole specimen with neutral axis nesting damage (55-2-3).

7.9 Moisture Content

Moisture content (MC) values for individual specimens were required for correction of the assumed shear strengths used in the SF and SBIF models and are given in Table 18. Moisture content samples were taken from each specimen at midspan during dissection. It was observed that moisture content varied along the length of poles with lowest values at the ends with small diameter, increasing towards ends with large diameter. This trend was attributed to the fact that larger diameter cross-sections required moisture to travel longer paths to exit the wood structure, reducing moisture loss.

Table 18. - Average new pole moisture contents.

Pole	MC_{avg} (%)	Pole	MC_{avg} (%)
45-1	30.22	55-3	29.23
45-2	30.75	60-1	33.27
50-1	25.91	60-2	52.40
50-2	24.69	60-3	38.91
50-3	28.84	60-4	40.55
55-1	27.84	55-2 (cedar)	19.11

7.10 Conclusions

Fifty-eight red pine and western red cedar beam specimens were sectioned from new utility poles into 4.25 m lengths for flexural beam testing. Based on observed in-service woodpecker damage levels, three idealized damage levels and orientations were categorized for introduction into the new beam specimens. Beam testing indicated that the introduction of woodpecker damage had a significant

effect on the behaviour of beam specimens. This was observed through a reduction in cross-section strength, increase in cross-section strain, and change in failure mode.

Experimental results confirm that the presence of different levels and orientations of woodpecker damage significantly reduce the cross-section strength. As the level of woodpecker damage became more severe the loss in cross-section strength increased. In addition, damage oriented in the neutral axis caused smaller reductions in strength in comparison to tension or compression orientations. Nesting level damage oriented in tension or compression locations caused severe strength reductions of over 40%. As a result, woodpecker damage was observed to cause strength reductions that would require replacement, according to CSA C22.3 No. 1 Cl. 8.3.1.3 (2006a), when in-service strength is reduced over 40%.

The three analytical models previously developed were used to analyze cross-sections with the presence of varying levels and orientations of woodpecker damage. Analytical predictions correlated well with experimental results when appropriate models were used according to failure mode. Based on comparison of analytical and experimental results, it was determined that bending failure effects are dominant in specimens with woodpecker damage introduced. An exception to this was observed in specimens with nesting level damage oriented in the neutral axis position which were observed to fail in shear. Overall, the BF analytical model was preferable for cross-section analysis due to the accuracy of the model predictions and the simplicity of required calculations.

Cross-section behaviour was investigated through the use of displacement transducers that allowed strain to be measured over the depth of the cross-section. Specimens with woodpecker damage oriented in tension and compression locations exhibited significant strain increases in the extreme fibres near hole locations. Experimental strain magnitudes for tension and compression damage at surface locations ranged from 2 to 7 and 4 to 9 times higher, respectively than predicted theoretically. Increased strain magnitudes at damage locations are attributed to stress concentrations that arise due to the discontinuity between damaged and undamaged cross-sections.

In order to better understand specimen failure modes, specimens were dissected at locations of failure. The majority of specimens failed due to tension fibre rupture at extreme tension fibre. Specimens with compression oriented damage underwent compression fibre crushing prior to tension fibre rupture, which was the ultimate failure mechanism. Specimens with nesting level neutral axis damage were unique since they failed in shear. After dissection it was observed that a horizontal shear failure plane developed at the base of the damage introduced.

Chapter 8 In-service Specimen Analysis, Results, and Discussion

Eleven in-service utility poles of varying length, class, and species were provided by HONI for experimental beam testing. These poles were removed from service due to the presence of woodpecker damage and wood decay. The purpose of the test program was to determine the effect of woodpecker damage and wood decay on utility pole cross-sectional strength. This was achieved by testing a single specimen from each in-service utility pole as a control specimen. Control specimens were useful in obtaining reference utility pole bending strengths. The remainder of the specimens were tested with natural woodpecker damage. The effect of woodpecker damage on cross-sectional strength was then determined based on reference control specimen bending strengths. The strength reduction caused by decay was determined by comparing control specimen bending strengths with undecayed wood bending strengths from literature (USDA 1999f).

8.1 In-service Test Specimens

The utility poles received were inspected and cut into 4.25 m segments for beam testing. The following naming system was developed for beam specimens: group – pole number – segment number. For example, D-1-3 is segment number 3 from the 1st in-service pole from group D. The symbols D and C stand for Damaged and Cedar, respectively. A summary of the beam test specimens are given in Table 19.

Table 19. - Received in-service pole details and specimens.

Pole	Species	Year	Class	Length (m)	Specimens
D-1	Lodgepole Pine	1979	-	12.19	D-1-1, D-1-2
D-2	Lodgepole Pine	Unknown	-	10.67	D-2-1, D-2-2
D-3	Lodgepole Pine	1985	-	12.19	D-3-1, D-3-2
D-4	Lodgepole Pine	1989	-	12.19	D-4-1, D-4-2, D-4-3
C-1	Western red cedar	2007	3	13.10	C-1-1, C-1-2, C-1-3
RP-1	Red Pine	2002	3	10.90	RP-1-1, RP-1-2
RP-2	Red Pine	2006	4	10.32	RP-2-1, RP-2-2
RP-3	Red Pine	2005	4	12.18	RP-3-1, RP-3-2
60-3	Red Pine	2004	2	18.29	60-3-1, 60-3-2
B-1	Red Pine	2009	2	18.29	B-1-1, B-1-2
B-2	Red Pine	2009	2	18.29	B-2-1, B-2-2

8.1.1 In-service Control Specimens

In order to determine a representative value of bending strength for each utility pole, one segment of each in-service pole was assigned as a control specimen. Unlike new poles, in-service poles had varying levels of deterioration and decay along their length. As a result, control specimens were taken from the middle segment of each pole to obtain an average value of bending strength from each pole. This was also advantageous for minimizing bending strength variation due to size effect.

8.1.2 In-service Specimens with Woodpecker Damage

The in-service utility poles received had varying levels and locations of woodpecker damage. As a result, specimens were sectioned from poles in a manner that allowed the influence of woodpecker damage to be investigated. Unlike the new pole specimen testing program, the experimental program for the in-service specimens did not use a factorial design to cover all levels and orientations of woodpecker damage.

8.2 Woodpecker Damage on In-service Poles

Eleven in-service utility poles were received from HONI. When received, these poles were fully documented in terms of woodpecker damage dimensions (Appendix C) and locations. It was observed that the majority of woodpecker damage occurred in the top half of poles as shown in Figure 67 to Figure 71. In these figure the symbols E, F, and N stand for exploratory, feeding, and nesting woodpecker damage, respectively. In wood pole analysis and design, the critical section for flexural failure is typically located between the groundline up to 1/3rd of a pole's height above ground (HAG). The fact that woodpecker damage was rarely observed in the critical design section is significant, since it indicates that the presence of woodpecker damage does not necessarily reduce the load carrying capacity of a pole.

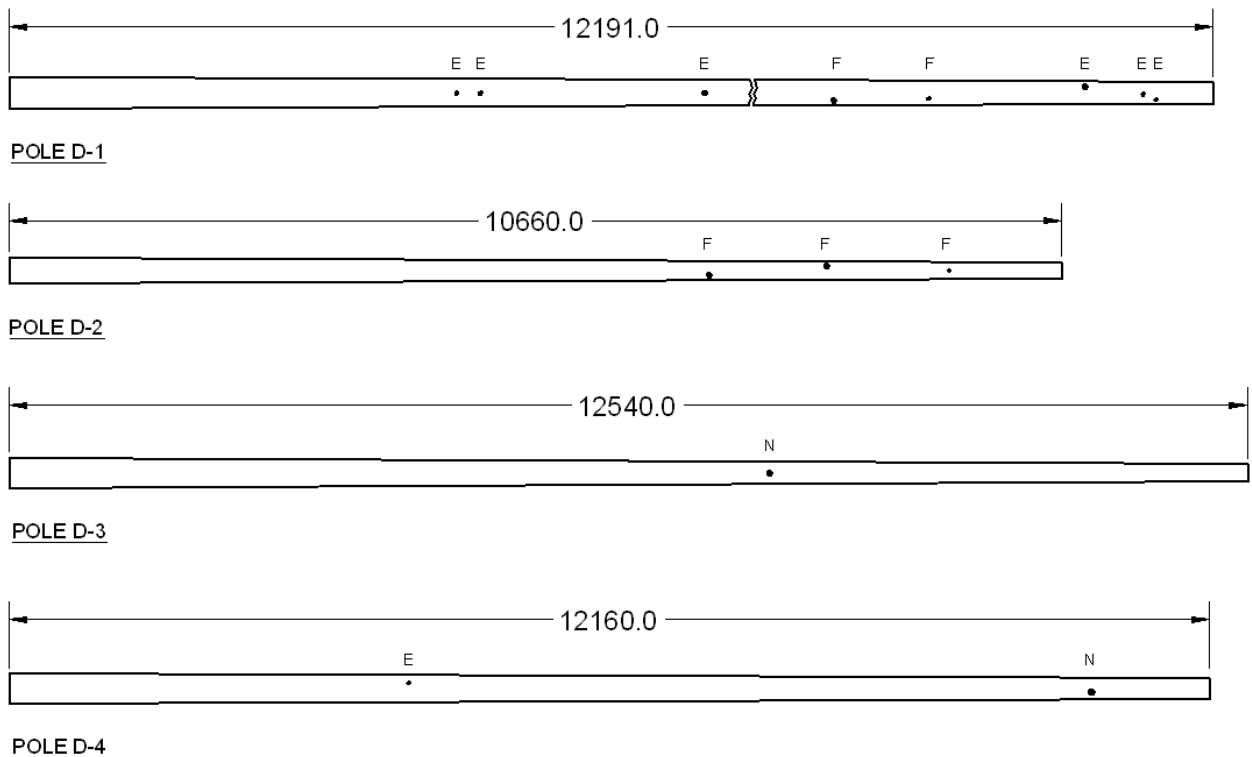
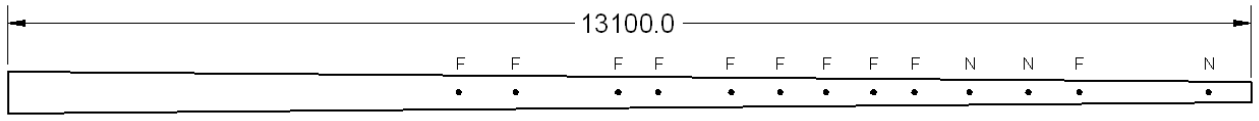
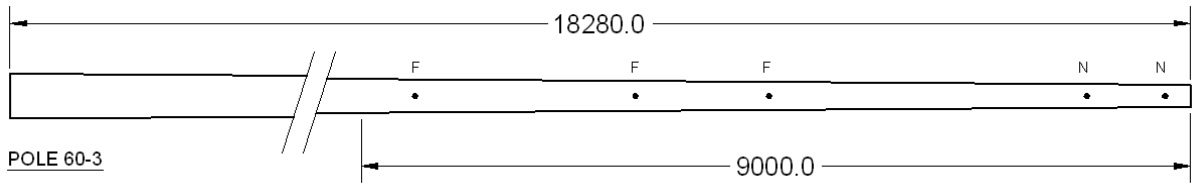


Figure 67. - Group D in-service poles with woodpecker damage locations.



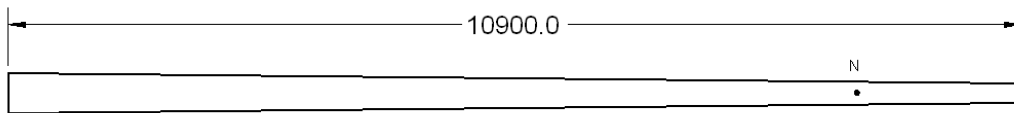
POLE C-1

Figure 68. - In-service pole C-1 with woodpecker damage locations.

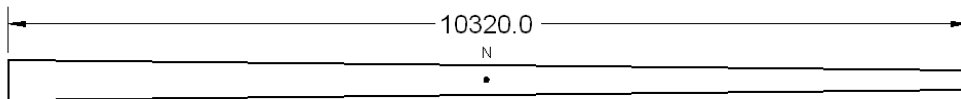


POLE 60-3

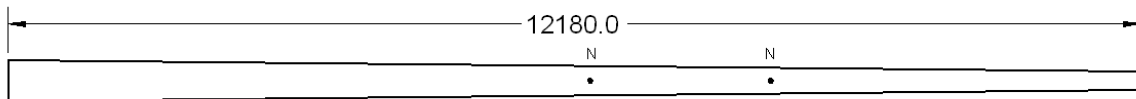
Figure 69. - In-service pole 60-3 with woodpecker damage locations.



POLE RP-1



POLE RP-2



POLE RP-3

Figure 70. - Group RP in-service poles with woodpecker damage locations.

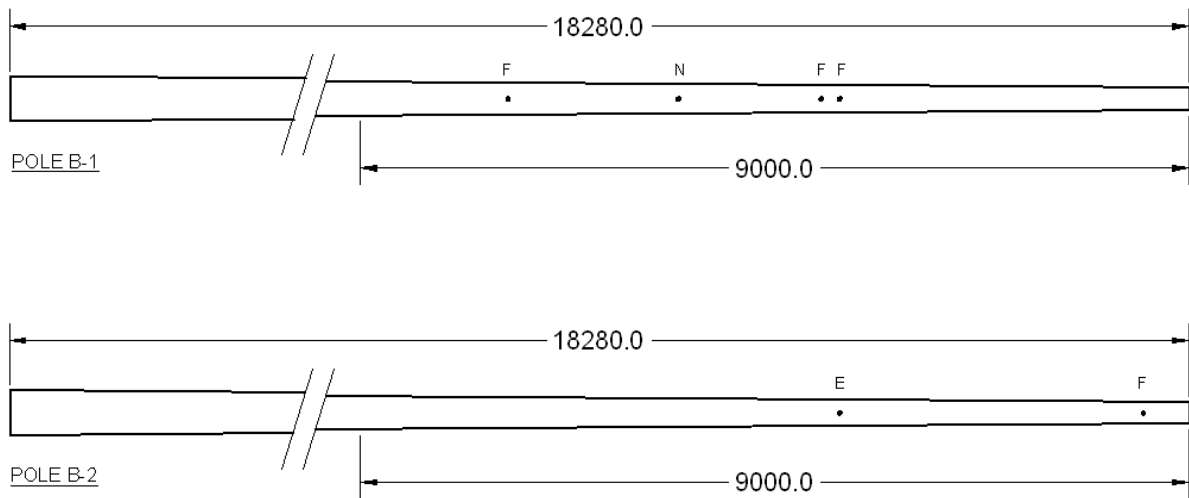














Figure 71. - Group B in-service poles with woodpecker damage locations.

8.3 In-service Specimen Condition Inspection

Once the in-service poles were cut to length, the specimens were inspected in terms of woodpecker damage, mechanical damage, and cracks and checks. An inspection of internal decay was performed during the dissection of specimens. Each of the four external indicators were separated into three levels of severity for a uniform inspection method.

Table 20 gives visual descriptions to aid in rating a specimen into a specific category based on external indicators. This method of visual rating was based on several research projects previously completed by others (Bhuyan 1998; McCarthy 2005; Pandey et al. 2010a; Vidor et al. 2010).

Table 20. - In-service specimen condition rating criteria.

Rating	1	2	3
Notes	Shallow indent	Medium depth hole	Deep cavity
Woodpecker Damage			
Notes	Minor	Intermediate	Major
Mechanical Damage			
Notes	Shallow and high density	Intermediate and low density	Deep and low density
Cracks and Checks			
Notes	Negligible decay	Intermediate decay	Advanced decay
Internal Decay			

8.4 Specimen Condition Inspection

Prior to strength testing, in-service specimens were rated in terms of woodpecker damage, mechanical damage, and cracks and checks as described in

Table 20. The purpose of the condition inspection was to correlate external indicators with levels of internal decay. Internal decay was rated after specimens were dissected and the interior of the specimens could be observed. Table 21 shows the received in-service specimen ratings. The external indicators observed are discussed in the following sections.

Table 21. - In-service specimen condition ratings.

Specimen	Cracks and Checks	Woodpecker Damage	Mechanical Damage	Internal Decay
D-1-1	3	3	3	3
D-1-2	3	2	1	3
D-2-1	1	2	1	1
D-2-2	1	1	1	1
D-3-1	1	2	1	2
D-3-2	1	1	1	2
D-4-1	3	3	2	3
D-4-2	3	1	1	3
D-4-3	2	1	1	2
C-1-1	1	2	1	1
C-1-2	1	2	1	1
C-1-3	1	1	1	1
RP-1-1	1	2	1	1
RP-1-2	1	1	1	1
RP-2-1	1	1	1	1
RP-2-2	1	2	1	1
RP-3-1	1	3	1	1
RP-3-2	1	1	1	1
60-3-1	1	2	1	1
60-3-2	1	1	1	1
B-1-1	1	1	1	1
B-1-2	1	1	1	1
B-2-1	1	1	1	1
B-2-2	1	1	1	1

8.4.1 Cracks and Checks

Based on previous research at the University of Waterloo (McCarthy 2005), the best external indicator of internal decay was found to be the presence of cracks and checks. Wide cracks and checks that penetrated deep into cross-sections were found to allow moisture and oxygen penetration, resulting in severe decay. This trend was evident in the received group D in-service specimens. Figure 72 shows an example of a very wide crack that penetrated into the cross-section core. The interior of this specimen at the crack location was observed to have severe decay.



Figure 72. - In-service specimen with deep crack and severe decay (D-1-1).

In contrast to deep cracks, high density cracks and checks that penetrated less deeply were shown to reduce moisture and oxygen penetration resulting in reduced decay. An example of an in-specimen with shallow checks at a high density, evenly distributed across the circumference of the cross-section is shown in Figure 73. The interior of this specimen was observed to be free from decay.



Figure 73. - In-service specimen with shallow and high density cracks with no decay (D-2-1).

8.4.2 Woodpecker Damage

The effect of woodpecker damage on decay was observed to have varying effects depending primarily on the depth of the damage and the age of the pole. Aged in-service specimens with severe woodpecker damage typically had advanced levels of decay as show in Figure 74. In contrast, relatively new in-service specimens with severe woodpecker damage were rarely decayed (Figure 75). This indicates that severe woodpecker damage may contribute to decay progression in older poles. Similar to the mechanism observed for cracks and checks, the presence of severe woodpecker damage exposes cross-section interiors to moisture and oxygen, increasing the rate decay.

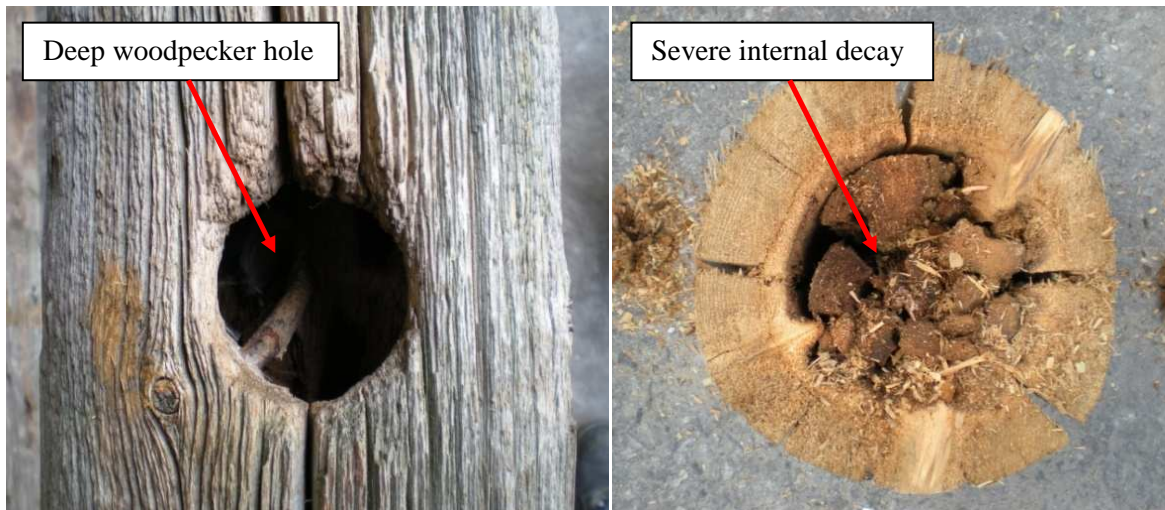


Figure 74. - In-service specimen with nesting level woodpecker damage and decay (D-4-1).



Figure 75. - In-service specimen with nesting level woodpecker damage and no decay (RP-3-1).

In specimen D-3-1, with a moderate level of decay present, woodpecker damage was found to be the initiator of decay as shown in Figure 76. Upon dissection of the specimen's midspan, it was found that the decay originated at the woodpecker hole and was less severe in sections more distant from it.



Figure 76. - In-service specimen with intermediate level woodpecker damage and decay (D-3-1).

In-service specimens with shallow depth woodpecker damage (Figure 77) were found to have little effect on cross-section decay. It appears that moisture was not able to pond in low depth holes due to environmental exposure that enabled quick evaporation of water. As a result, cross-sections did not become saturated with water, as occurred in nesting holes, reducing the effects of premature decay due to moisture and oxygen penetration.

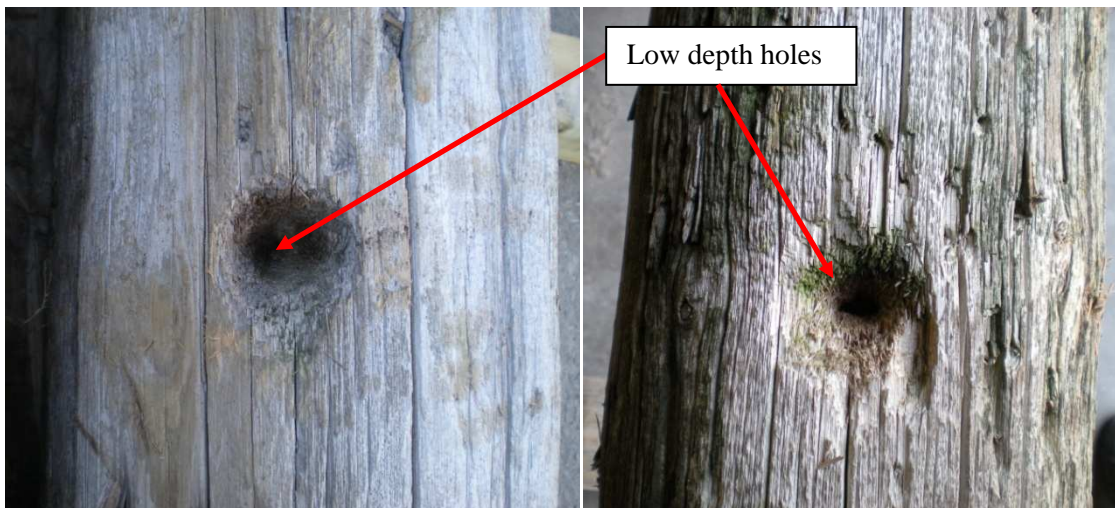


Figure 77. - In-service specimens with minor woodpecker damage and no decay (D-4-1).

8.4.3 Mechanical Damage

Mechanical damage was present on several in-service specimens where bolted attachments were previously installed (Figure 78). As shown in Figure 78 and Figure 79, mechanical damage contributed to severe crack formation and cross-section crushing in aged specimens. Both of these by-products resulted in cross-section interiors being exposed to the external environment. Upon interior exposure, mechanical damage advanced cross-sectional decay and deterioration due to moisture and oxygen exposure over time. Relatively new in-service specimens were also observed to have mechanical damage as shown in Figure 80. These specimens had no signs of internal decay due to the relatively short length of environmental exposure time.

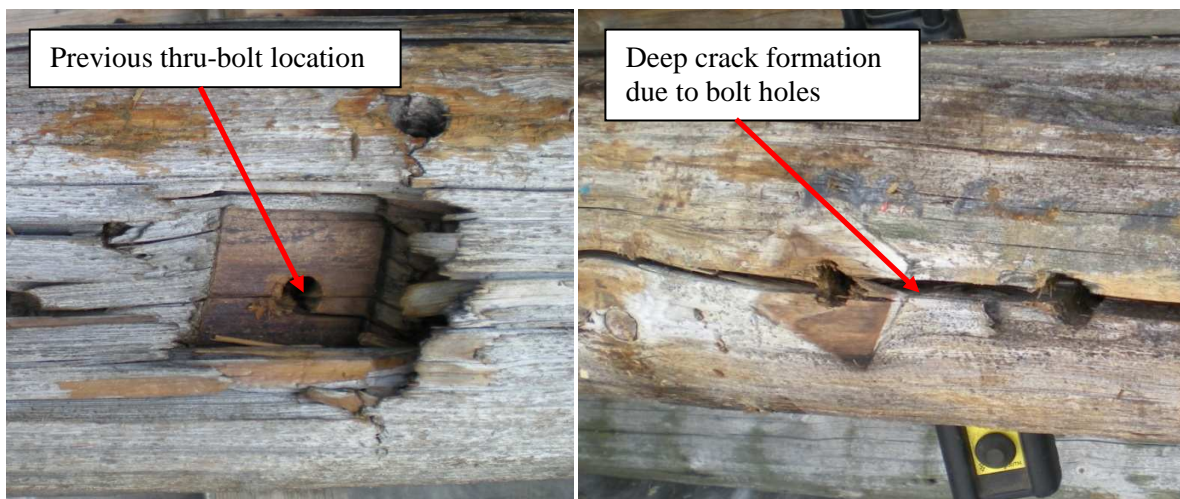


Figure 78. - In-service specimen with severe mechanical damage and decay (D-1-1).



Figure 79. - In-service specimen with mechanical damage and crack formation (D-1-1).



Figure 80. - In-service specimens with mechanical damage and no decay (60-4-2).

8.4.4 Significance of External Indicators

Cracks and checks, woodpecker damage, and mechanical damage have all been shown to contribute to decay and degradation of in-service specimens. It appears that the same mechanism is responsible for decay regardless of the external indicator present. This mechanism can be described by the following procedure:

1. The interior of a specimen cross-section is exposed to the external environment by cracks and checks, woodpecker damage, mechanical damage, or any other means.
2. Environmental exposure allows moisture and oxygen penetration into the cross-section interior.
3. Extended time periods of exposure result in internal decay occurring.
4. Decay results in significant strength reductions (see Section 8.7.5).

All external indicators were shown to contribute to decay in certain situations, although some were consistently more significant than others. Cracks and checks were the most significant indicator based on the specimen ratings and previous research. Every specimen that had severe cracks and checks also had severe internal decay (Table 21). An important note is that severe cracks and checks were not present in new in-service specimens; rather they required time to develop. This indicated that time was also a required factor for significant decay. In contrast to cracks and checks, woodpecker damage and mechanical damage were found in aged and new in-service poles. These two external indicators were only applicable after a significant period of time had elapsed, allowing development of decay.

8.5 General Behaviour

Typical load-deflection curves are shown in Figure 81 and Figure 82 for in-service pole specimens failing in bending and shear, respectively. In-service specimens failed in both bending and shear with similar load-deflection behaviour as was observed for the new specimens. Bending failures were ductile and gradual while shear failures were brittle and sudden. The number of specimens that experienced a shear failure significantly increased in comparison to the new pole specimen testing. The majority of shear failures occurred in specimens with heavy decay and checking as shown in Figure 83. Decay was found to most significantly affect the interior core of specimens, rendering interior fibres ineffective in strength contribution. As a result, decay caused a large reduction in shear strength since the thickness of the shear plane carrying shear force was significantly reduced. In addition, locations of checking acted as initiation planes for shear failure. In contrast to this, bending strength was affected to a lesser degree by decay since the outer shell fibres, which contribute to the majority of bending strength, were subjected to minimal decay. This mechanism accounts for the significant increase in proportion of shear failures observed during the testing of in-service specimens.

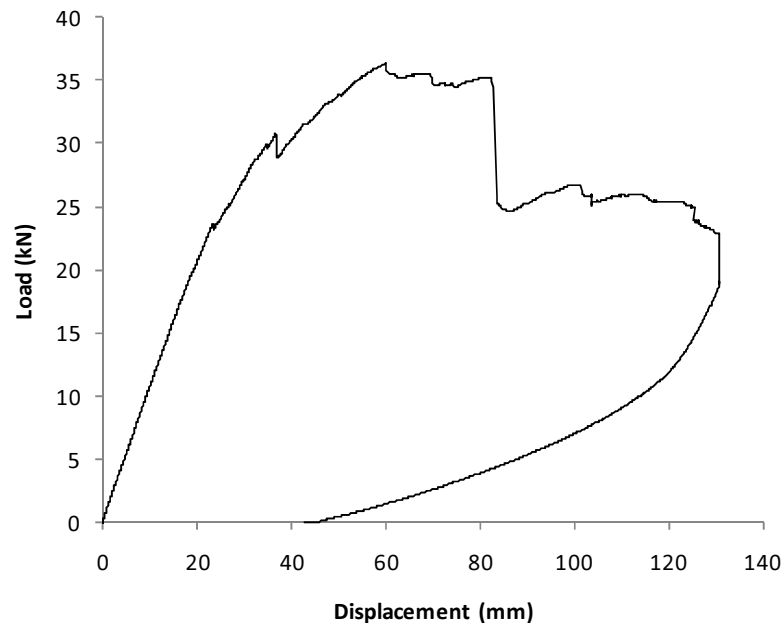


Figure 81. - Typical load-deflection curve for in-service specimen failing in bending (D-4-2).

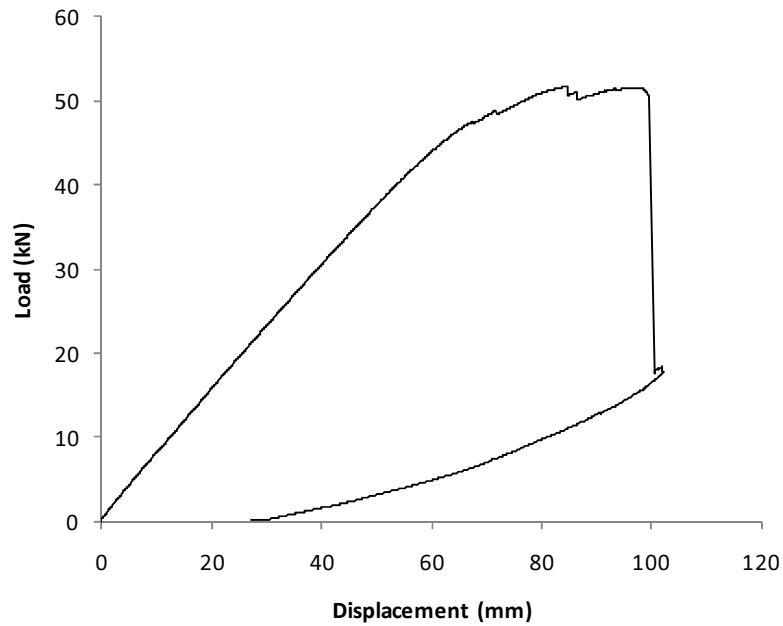


Figure 82. - Typical load-deflection curve for in-service specimen failing in shear (D-2-2).



Figure 83. - Heavily decayed in-service specimen that failed in shear (D-4-1).

8.6 Influence of Knots and Checks

The influence of knots and checks on specimen strength was monitored throughout beam testing and dissection of failure locations. Specimens with low levels of decay performed in the same manner as new specimens with knots and checks. When significant levels of decay were present, decay was observed to dominate strength reduction over the effect of knots. Many aged in-service specimens with high levels of decay had significant checking that often times penetrated the entire depth of the outer shell. These locations of checking acted as initiation planes for shear failure, as shown in Figure

84. It was also observed that shear failure planes did not necessarily develop at the neutral axis, as predicted theoretically, when checks were present. This indicated that the presence of checks caused shear failure at lower loads than required to normally cause shear failure. As a result, the presence of checking in decayed in-service specimens was observed to control the location of shear failure plane development, causing reduced strength.

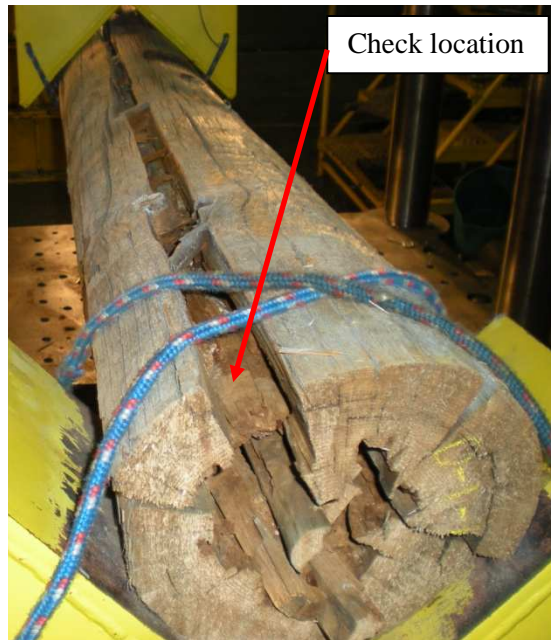


Figure 84. - In-service specimen with shear failure plane coinciding with check (D-1-1).

8.7 In-service Control Specimens

In-service control specimens were tested in three-point loading and did not consistently fail in bending as observed with the new specimens tested. Rather, specimens failed in bending and shear as shown in Figure 85 and Figure 86, respectively. Several specimens with woodpecker damage present had failures that were not influenced by the damage. These specimens were also included as control specimens since their strengths were unaffected by the woodpecker damage. The bending and shear strengths of control specimens were calculated using gross section properties as well as effective section properties that neglected strength contribution from decayed wood fibres. Specimens were analyzed using the previously developed BF and SF analytical models.

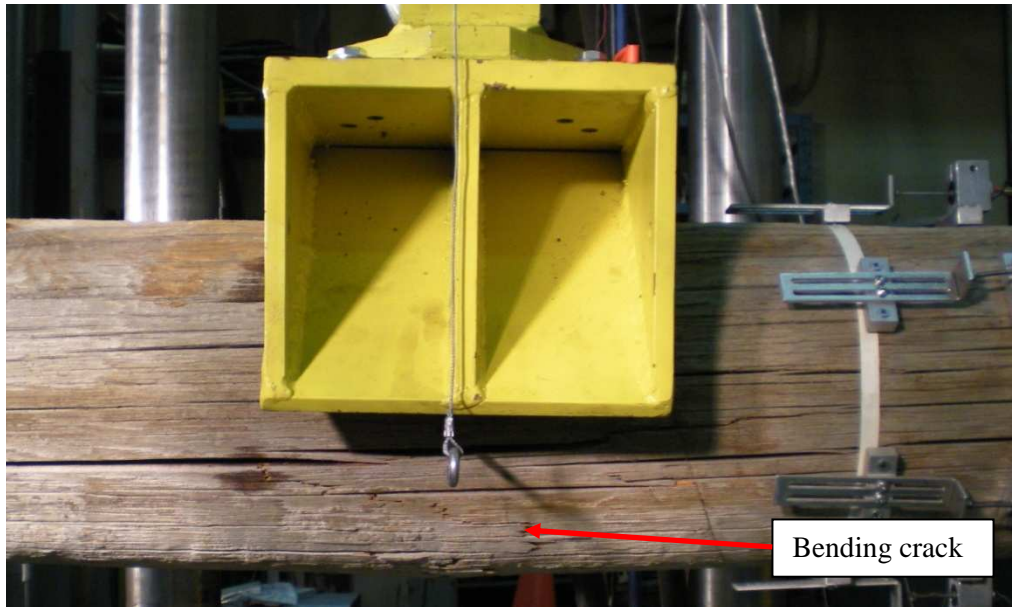


Figure 85. - In-service control specimen bending failure (D-3-2).

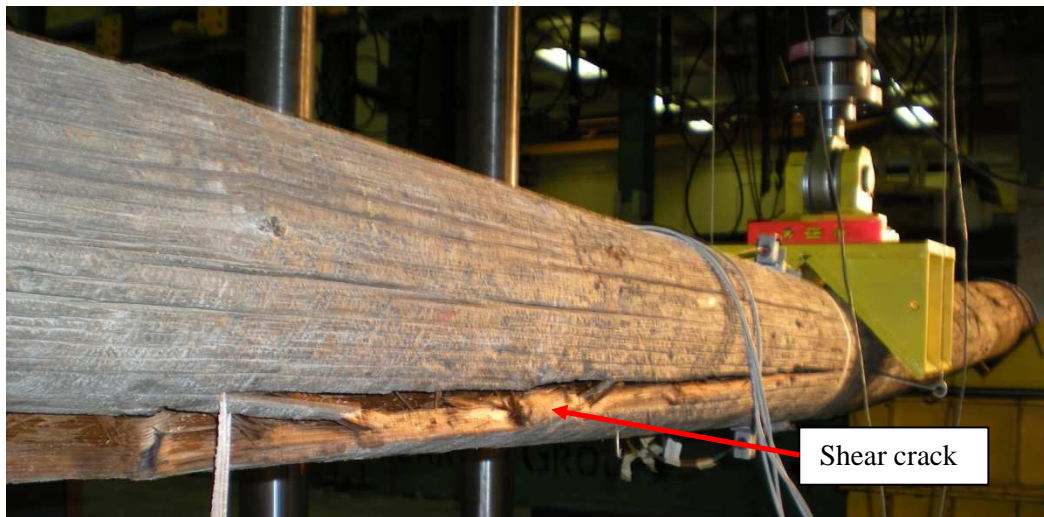


Figure 86. - In-service control specimen shear failure (D-4-1)

8.7.1 Bending Failure Analysis Using Gross Cross-section Properties

The procedure followed for bending failure analysis of in-service specimens using gross cross-section properties was the same as that used for new control specimens. See Section 7.4.1 for details.

8.7.2 Shear Failure Analysis Using Gross Cross-section Properties

Shear failure analysis using gross cross-section properties was performed based on several assumptions. The first assumption was that shear failure would occur at the neutral axis of control

specimens as predicted theoretically. The two geometric assumptions were that moment of inertia and moment of area values were accurately represented by the following theoretical equations:

$$I = \frac{\pi D^4}{64} \quad \text{Equation 51}$$

$$Q = \frac{D^3}{12} \quad \text{Equation 52}$$

where D is cross-section diameter at the failure location. The experimental shear strengths of the control specimens were then computed directly using the following equation (USDA 1999f):

$$f_v = \frac{4V}{3A} \quad \text{Equation 53}$$

where V is the value of shear at the failure location and A is the gross cross-section area.

8.7.3 Bending Failure Analysis Using Effective Cross-section Properties

A modified bending failure analysis was conducted for in-service pole specimens with significant internal decay. This modified bending failure analysis was based on an effective shell width assuming internally decayed wood to be ineffective in providing bending resistance. Based on this assumption, geometric section properties were calculated using the following equations:

$$Z = \frac{2I}{D} \quad \text{Equation 54}$$

$$I = \frac{\pi D^4}{64} - \frac{\pi(D-2t_{shell})^4}{64} \quad \text{Equation 55}$$

where t_{shell} is the average width of sound wood shell. The experimental bending strength of the decayed control specimens were then computed directly using the following equation:

$$f_b = \frac{M}{Z} \quad \text{Equation 56}$$

where M is the moment at the failure location.

8.7.4 Shear Failure Analysis Using Effective Cross-section Properties

A modified shear failure analysis was also conducted based on an effective shell width assuming internally decayed wood was ineffective in providing shear resistance. Based on this assumption, moment of inertia was calculated as previously described and moment of area about the neutral axis was calculated using the following equation:

$$Q = \frac{D^3}{12} - \frac{(D-2t_{shell})^3}{12} \quad \text{Equation 57}$$

where t_{shell} is effective shell thickness. The experimental shear strength of the decayed control specimens was then computed directly using the following equation:

$$f_v = \frac{vQ}{It} \quad \text{Equation 58}$$

where V is the shear at the failure location and t is $2 \cdot t_{\text{shell}}$.

8.7.5 Experimental Results

Bending and shear strengths of control specimens based on gross and effective section properties were calculated as previously described and are given in Table 22. If a specimen failed in bending, the bending strength of the specimen was determined, whereas if a specimen failed in shear, the shear strength of the specimen was determined (pole failure modes are listed in Appendix C). For in-service specimens with significant decay, the shell thickness of sound wood is also included. For comparison with in-service experimental values provided in Table 23, bending and shear strengths for new wood at a moisture content of 20% have been provided in Table 24 (USDA 1999f).

Table 22. - In-service control specimen bending and shear strengths.

Specimen	Gross Cross-section		Effective Cross-section		t_{shell} (mm)	Internal Decay Level
	f_b (MPa)	f_v (MPa)	f_b (MPa)	f_v (MPa)		
D-1-1	-	0.17	-	0.43	40.00	3
D-1-2	-	0.30	-	0.92	35.00	3
D-2-2	-	0.89	-	-	-	1
D-3-2	26.89	-	-	-	-	2
D-4-1	-	0.29	-	0.66	45.00	3
D-4-2	-	0.55	-	1.43	40.00	3
D-4-3	21.45	-	30.10	-	37.50	2
C-1-3	40.13	-	-	-	-	1
RP-1-2	35.73	-	-	-	-	1
RP-2-1	26.87	-	-	-	-	1
RP-2-2	27.31	-	-	-	-	1
RP-3-2	39.74	-	-	-	-	1
60-3-2	35.02	-	-	-	-	1
B-1-2	34.87	-	-	-	-	1
B-2-2	28.58	-	-	-	-	1

Table 23. - In-service control specimen average bending and shear strengths and COV's.

Species	$f_{b \text{ avg}}$ (MPa)	COV (%)	$f_{v \text{ avg}}$ (MPa)	COV (%)
Lodgepole pine	24.17	15.92	0.44	65.24
Red pine	32.59	15.28	-	-
Western red cedar	40.13	-	-	-

Table 24. - Published bending strengths, shear strengths, and COV's (USDA 1999f).

Species	$f_{b \text{ avg}}$ (MPa)	COV (%)	$f_{v \text{ avg}}$ (MPa)	COV (%)
Lodgepole pine	45.37	16.00	5.52	13.95
Red pine	30.60	16.00	4.41	14.06
Western red cedar	43.11	16.01	5.14	13.94

The in-service control specimens displayed a large variation in bending and shear strengths due to the large variation in specimen condition. In general, aged in-service specimens with significant decay had severely reduced bending and shear strengths in comparison to new specimens. In contrast to this,

newer in-service specimens had minimal decay with strengths equivalent to new pole specimens. In order to better understand the relationship between wood decay and strength, experimental results based on gross cross section properties were grouped based on decay level and are given in Table 25.

Table 25. - Relationship between decay level and in-service bending and shear strength.

Internal Decay Level	$f_{b \text{ avg}}$ (MPa)	COV (%)	$f_{v \text{ avg}}$ (MPa)	COV (%)	Average age (years)
1	33.53	15.88	0.89	-*	7
2	24.17	15.92	-**	-**	24
3	-**	-**	0.33	48.75	27

* only one specimen was used to determine f_v

** no specimens failed in bending or shear at this decay level

It is evident that as the level of in-service specimen decay increased, reductions in bending and shear strength increased. Specimens with level 3 decay all failed in shear, supporting the previous observation that decay caused a larger reduction in shear strength than in bending strength. In addition, it is evident that in-service specimens with lower strengths were from older in-service poles. In order to determine the strength reduction (SR) caused by decay, the ultimate load capacity of each specimen was calculated assuming decay was not present and compared with experimental ultimate loads. The strength reductions for different specimens were grouped based on decay level and results are given in Table 26.

Table 26. - Strength reductions caused by decay.

Decay Level	SR (%)	Standard Deviation (%)	Average age (years)
1	≈ 0	15	7
2	47	8	24
3	73	18	27

The computed strength reductions indicated that in-service specimens with negligible decay (level 1) had strengths close in magnitude to new specimen strengths. As the level of decay increased to intermediate and advanced levels (levels 2 and 3), significant average strength reductions of 47% and 73%, respectively were observed. The presence of internal decay on in-service wood poles could cause significant strength reductions, and in some cases would require wood pole replacement according to CSA C22.3 No. 1 Cl. 8.3.1.3 (2006a) due to strength reductions of over 40%.

8.8 In-service Specimens with Natural Woodpecker Damage

In-service specimens with natural woodpecker damage in tension, compression, and neutral axis orientations failed due to tension fibre rupture as shown in Figure 87 to Figure 89. This contrasted with new specimen behaviour in which specimens with compression damage underwent compression fibre crushing prior to tension fibre rupture. This change in behaviour appears to be caused by the brittle nature of the decayed in-service wood that withstood smaller cross-section deformations prior to failure. As a result, tension fibre rupture occurred at low strain levels before compression fibre crushing would normally occur. Shear failure was not observed in specimen C-1-2 with neutral axis

damage, due to the low severity of woodpecker damage present. Specimens with multiple damage locations were tested in a manner that caused failure to occur at a desired damage location.

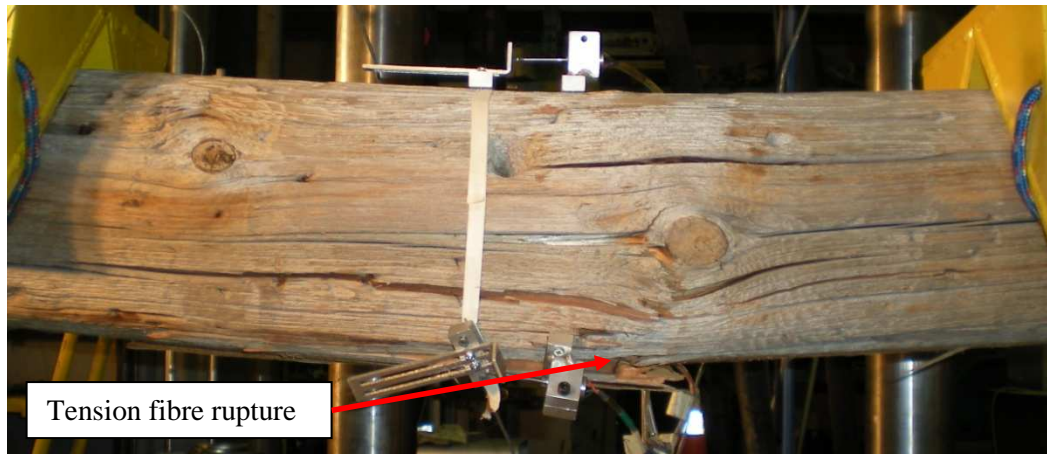


Figure 87. - Tension fibre rupture of in-service specimen with tension damage (D-3-1).

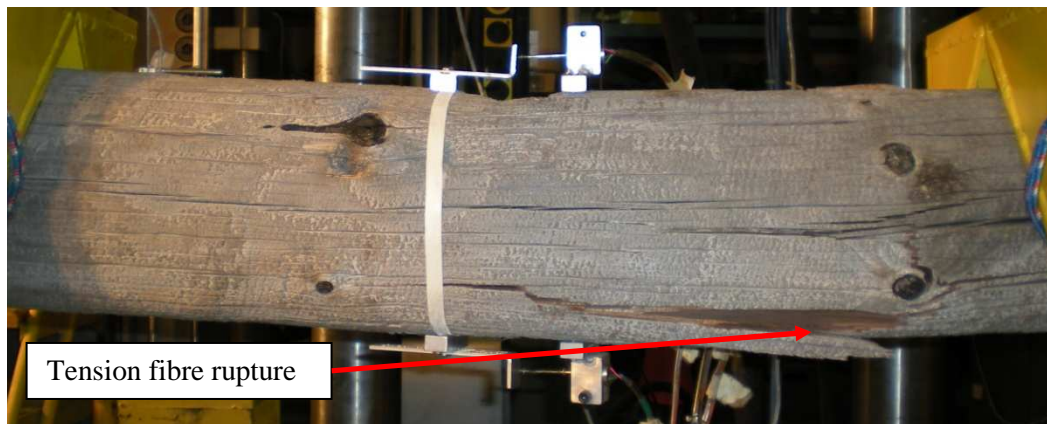


Figure 88. - Tension fibre rupture of in-service specimen with compression damage (D-2-1).



Figure 89. - Tension fibre rupture of in-service specimen with neutral axis damage (C-1-2).

8.8.1 Bending Failure Analysis Using Gross Cross-section Properties

In-service specimens that failed at locations of woodpecker damage were analyzed using gross cross-section properties. This was appropriate since the subject specimens had minimal internal decay at locations of woodpecker damage. The same procedure used for bending failure analysis of new woodpecker damaged specimens (Section 7.5.1) was implemented for in-service specimens. It was observed that failures at locations of woodpecker damage were due exclusively to bending. Assumed bending strengths were obtained from control specimen analysis results previously determined. This allowed the effect of woodpecker damage on cross-section strength to be determined. Woodpecker damage dimensions were recorded during dissection of specimens after strength testing. Based on these dimensions, corresponding theoretical geometric section properties were calculated using the previously developed BF analytical model. This enabled experimental results and theoretical predictions to be compared.

8.8.2 Experimental Strength Reduction

It was assumed that the bending strengths of in-service control specimens were representative of the bending strengths of the utility poles they were obtained from. As a result, the bending and shear strengths of specimens with woodpecker damage were known prior to analysis. This enabled the strength reduction (SR) caused by the presence of woodpecker damage to be determined from the experimental and theoretical failure loads. Strength reductions are given in Table 27 for different levels and orientations of woodpecker damage.

Table 27. - In-service specimen strength reductions caused by woodpecker damage.

Specimen	SR (%)	Damage Orientation	Damage Dimensions		Category
			Width (D)	Depth (D)	
D-2-1	44	Compression	0.32	0.40	Feeding
D-3-1	16	Tension	0.24	0.41	Feeding
C-1-1	32	Compression	0.23	0.50	Feeding
C-1-2	≈ 0	Neutral Axis	0.25	0.53	Feeding
RP-1-1	20	Tension	-	-	-
RP-3-1	57	Compression	50 mm shell and 200 mm wide opening		Nesting
60-3-1	25	Tension	0.29	0.61	Feeding
B-1-1	55	Tension	50 mm shell and 90 mm wide opening		Nesting
B-2-1	33	Tension	0.30	0.70	Nesting

The values of strength reduction computed indicate that the presence of natural woodpecker damage can cause severe reductions in cross-section strength up to 57%. As a result, naturally occurring woodpecker damage is significant and could require in-service wood utility poles to be replaced according to CSA C22.3 No. 1 Cl. 8.3.1.3 (2006a), which requires replacement with strength reductions over 40%.

8.8.3 Comparison of Analytical Model with Experimental Results

Experimental results were compared with the analytical model predictions in terms of member section properties (moment of inertia, I) calculated using the measured failure loads and material properties through back-calculation of the analytical models. Results were expressed as the ratio of experimental to theoretical moment-of-inertia (I_e/I_t), and are listed in Table 28. Note that the theoretical moments of inertia account for the section reduction due to the presence of the natural woodpecker damage. Thus, differences between the values calculated using experimental data (failure load and material strength) and the theoretical values must result from assumptions in the analytical models and other factors as discussed below. Specimen RP-1-1 was not included in the analysis since woodpecker damage was not located at the failure cross-section. Despite this, failure of this specimen was initiated by woodpecker damage at another location on the pole.

Table 28. - In-service specimen I_e/I_t values for bending failure criteria.

Specimen	Damage Orientation	Damage Dimensions		I_e/I_t	Internal Decay Level
		Width (D)	Depth (D)		
D-2-1	Compression	0.32	0.40	0.81	1
D-3-1	Tension	0.24	0.41	1.13	2
C-1-1	Compression	0.23	0.50	0.91	1
C-1-2	Neutral Axis	0.25	0.53	1.03	1
RP-3-1	Compression	50 mm shell and 200 mm wide opening		0.80	1
60-3-1	Tension	0.29	0.61	1.11	1
B-1-1	Tension	50 mm shell and 90 mm wide opening		0.79	1
B-2-1	Tension	0.30	0.70	1.00	1

Results indicate that the I_e values for natural woodpecker damage were predicted well using the BF model. On average, analysis predicts $I_e/I_t = 0.95$ with a 14.72 % COV, which is similar in accuracy to predictions for new specimens with woodpecker damage. A major assumption in calculating I_e was that the control specimen bending strength from a specific utility pole has the same bending strength as other specimens from the same pole. This is a practical assumption for research purposes, although it is not strictly correct. Due to the highly variable nature of wood from checks, knots, and local cellular structure, bending strength within a wood pole has some unknown variation. Additional variation was introduced by the presence of low levels of wood decay that varied throughout the length of poles. These assumptions, with unknown errors, contributed to the differences between the theoretical predictions and experimental results.

8.9 In-service Experimental Strain Data

Strain data from in-service control and woodpecker damaged specimens was analyzed in order to better understand cross-section behaviour. Strain profiles provided represent strain levels at one-third of the ultimate load, which are well within the linear-elastic range of cross-section behaviour.

8.9.1 Control Cross-sections

In-service control specimens exhibited a linear strain profile as shown in Figure 90. Linear behaviour is predicted by theoretical section analysis. The magnitude of strain predicted by theoretical analysis is very close to what is observed experimentally for specimen D-3-2, indicating that the assumed modulus of elasticity closely approximates the actual.

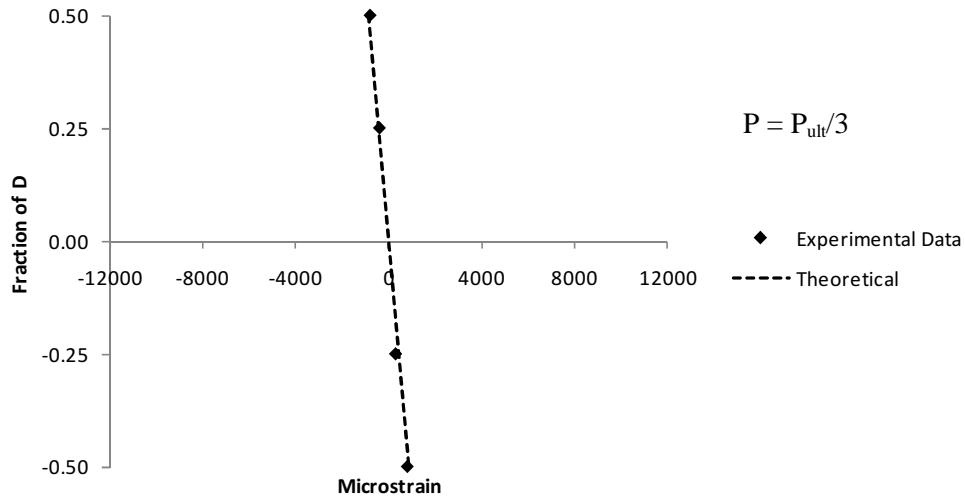


Figure 90. - In-service control specimen strain profile (D-3-2).

8.9.2 Cross-sections with Tension Damage

Specimens with tension fibre damage exhibited linear strain profiles similar to that predicted by theoretical analysis (Figure 91 and Figure 92). This differed considerably from new specimens with tension damage that exhibited tension fibre strains from 2 to 7 times higher than predicted theoretically. Based on observations during dissection, it appears that these differences were due to specimen conditions. In-service specimen D-3-1 was decayed around the surface of the tension hole as shown in Figure 100. As a result, these fibres were ineffective in load resistance and did not undergo stress concentrations and corresponding increased strains as typically observed in new pole specimen cross-sections. During dissection it was observed that the interior core of in-service specimen D-4-3 was decayed and separated from the intact outer shell. As a result, the extreme tension fibres underwent less significant stress concentrations when woodpecker damage was introduced since the interior fibres were already ineffective in load resistance prior to damage introduction. Due to lower stress concentrations, the large strains that were observed in new specimens were not developed in the cross-section of specimen D-4-3.

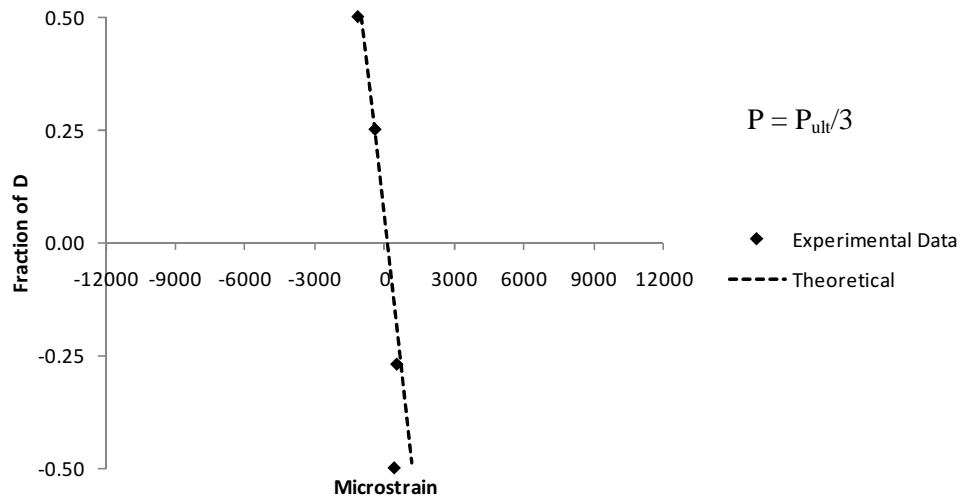


Figure 91. - Strain profile of in-service specimen with tension damage (D-3-1).

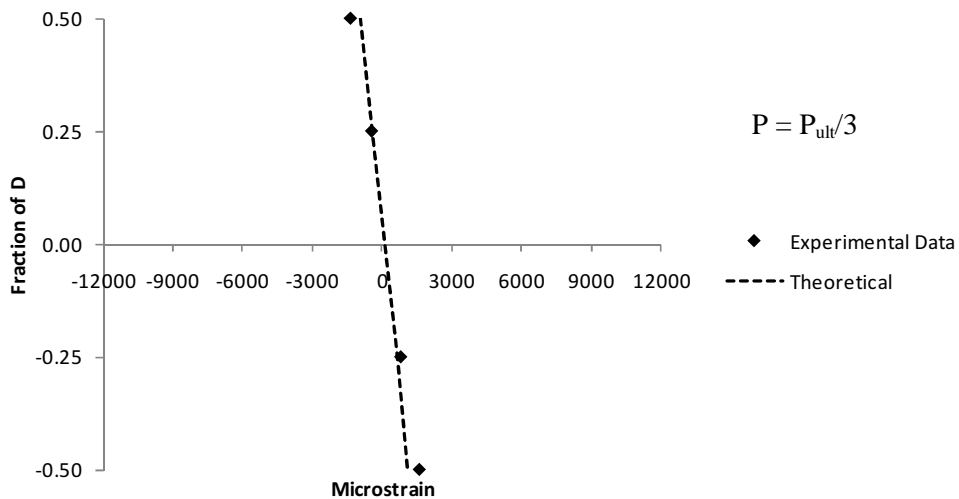


Figure 92. - Strain profile of in-service specimen with tension damage (D-4-3).

8.9.3 Cross-sections with Compression Damage

The in-service specimens with compression fibre damage exhibited similar strain profiles to new specimens with compression damage as shown in Figure 93 and Figure 94. Strain profiles were linear over the majority of the cross-section and rapidly increased near the compression surface where woodpecker damage was present. Experimental results for compression fibre strain were from 2 to 8 times higher than those predicted theoretically.

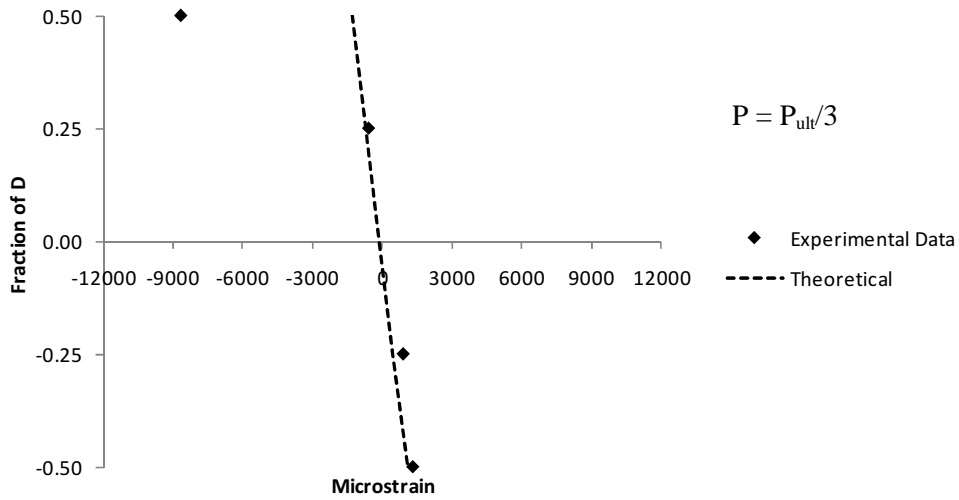


Figure 93. - Strain profile of in-service specimen with compression damage (D-2-1).

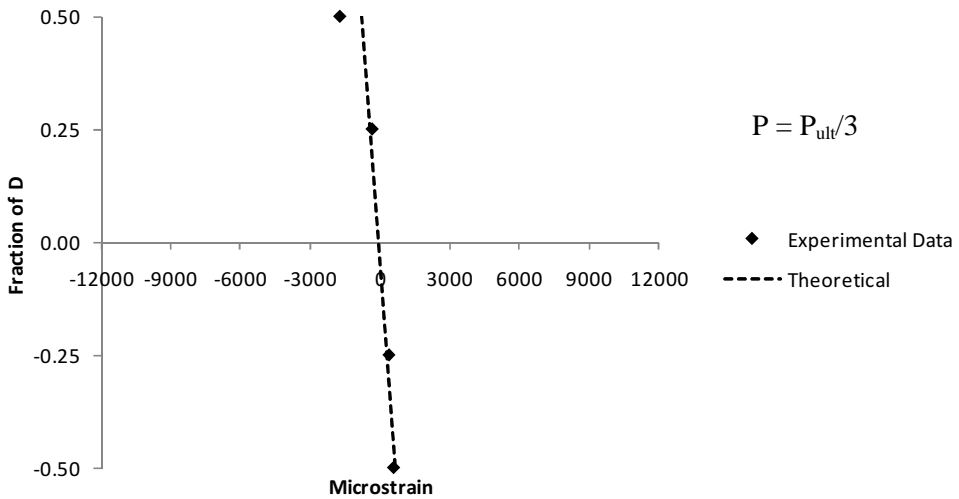


Figure 94. - Strain profile of in-service specimen with compression damage (C-1-1).

8.9.4 Cross-section with Neutral Axis Damage

Specimen C-1-2 with neutral axis damage behaved in a similar manner to the control specimens. This was due to symmetry of damage about the horizontal axis that resulted in similar magnitudes of strain in tension and compression. A strain profile of specimen C-1-2 with neutral axis woodpecker damage is given in Figure 95. This strain profile was modeled well by the theoretical strain profile that incorporated modified moment of inertia due to damage.

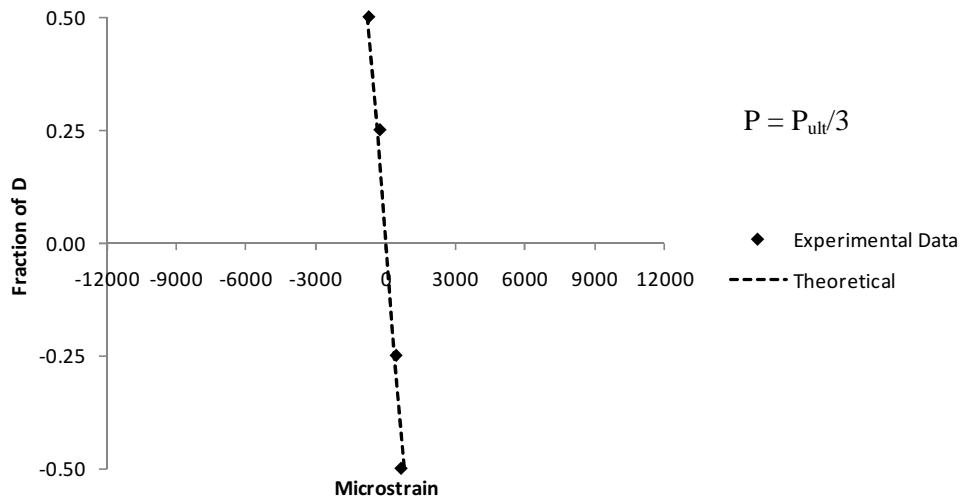


Figure 95. - Strain profile of in-service specimen with neutral axis damage (C-1-2).

8.10 Experimentally Determined Modulus of Elasticity

8.10.1 Modulus of Elasticity Determined from Deflection

Average modulus of elasticity based on deflection for in-service control specimens were calculated using the double integration method with numerical integration as done with the new pole specimens. Strain based modulus of elasticity values were not calculated due to inconsistent data due to surface conditions of the specimens. Shear deflection was not taken into account since depth to span ratios of the specimens were low, making shear deflection negligible. Table 29 provides a summary of modulus of elasticity values for in-service control specimens.

Table 29. - In-service control specimen average modulus of elasticity values.

Specimen	E_{avg} (MPa)	Internal Decay Level	Specimen	E_{avg} (MPa)	Internal Decay Level
D-1-1	2709	3	D-3-2	9118	2
D-1-2	4978	3	D-4-1	4925	3
D-2-1	6566	1	D-4-2	7574	3
D-2-2	7499	1	D-4-3	7468	2
D-3-1	8328	2	-	-	-

The general trend is that specimens with lower modulus of elasticity also have higher levels of internal decay. Modulus of elasticity values averaged 6574 MPa with 31% COV. The Wood Handbook (USDA 1999f) predicts a modulus of elasticity value of 9555 MPa with 22% coefficient-of-variation for lodgepole pine. In-service specimens clearly have reduced modulus of elasticity due to internal decay. The coefficient-of-variation is also very high for in-service specimens due to the large range of internal decay present.

8.10.2 Relationship of Modulus of Elasticity, Bending Strength, and Age

Modulus of elasticity, bending strength, and age are graphed in Figure 96 and Figure 97. It is evident that as the modulus of elasticity of a specimen increases, the bending strength also increases. This trend is somewhat stronger for in-service specimens in comparison to the new pole specimens. In addition, there is a trend that as the age of a specimen increases, the modulus of elasticity decreases.

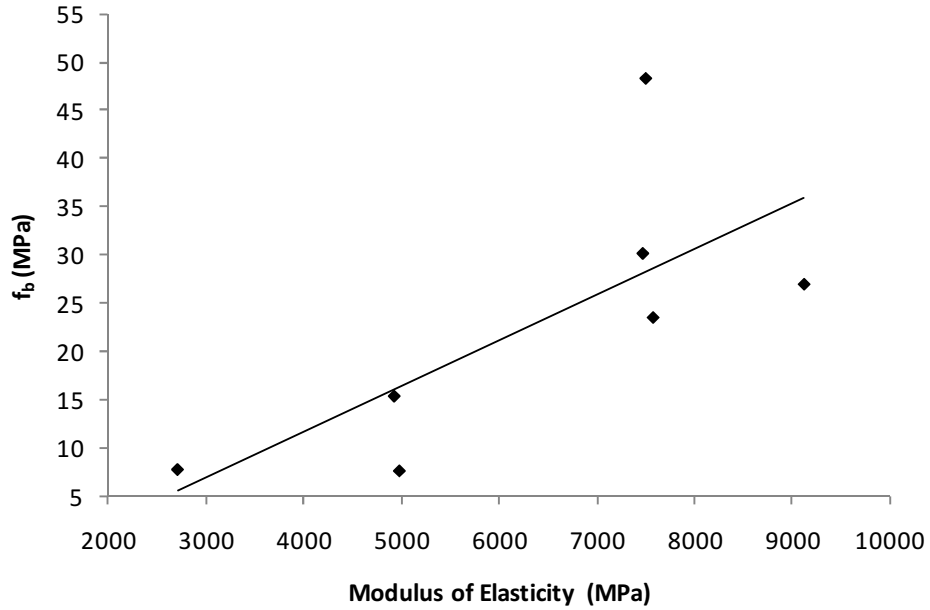


Figure 96. - Bending strength vs. modulus of elasticity for in-service specimens.

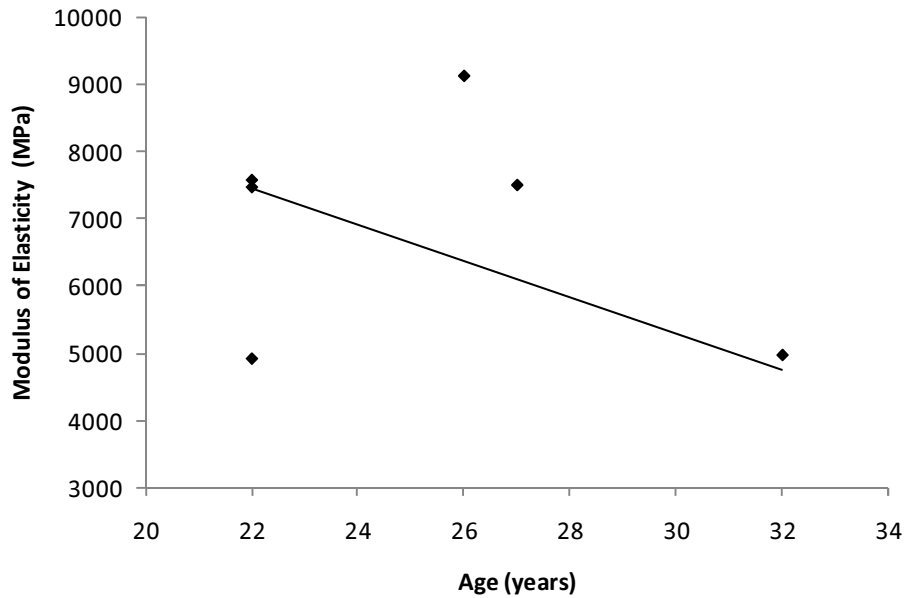


Figure 97. - Modulus of elasticity vs. age for in-service specimens.

8.11 Dissection of Specimen Failure Locations

In order to better understand the behaviour of in-service control and woodpecker damaged cross-sections at failure, specimens were dissected after beam testing. Dissection consisted of cross-sectioning failure locations in 150 mm long segments along the pole length.

8.11.1 Control Specimens

Dissection of control specimens at failure locations indicated tension fibre rupture and shear cracking were the primary modes of failure. As shown in Figure 98, tension fibre rupture typically occurred in the extreme tension fibres since they were under the maximum tensile stress. An example of shear failure can be seen in Figure 99, where a shear crack formed at the neutral axis.

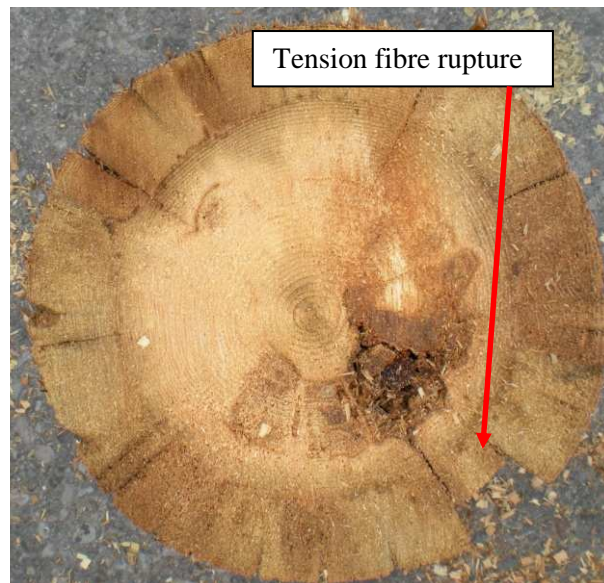


Figure 98. - Cross-section of in-service control specimen (D-3-2).

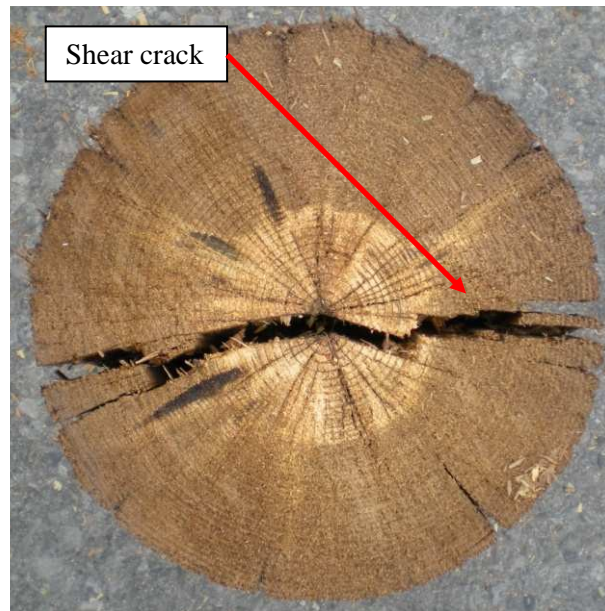


Figure 99. - Cross-section of in-service control specimen (D-2-2).

8.11.2 Tension Oriented Damage Specimens

Specimens with tension oriented damage typically failed due to tension fibre rupture. Similar to the control specimens, tension fibre rupture initiated at the extreme tension fibres and caused fracture of the cross-section. Examples of failure cross-sections of tension specimens with varying levels of damage are shown in Figure 100 and Figure 101.

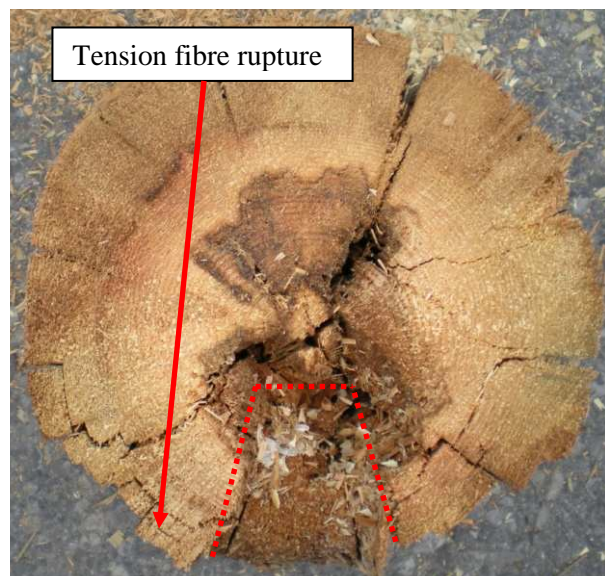


Figure 100. - Cross-section of in-service specimen with tension damage (D-3-1).

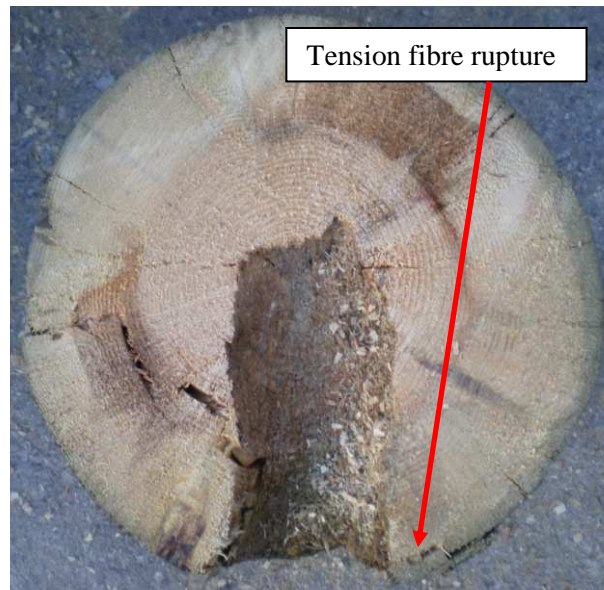


Figure 101. - Cross-section of in-service specimen with tension damage (60-3-1).

8.11.3 Compression Oriented Damage Specimens

Specimens with compression oriented damage typically failed due to tension fibre rupture as shown in Figure 102 and Figure 103. This contrasted the new pole specimen behaviour in which specimens with compression damage underwent compression fibre crushing prior to tension fibre rupture. This change in behaviour appeared to be caused by the brittle nature of the decayed in-service wood that withstood smaller longitudinal deformation prior to failure. As a result, tension fibre rupture occurred at low strain levels before compression fibre crushing would normally occur. An extreme case of nesting level woodpecker damage is shown in Figure 104. Due to the significant reduction in cross-section, tension fibre rupture occurred in a brittle manner with little post-failure strength remaining.

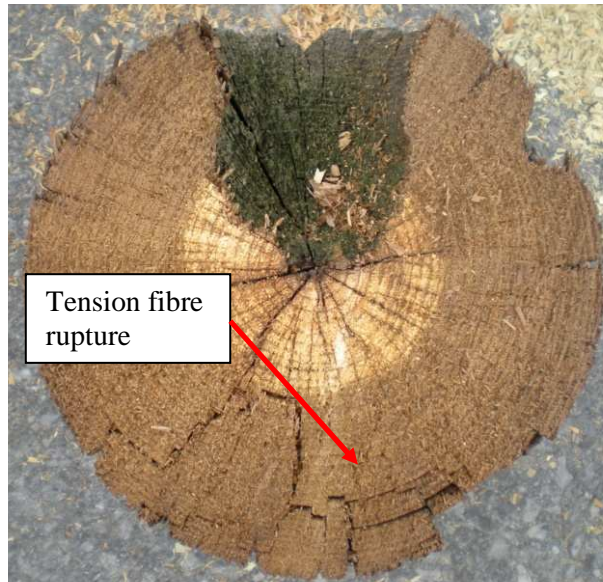


Figure 102. - Cross-section of in-service specimen with compression damage (D-2-1).

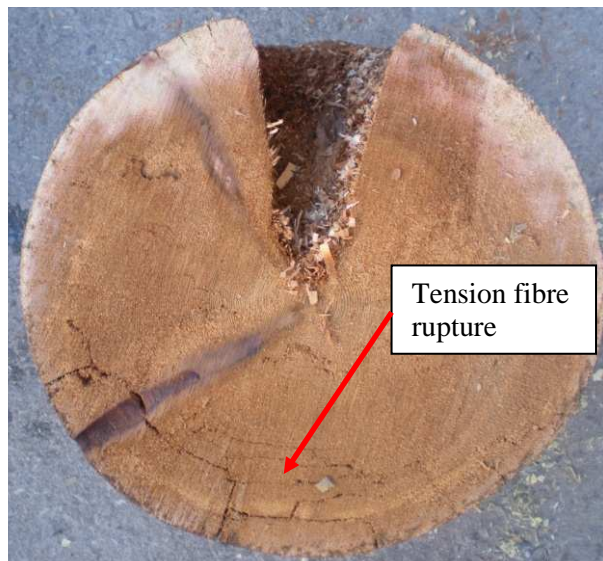


Figure 103. - Cross-section of in-service specimen with compression damage (C-1-1).

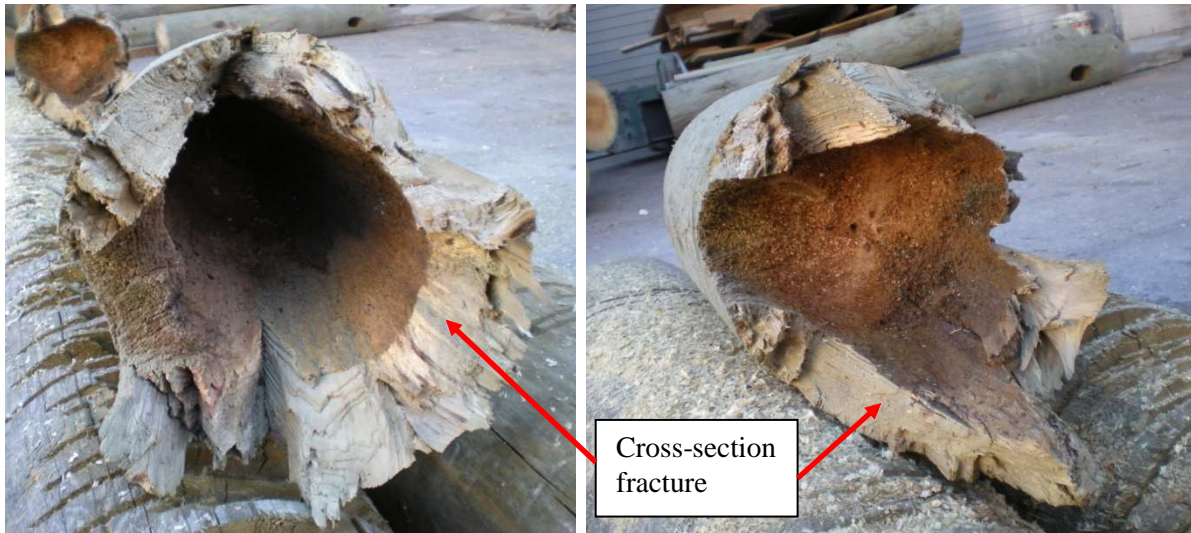


Figure 104. - Cross-section of in-service specimen with compression damage (RP-3-1).

8.11.4 Neutral Axis Oriented Damage Specimens

Specimen C-1-2 with neutral axis oriented damage (Figure 105) was observed to fail due to tension fibre rupture in the same manner as the control specimens.

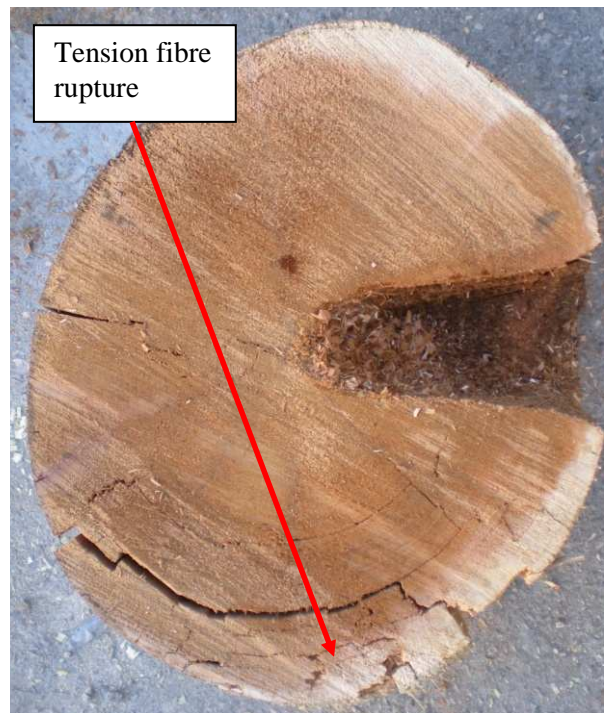


Figure 105. - Cross-section of in-service specimen with neutral axis exploratory damage (C-1-2).

8.12 In-service Specimen Moisture Content

Moisture content samples were taken from each specimen at midspan locations during dissection and are given in Table 30. It was observed that moisture content varied along the length of poles with lowest values at the ends with small diameter, increasing towards ends with large diameter. This trend was attributed to the fact that larger diameter cross-sections require moisture to travel longer paths to exit the wood structure, reducing moisture loss.

Table 30. - Average in-service pole moisture contents.

Pole	MC_{avg} (%)	Pole	MC_{avg} (%)
D-1	25.64	RP-1	38.11
D-2	13.72	RP-2	44.30
D-3	24.42	RP-3	21.95
D-4	19.78	60-3	38.91
C-1	23.02	-	-

8.13 Conclusions

Twenty-four lodgepole pine, western red cedar, and red pine beam specimens were sectioned from in-service utility poles into 4.25 m lengths for flexural beam testing. The in-service poles received had varying levels of natural woodpecker damage and decay. Beam testing indicated that the presence of both woodpecker damage and decay had significant effects on the behaviour of beam specimens. This was observed through reductions in cross-section strength, increases in cross-section strain, and changes in failure modes.

Condition inspections of the in-service specimens was undertaken in order to correlate external indicators with level of decay. Cracks and checks were the most significant indicator based on the specimen ratings and previous research. In-service specimens with severe cracks and checks were consistently observed to have decay. In contrast, woodpecker damage and mechanical damage were not found to be consistent external indicators of decay. These two external indicators were only found to be informative of decay after a significant period of time had elapsed, allowing development of decay. It appears that the same mechanism is responsible for decay regardless of the external indicator present. This mechanism is described as follows:

1. The interior of a specimen's cross-section is exposed to the external environment by cracks and checks, woodpecker damage, mechanical damage, or any other means.
2. Environmental exposure allows moisture and oxygen penetration into the cross-section interior.
3. Extended time periods of exposure result in internal decay occurring.
4. Decay results in significant strength reductions.

Experimental results confirmed that the presence of different levels of decay significantly reduced cross-section strength. Intermediate and advanced levels of decay (levels 2 and 3) caused strength reductions of 47% and 73%, respectively in in-service specimens. The presence of different

levels and orientations of woodpecker damage were also observed to significantly reduce in-service specimen cross-section strength. Strength reductions varied from 0% to 57% depending on the severity of damage present. As the level of woodpecker damage became more severe, the loss in cross-section strength increased. The presence of both woodpecker damage and decay on in-service wood poles was significant and in some cases would require pole replacement according to CSA C22.3 No. 1 Cl. 8.3.1.3 (2006a) when strength is reduced over 40%. Woodpecker damage and internal decay on in-service specimens were independently shown to cause strength reductions of over 40%.

The BF analytical model was used to analyze cross-sections with the presence of varying levels and orientations of woodpecker damage. Analytical predictions correlated well with experimental results which predicted an average value of $I_c/I_t = 0.95$ with a 14.72 % COV, which is similar in accuracy to predictions for new pole specimens with woodpecker damage. This indicates that the BF model provided a good indication of section property reduction for natural woodpecker damage on in-service poles.

Cross-section behaviour was investigated through the use of displacement transducers that allowed the strain profile to be measured. Control specimens and specimens with compression and neutral axis oriented damage behaved in a similar fashion to new pole specimens. In contrast, the strain profiles of in-service specimens with tension oriented damage did not have strain increases at hole locations. This was due to the presence of decay in many tension specimens which rendered interior fibres ineffective in transferring tensile force. As a result, the presence of a hole in a decayed cross-section did not significantly affect cross-sectional behaviour since the removed fibres were ineffective prior to hole introduction. Thus, the strain increases observed in new pole tension specimens were not observed in the in-service tension specimens.

In order to better understand specimen failure modes, specimens were dissected at locations of failure. The majority of specimens failed due to tension fibre rupture and shear crack formation. An important finding was that the proportion of in-service specimen shear failures observed significantly increased in comparison to new specimen testing. The majority of these shear failures occurred in specimens with heavy decay. Decay was found to most significantly affect the interior core of specimens, rendering interior fibres ineffective in strength contribution. As a result, decay caused a large reduction in shear strength since the thickness of the cross-section carrying shear force was significantly reduced. In-service specimens with compression oriented damage typically failed due to tension fibre rupture. This contrasted with new pole specimen behaviour in which specimens with compression damage underwent compression fibre crushing prior to tension fibre rupture. This change in behaviour appears to be caused by the brittle nature of the decayed in-service wood. As a result, tension fibre rupture occurred at low strain levels before compression fibre crushing would normally occur.

Chapter 9 Application to Utility Pole Replacement

The previously described analytical and experimental research helped develop an improved understanding of the strength reducing effect of woodpecker damage and wood decay on utility poles. This research has been condensed into three different methods that allow the strength reducing effect of woodpecker damage on utility poles to be determined for field applications. The three methods developed have varying levels of analysis refinement and ease of application.

9.1 CSA C22.3 No. 1 Criteria

Due to woodpecker damage and wood decay, wood utility poles require replacement or reinforcement. According to CSA C22.3 No. 1 Cl. 8.3.1.3 (2006a), “When the strength of a structure has deteriorated to 60% of the required capacity, the structure shall be reinforced or replaced”. This replacement criteria is applied to structures using simplified or more detailed analysis methods.

9.2 Wood Decay

Based on a limited amount of experimental tests, the presence of wood decay was observed to cause large strength reduction in wood utility poles. The presence of wood decay at the lowest level detectable by visual methods caused strength reduction over 40%. This level of strength reduction exceeds the allowable limit according to CSA C22.3 No.1 (2006a), indicating that pole replacement is necessary. Based on current experimental results, if wood decay is present at any level, wood pole replacement is necessary.

9.3 Woodpecker Damage

The BF analytical model developed to predict strength reduction caused by woodpecker damage was verified by experimental beam testing. According to experimental results, the BF analytical model is a good predictor of strength reduction caused by woodpecker damage. As a result, the BF analytical model was used to predict strength reduction when developing methods of determining whether utility pole replacement is necessary or not when woodpecker damage is present.

9.3.1 Simplified Method

The simplified method of determining wood utility pole replacement is practical for use in field applications. This method is based on identifying the most severe level of woodpecker damage present in a wood utility pole. All woodpecker damage is assumed to occur in the most critical orientation and location along the pole length, maximizing strength reduction. The strength reduction present in a wood utility pole can then be determined from Table 31.

Table 31. - Strength reduction caused by woodpecker damage.

Damage Level	SR (%)
Exploratory	21
Feeding	33
Nesting	41

Using the simplified method, only wood utility poles with nesting level woodpecker damage require replacement according to CSA C22.3 No. 1 (2006a). A disadvantage of this method is that it is conservative in many situations due to simplifications.

9.3.2 Chart Method

The chart method of determining wood utility pole replacement is practical for use in field applications and allows more parameters to be varied than when using the simplified method. This method is very similar to the HONI method that was presented in Section 3.2 that categorizes woodpecker damage into exploratory, feeding, and nesting levels. Based on the level of damage present (determined by hole depth), one of the charts in Figure 106, Figure 107, Figure 108 is referred to. These charts were developed using the previously described woodpecker damage BF analytical model that was verified by experimental results. Once one of the three charts is chosen, the width of hole and circumference of the pole at the damage location is determined and the remaining strength of the cross-section is read off of the graph. If the remaining strength of a cross-section is less than 60%, the utility pole should be replaced according to CSA C22.3 No. 1 (2006a). This process is repeated for all the holes present on a pole. The following steps outline this procedure:

1. Choose the exploratory, feeding, or nesting level graph for remaining strength based on the depth of the hole present.
2. Read off the cross-section strength reduction from the graph previously chosen based on hole width and cross-section circumference at the damage location.
3. If the remaining strength of a cross-section is less than 60% the utility pole should be replaced.
4. Repeated for all the holes present on a pole.

The charts developed for exploratory and feeding level damage have very similar trends to the charts developed by HONI. In contrast, the chart developed for nesting level damage has a much different trend than the chart developed by HONI. This is due to the assumption in the undertaken research that a constant 2” shell thickness is present in wood utility poles with nesting damage, regardless of the width of the hole opening. This assumption was supported by observations made of received in-service poles from HONI.

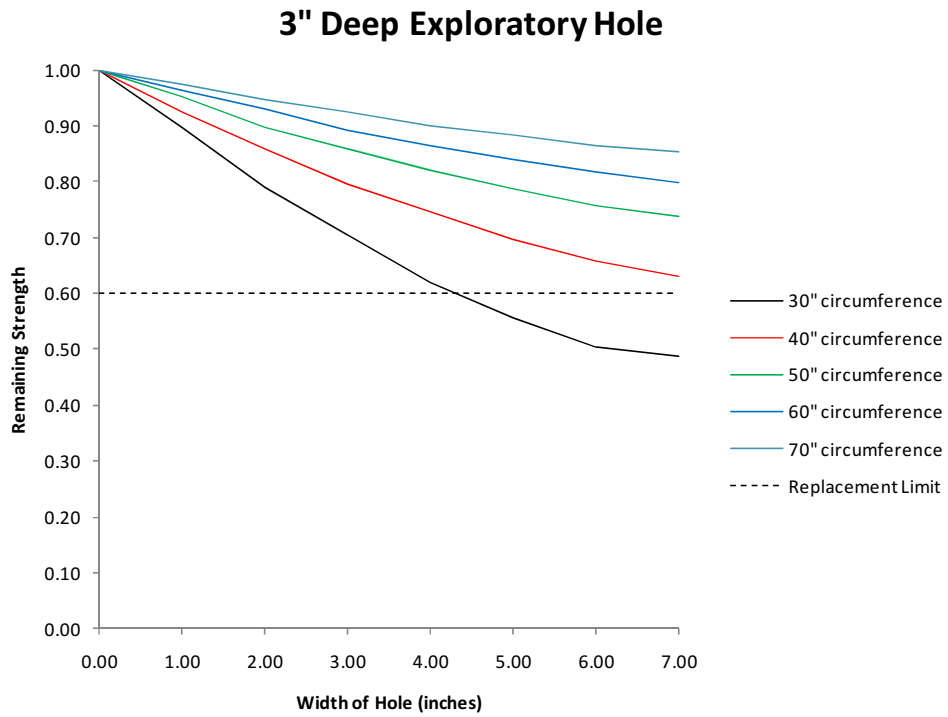


Figure 106. - Remaining strength due to exploratory level woodpecker damage.

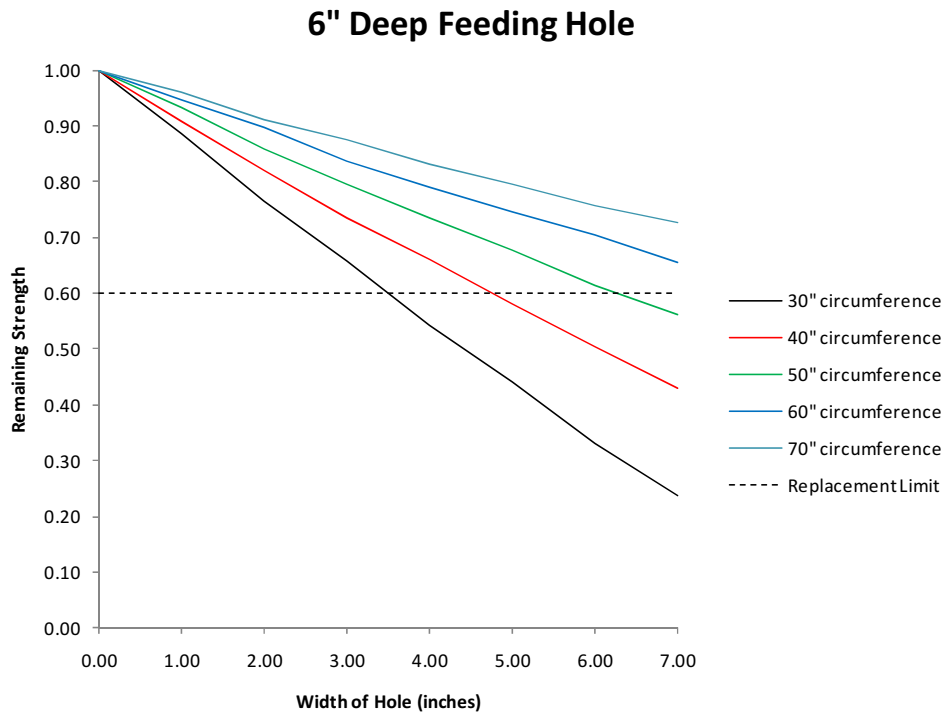


Figure 107. - Remaining strength due to feeding level woodpecker damage.

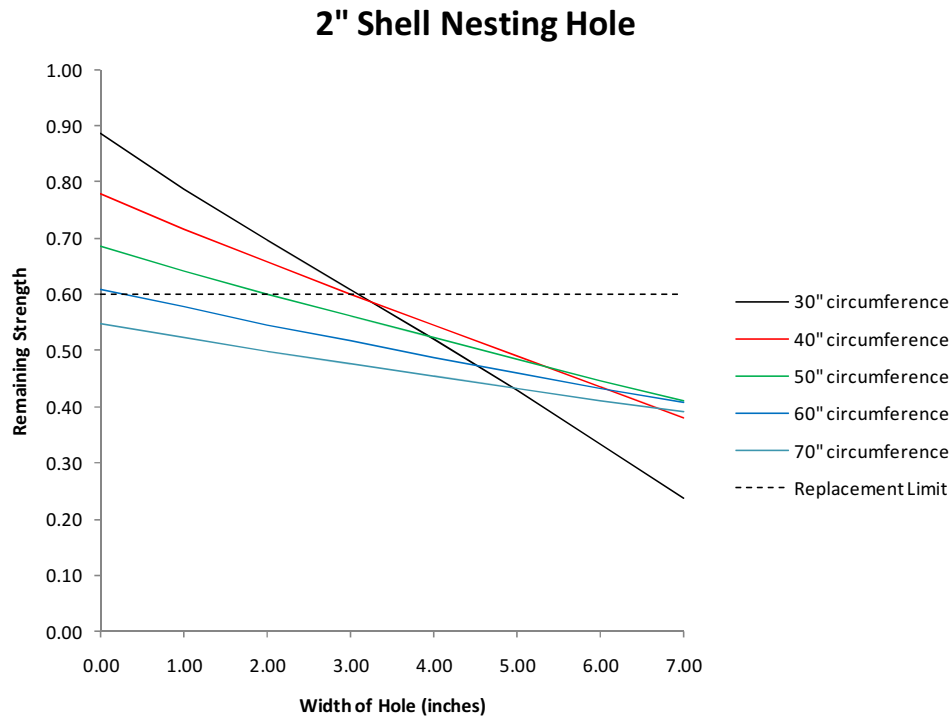


Figure 108. - Remaining strength due to nesting level woodpecker damage.

9.3.3 Case-specific Method

The case-specific method of determining wood utility pole replacement requires more rigorous analysis and yields more accurate results. This method requires woodpecker holes to be determined in terms of level and orientation, as well as location along the length of the pole. A structural analysis of the pole is then performed to determine the effect of woodpecker damage at different locations. The previously derived woodpecker damage BF analytical model (Chapter 4) is incorporated to model the effects of woodpecker damage. If a structure has less than 60% of the required resistance due to the presence of woodpecker damage, the pole must be replaced according to CSA C22.3 No. 1 (2006a). This approach explicitly accounts for the strength reducing effect caused by multiple damage locations. The following steps outline this procedure:

1. Determine woodpecker damage level, orientation, and location along the length of the pole (for each damage location).
2. Perform a structural analysis of the pole with woodpecker damage effects included.
3. Determine if the structure has less than 60% of the required resistance required due to the presence of woodpecker damage.

This method results in a more accurate prediction of strength reduction since it is not assumed that woodpecker damage is located at the critical design section and orientation, rather the actual location of woodpecker damage and orientation is used in analysis. A disadvantage of this method is that it

requires more rigorous analysis compared to the simplified method. The following example displays this method:

Assume a new pole is designed with an allowable bending stress of 30 MPa as shown in Figure 109, using the previously developed structural analysis model.

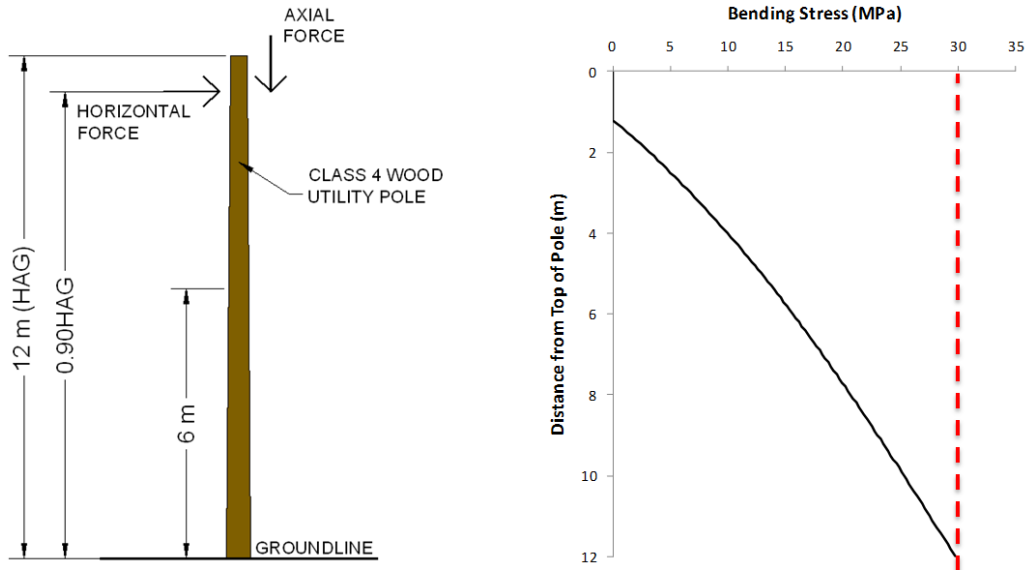


Figure 109. - New pole design.

The pole is then damaged by a woodpecker creating a 4” wide nesting hole in the extreme bending fibres at 6 m from the pole base and is re-analyzed as shown in Figure 110.

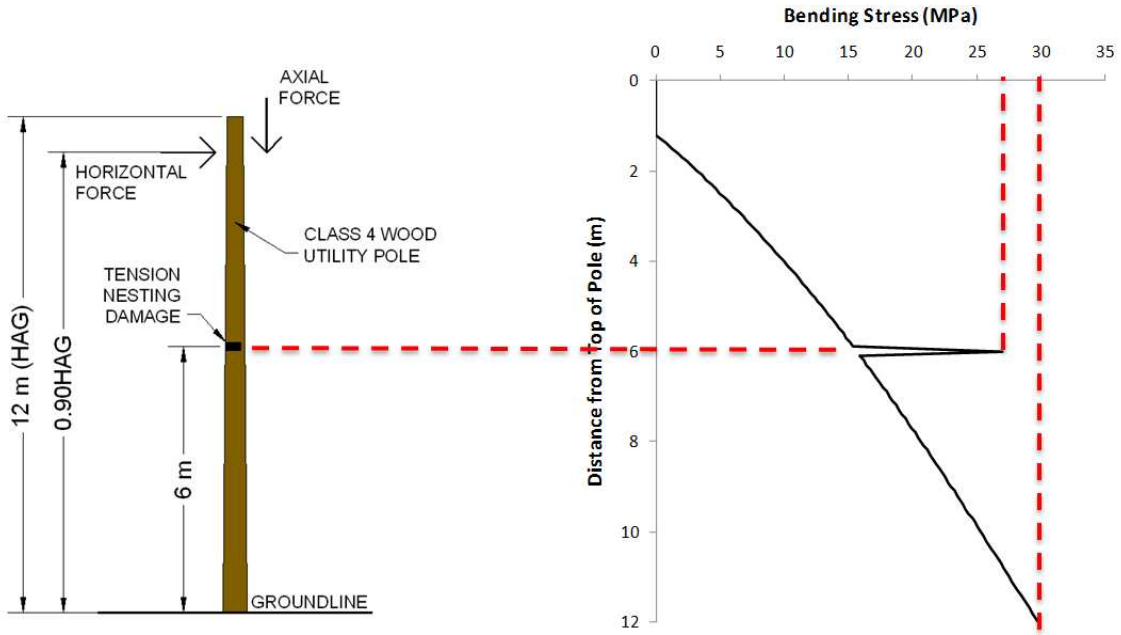


Figure 110. - Analysis of pole with woodpecker damage.

It is evident from the second analysis that the wood utility pole was significantly damaged by the woodpecker hole, resulting in a stress increase at the damage location. Despite this damage, the pole is suitable to remain in-service since the pole has greater than 60% of the required strength to resist the imposed loads. According to the simplified and chart method, this pole would require replacement. This shows how the case-specific method is more accurate and results in a less conservative pole assessment.

Chapter 10 Conclusions and Recommendations

In order to determine the effect of woodpecker damage and wood decay on the strength of wood utility poles, background literature review and analytical work was performed. The literature review involved reviewing current design standards for wood utility poles, the mechanical properties of wood, the effect of decay on wood strength, and the effect of woodpecker damage on wood utility pole strength. The Hydro One Networks Incorporated (HONI) current approach to determining the effects of woodpecker damage and wood decay on wood utility pole strength was reviewed. Based on the HONI classification of woodpecker damage, woodpecker damage levels were organized into three levels of severity for research purposes.

Three analytical models were developed that predicted the theoretical strength reduction caused by the presence of woodpecker damage in a cross-section. The models developed were based on mechanics of materials principles using modified cross-section geometry due to woodpecker damage. A bending failure model was developed since, in the structural design of utility poles, bending moment stresses are known to be the critical design parameter. It was decided that the significance of shear stress in a cross-section should also be considered since the presence of woodpecker damage could cause shear stresses to be a significant parameter. As a result, a shear-bending and a shear failure model was developed to determine the significance of shear stress on cross-section behaviour. These models were developed for analysis purposes and were verified by the subsequent experimental program. In order to develop an experimental beam test setup that simulated the load effects representative of in-service utility poles, a utility pole structural analytical model was developed. This analytical model incorporated the theoretical effect of woodpecker damage using the previously developed woodpecker damage analytical models. Using the utility pole structural analytical model, a parametric study was performed with varying levels and orientation of woodpecker damage. Based on this study, two experimental beam test setups were developed for use in the experimental program for testing of new and in-service utility poles.

A total of 28 new and in-service utility poles were received from HONI for experimental testing. The poles received were cut into 4.25 m for beam testing. A single new pole and in-service specimen from each pole was tested as a control specimen without woodpecker damage for reference wood strength. The remainder of the new pole specimens were mechanically introduced with woodpecker damage. The remainder of the in-service specimens were tested with natural woodpecker damage. Tested specimens were analyzed and results were compared with the woodpecker damage analytical model predictions. Results indicated that the effect of woodpecker damage is well modelled by the woodpecker damage analytical models. Overall, the BF analytical model was preferable for cross-section analysis due to the accuracy of the model predictions and the simplicity of required calculations. The effect of decay on wood strength was also determined from experimental in-service specimen results. Results indicated that by the time wood decay can be detected in wood utility poles, severe reduction in wood strength has occurred.

Analytical and experimental results were used to develop three application methods for determining whether utility pole replacement is necessary due to the presence of woodpecker damage. These three methods include the simplified method, the chart method, and the case-specific method. The simplified method allows determination of whether a utility pole should be replaced based only

on knowledge of the most severe level of woodpecker damage present in a pole. The chart method takes into account additional factors such as the diameter of the pole at the location of the woodpecker damage and the width of the hole opening. The case-specific method is advantageous since it accounts for the parameters used in the chart method and allows the location of woodpecker damage along the length of a pole to be accounted for. The simplified and chart methods are preferable since they are relatively simple and easy to implement in the field. The case-specific method requires a full structural analysis of the utility pole in question to be undertaken and is useful for more accurately assessing whether replacement is necessary.

10.1 Conclusions

The main objective of this thesis was to determine the effect of woodpecker damage and wood decay on the strength of wood utility poles.

10.1.1 New Specimen Experimental Results

- Experimental results confirmed that the presence of different levels and orientations of woodpecker damage significantly reduced cross-section strength.
- As the level of woodpecker damage became more severe the loss in cross-section strength increased.
- Damage oriented in the neutral axis position caused smaller reductions in strength in comparison to tension or compression orientations.
- Nesting level damage oriented in tension or compression locations caused severe strength reduction of over 40%.
- The presence of woodpecker damage was observed to cause significant strength reduction that would in some cases require replacement according to CSA C22.3 No. 1 Cl. 8.3.1.3 (2006a).

10.1.2 In-service Specimen Experimental Results

- Experimental results confirmed that the presence of different levels of decay significantly reduced cross-section strength.
- Intermediate and advanced levels of decay (levels 2 and 3) caused strength reductions of 47% and 73%, respectively.
- The incidence of shear failures increased in poles with decay. Even beams such as control specimens, that were predicted to fail in bending, failed in shear due to the effects of decay.
- The presence of different levels and orientations of woodpecker damage were observed to significantly reduce in-service specimen cross-section strength. Strength reductions varied from 0% to 57% depending on the severity of damage present.
- As the level of woodpecker damage became more severe, the loss in cross-section strength increased.
- The presence of both woodpecker damage and decay on in-service wood poles was significant and in some cases would require pole replacement according to CSA C22.3 No. 1 Cl. 8.3.1.3 (2006a).

10.1.3 Comparison of Analytical Model with Experimental Results

- Analytical predictions correlated well with experimental results for new and in-service specimens when the appropriate model was used according to failure mode.
- Bending failure effects were dominant in specimens with woodpecker damage introduced.
- The BF analytical model was preferable for cross-section analysis due to the accuracy of the model predictions and the simplicity of required calculations.
- The analytical models developed are suitable for estimating strength reduction caused by varying levels and orientations of woodpecker damage in in-service utility poles.

10.1.4 Application to Utility Pole Replacement

- “When the strength of a structure has deteriorated to 60% of the required capacity, the structure shall be reinforced or replaced” according to CSA C22.3 No. 1 Cl. 8.3.1.3 (2006a). This criteria was used in developing application methods.
- Analytical and experimental results were sufficient for developing application methods for determining whether utility pole replacement is necessary or not.
- The presence of wood decay at any level in wood utility poles requires replacement due to strength reductions in excess of 40%.
- At the most simplified level of application, the presence of nesting level woodpecker damage requires utility poles to be replaced.
- Using the chart method, woodpecker hole severity and width of opening are considered in determining whether replacement of a utility pole is necessary.
- Using a more rigorous and thorough method, determination of whether pole replacement is necessary can be more accurately assessed. This method requires woodpecker holes to be determined in terms of level and orientation, as well as location along the length of the pole. A structural analysis of the pole is then performed to determine the effect of woodpecker damage at different locations.

10.2 Recommendations for Future Research

- It is recommended that further experimental testing be undertaken in order to improve the data set on the effects of woodpecker damage and wood decay on wood utility pole strength. This would increase the sample size of experimental results and allow statistical analysis to be applied to the data.
- Conduct direct shear tests on new and in-service poles to assess shear strength of wood poles and effect of damage and decay on f_v .
- It is recommended that a wood utility pole structural-reliability model be developed that incorporates the effect of woodpecker damage and wood decay. Using this model a parametric study could be undertaken to determine the reliability levels achieved along the length of poles with the following strength reducing parameters: level of woodpecker damage, orientation of woodpecker damage, and level of decay.

References

- ANSI. O5.1 - Wood Poles - Specifications & Dimensions. 2008.
- ASTM. D 1036 - Standard Test Methods of Static Tests of Wood Poles. West Conshohocken, Pennsylvania: American Society of Testing and Materials, 2005a.
- . D 143 - Standard Practice for Small Clear Specimens of Timber. West Conshohocken, Pennsylvania: American Society of Testing and Materials, 2009b.
- . D 2225 - Standard Practice for Establishing Clear Wood Strength Values. West Conshohocken, Pennsylvania: American Society of Testing and Materials, 2006c.
- . D 245 - Standard Practice for Establishing Structural Grades and Related Allowable Properties for Visually Graded Lumber. West Conshohocken, Pennsylvania: American Society of Testing and Materials, 2006d.
- . D 2899 - Standard Practice for Establishing Allowable Stresses for Round Timber Piles. West Conshohocken, Pennsylvania: American Society of Testing and Materials, 2003e.
- . D 3200 - Standard Specification and Test Method for Establishing Recommended Design Stresses for Round Timber Construction Poles. West Conshohocken, Pennsylvania: American Society of Testing and Materials, 2005f.
- . D 4442 - Standard Test Methods for Direct Moisture Content Measurement of Wood and Wood-Based Materials. West Conshohocken, Pennsylvania: American Society of Testing and Materials, 2007g.
- . D 4933 - Standard Guide for Moisture Conditioning of Wood and Wood-Based Materials. West Conshohocken, Pennsylvania: American Society of Testing and Materials, 2004h.
- Bhuyan, G. "Condition Based Serviceability and Reliability Assessment of Wood Pole Structures." IEEE (1998): 333-9.
- CSA. C22.3 no. 1-06 - Overhead Systems. Mississauga, ON: Canadian Standards Association, 2006a.
- . C22.3 no. 60826-06 - Design Criteria of Overhead Transmission Lines. Mississauga, ON: Canadian Standards Association, 2006b.
- . O116 - Power and Communication Sawn Wood Crossarms. Mississauga, ON: Canadian Standards Association, 2008c.
- . O15 - Wood Utility Poles and Reinforcing Stubs. Mississauga, ON: Canadian Standards Association, 2005d.

---. O86 - Engineering Design in Wood. Mississauga, ON: Canadian Standards Association, 2009e.

Gaiotti, Regina, and Bryan Strafford Smith. "P-Delta Analysis of Building Structures." Journal of Structural Engineering. 115.4 (1989): 755-70.

Grigsby, L. L. The Electric Power Engineering Handbook. USA: CRC Press, 2001.

Harness, Richard E., and Eric L. Walters. "Knock on Wood." IEEE Industry Application Magazine. 2005: 68-73.

HONI. 2009 Annual Information Report. Hydro One Networks Incorporated, 2009.

HONI. Woodpecker Damage and Wood Decay on Wood Utility Poles. Hydro One Networks Incorporated, 2010.

Jones, James. "One-Way ANOVA." August 25, 2010 2010.
<<http://people.richland.edu/james/lecture/m170/ch13-1wy.html>>.

Li, H., J. Zhang, and G. Bhuyan. "Reliability Assessment of Electrical Overhead Distribution Wood Poles." Probabilistic Methods Applied to Power Systems, 2006. PMAPS 2006. (2006): 1-4.

McCarthy, Francis J. Condition Assessment of Wooden Cross Arms in 230 kV Transmission Structures. M.A.Sc University of Waterloo, 2005.

Mikhelson, Ilya. "Structural Engineering Formulas." New York, NY: McGraw-Hill, 2004.

Pandey, M. D., et al. "Development of a Condition Assessment Model for Transmission Line in-Service Wood Crossarms." Canadian Journal of Civil Engineering. 3 (2010a): 480-9. .

Pandey, M. D., et al. "Experimental Evaluation of Remaining Strength of Crossarms in Gulfport Transmission Line Wood Structures." Canadian Journal of Civil Engineering. 37 (2010b): 638-47.

Rumsey, R. L., and G. E. Woodson. "Strength Loss in Southern Pine Poles Damaged by Woodpeckers." Forest Products Journal. 23.12 (1973): 47-50.

USDA. Derivation of Fiber Stresses from Strength Values of Wood Poles. Vol. FPL-39. Madison, WI: Forest Products Laboratory, 1965a.

---. Derivation of Nominal Strength for Wood Utility Poles. Vol. FPL-GTR-128. Madison, WI: Forest Products Laboratory, 2001b.

---. Design Manual for High Voltage Transmission Lines. Vol. 1724E-200. Rural Utilities Services, 2009c.

- . Designated Fiber Stress for Wood Poles. Vol. FPL–GTR–158. Madison, WI: Forest Products Laboratory, 2005d.
- . Strength of Orthotropic Materials Subject to Combined Stresses. Vol. 1816. Madison, WI: Forest Products Laboratory, 1962e.
- . Wood Handbook. Vol. FPL–GTR–113. Madison, WI: Forest Products Laboratory, 1999f.
- van der Put, T. A. C. M. "Failure Criterion for Timber Beams Loaded in Bending, Compression and Shear." Wood Material Science and Engineering. 5.1 (2010): 41-9.
- Vidor, Flavio L. R., et al. "Inspection of Wooden Poles in Electrical Power Distribution Networks in Southern Brazil." IEEE Transactions on Power Delivery. 25.1 (2010): 479-84.
- Yoshihara, H., and T. Kawasaki. "Failure Behavior of Spruce Wood Under Bending-Shear Combined Stress Field." Journal of Materials in Civil Engineering. 18.1 (2006): 93-8.

Appendix A: C_b and C_s Constants for Analytical Models

Table 32. - Analytical model C_b and C_s constants for vertically oriented damage.

Woodpecker Damage Ordinate From Undamaged Face (D)	Vertical Exploratory		Vertical Feeding		Vertical Nesting	
	C_b	C_s	C_b	C_s	C_b	C_s
0	8.56E-02	0.00	7.66E-02	0.00	6.07E-02	0.00
0.05	9.58E-02	0.37	8.63E-02	0.41	6.81E-02	0.52
0.1	1.09E-01	0.69	9.88E-02	0.77	7.76E-02	0.98
0.15	1.26E-01	0.98	1.16E-01	1.08	9.02E-02	2.69
0.2	1.49E-01	1.22	1.39E-01	1.34	1.08E-01	2.64
0.25	1.83E-01	1.42	1.75E-01	1.55	1.34E-01	2.70
0.3	2.38E-01	1.58	2.35E-01	1.70	1.76E-01	2.77
0.325	N/A	N/A	N/A	N/A	N/A	N/A
0.35	3.38E-01	1.69	3.59E-01	1.81	2.57E-01	2.83
0.4	5.84E-01	1.76	7.61E-01	1.86	4.78E-01	2.86
0.4448	N/A	N/A	0.00E+00	1.87	N/A	N/A
0.45	2.15E+00	1.79	6.55E+00	1.86	3.39E+00	2.85
0.4582	N/A	N/A	N/A	N/A	0.00E+00	2.85
0.4687	0.00E+00	1.79	N/A	N/A	N/A	N/A
0.5	1.28E+00	1.77	6.17E-01	1.81	6.65E-01	2.80
0.55	4.93E-01	1.71	3.24E-01	2.43	3.03E-01	2.70
0.6	3.06E-01	1.60	2.20E-01	2.30	1.96E-01	2.56
0.65	2.21E-01	1.83	1.66E-01	2.12	1.45E-01	2.36
0.7	1.73E-01	1.66	1.34E-01	1.90	1.15E-01	2.11
0.75	1.43E-01	1.46	1.12E-01	1.64	9.53E-02	1.81
0.8	1.21E-01	1.22	9.59E-02	1.34	8.13E-02	1.47
0.85	1.05E-01	0.94	8.41E-02	1.00	7.10E-02	1.08
0.9	9.30E-02	0.62	7.49E-02	0.62	6.29E-02	0.64
0.95	8.33E-02	0.28	6.74E-02	0.22	5.65E-02	0.17
0.9684	N/A	N/A	N/A	N/A	5.45E-02	0.00
0.977	N/A	N/A	6.40E-02	0.00	N/A	N/A
0.9899	7.70E-02	0.00	N/A	N/A	N/A	N/A
1	N/A	N/A	N/A	N/A	N/A	N/A

Table 33. - Analytical model C_b and C_s constants for horizontally oriented damage.

Ordinate (D)	Horizontal Exploratory		Horizontal Feeding		Horizontal Nesting	
	C_b	C_s	C_b	C_s	C_b	C_s
0	9.77E-02	0.00	9.62E-02	0.00	9.22E-02	0.00
0.05	1.09E-01	0.32	1.07E-01	0.33	1.02E-01	0.34
0.1	1.22E-01	0.61	1.20E-01	0.62	1.15E-01	0.65
0.15	1.40E-01	0.87	1.37E-01	0.88	1.32E-01	0.92
0.2	1.63E-01	1.09	1.60E-01	1.11	1.54E-01	1.16
0.25	1.95E-01	1.28	1.92E-01	1.30	1.84E-01	1.36
0.3	2.44E-01	1.43	2.41E-01	1.46	2.31E-01	1.52
0.325	N/A	N/A	N/A	N/A	2.64E-01	12.55
0.35	3.26E-01	1.55	3.21E-01	2.85	3.07E-01	11.79
0.4	4.89E-01	2.51	4.81E-01	2.91	4.61E-01	10.83
0.45	9.77E-01	2.55	9.62E-01	2.95	9.22E-01	10.35
0.5	0.00E+00	2.57	0.00E+00	2.96	0.00E+00	10.21
0.55	9.77E-01	2.55	9.62E-01	2.95	9.22E-01	10.35
0.6	4.89E-01	2.51	4.81E-01	2.91	4.61E-01	10.83
0.65	3.26E-01	1.55	3.21E-01	2.85	3.07E-01	11.79
0.675	N/A	N/A	N/A	N/A	2.64E-01	12.55
0.7	2.44E-01	1.43	2.41E-01	1.46	2.31E-01	1.52
0.75	1.95E-01	1.28	1.92E-01	1.30	1.84E-01	1.36
0.8	1.63E-01	1.09	1.60E-01	1.11	1.54E-01	1.16
0.85	1.40E-01	0.87	1.37E-01	0.88	1.32E-01	0.92
0.9	1.22E-01	0.61	1.20E-01	0.62	1.15E-01	0.65
0.95	1.09E-01	0.32	1.07E-01	0.33	1.02E-01	0.34
1	9.77E-02	0.00	9.62E-02	0.00	9.22E-02	0.00

Appendix B: Pre-experimental Study M/V Ratios

Table 34. - 13.72 m pole M/V ratios (bending failure).

Resultant Height (m)	Damage Level	Vertical M/V Ratio	Horizontal M/V Ratio
0.90HAG	Undamaged	9.94	9.94
	Exploratory	3.97 - 11.24	9.00 - 11.35
	Feeding	2.85 - 10.84	7.84 - 11.79
	Nesting	2.19 - 10.53	6.46 - 11.68
0.80HAG	Undamaged	10.40	10.40
	Exploratory	4.23 - 9.95	9.47 - 10.39
	Feeding	3.11 - 9.65	8.32 - 10.36
	Nesting	2.44 - 9.42	6.72 - 10.28

Table 35. - 15.24 m pole M/V ratios (bending failure).

Resultant Height (m)	Damage Level	Vertical M/V Ratio	Horizontal M/V Ratio
0.90HAG	Undamaged	10.31	10.31
	Exploratory	4.08 - 12.71	9.14 - 11.49
	Feeding	2.95 - 12.21	7.98 - 13.16
	Nesting	2.29 - 11.82	6.60 - 13.27
0.80HAG	Undamaged	11.13	11.13
	Exploratory	4.44 - 11.26	9.95 - 11.83
	Feeding	3.10 - 10.89	8.56 - 11.79
	Nesting	2.43 - 10.59	6.95 - 11.68

Table 36. - 16.76 m pole M/V ratios (bending failure).

Resultant Height (m)	Damage Level	Vertical M/V Ratio	Horizontal M/V Ratio
0.90HAG	Undamaged	11.47	11.47
	Exploratory	4.55 - 14.02	10.30 - 12.89
	Feeding	3.21 - 13.47	8.90 - 14.80
	Nesting	2.53 - 13.04	7.28 - 14.64
0.80HAG	Undamaged	12.36	12.36
	Exploratory	4.96 - 12.43	10.95 - 13.05
	Feeding	3.61 - 12.01	9.55 - 13.01
	Nesting	2.73 - 11.68	7.93 - 12.89

Table 37. - 18.29 m pole M/V ratios (bending failure).

Resultant Height (m)	Damage Level	Vertical M/V Ratio	Horizontal M/V Ratio
0.90HAG	Undamaged	11.85	11.85
	Exploratory	4.69 - 15.51	10.67 - 13.27
	Feeding	3.34 - 14.84	9.27 - 15.44
	Nesting	2.66 - 14.31	7.64 - 16.27
0.80HAG	Undamaged	12.84	12.84
	Exploratory	5.17 - 13.74	11.42 - 14.50
	Feeding	3.61 - 13.24	10.02 - 14.45
	Nesting	2.92 - 12.84	8.16 - 14.31

Table 38. - 13.72 m pole M/V ratios (shear-bending interaction failure).

Resultant Height (m)	Damage Level	Vertical M/V Ratio	Horizontal M/V Ratio
0.90HAG	Undamaged	9.89	9.89
	Exploratory	4.01 - 9.58	8.79 - 9.88
	Feeding	2.84 - 9.43	7.90 - 9.84
	Nesting	2.13 - 9.35	6.32 - 9.75
0.80HAG	Undamaged	10.40	10.40
	Exploratory	4.21 - 9.92	9.11 - 10.39
	Feeding	2.84 - 9.60	8.24 - 10.36
	Nesting	2.14 - 9.36	6.69 - 10.27

Table 39. - 15.24 m pole M/V ratios (shear-bending interaction failure)

Resultant Height (m)	Damage Level	Vertical M/V Ratio	Horizontal M/V Ratio
0.90HAG	Undamaged	10.60	10.60
	Exploratory	4.20 - 10.01	9.27 - 10.59
	Feeding	2.76 - 9.81	8.14 - 10.55
	Nesting	2.28 - 9.70	6.77 - 10.45
0.80HAG	Undamaged	11.19	11.19
	Exploratory	4.25 - 10.42	9.67 - 11.18
	Feeding	3.08 - 10.25	8.57 - 11.14
	Nesting	2.37 - 10.15	7.00 - 10.83

Table 40. - 16.76 m pole M/V ratios (shear-bending interaction failure).

Resultant Height (m)	Damage Level	Vertical M/V Ratio	Horizontal M/V Ratio
0.90HAG	Undamaged	9.79	9.79
	Exploratory	3.98 - 9.49	8.65 - 9.78
	Feeding	2.78 - 9.35	7.73 - 9.74
	Nesting	2.06 - 9.10	6.34 - 9.87
0.80HAG	Undamaged	10.50	10.50
	Exploratory	4.11 - 10.21	9.16 - 10.49
	Feeding	2.94 - 9.88	8.26 - 10.46
	Nesting	2.23 - 9.83	6.89 - 10.37

Table 41. - 18.29 m pole M/V ratios (shear-bending interaction failure).

Resultant Height (m)	Damage Level	Vertical M/V Ratio	Horizontal M/V Ratio
0.90HAG	Undamaged	12.32	12.32
	Exploratory	4.68 - 11.57	10.98 - 12.31
	Feeding	3.47 - 11.28	9.62 - 12.26
	Nesting	2.74 - 11.10	8.00 - 12.12
0.80HAG	Undamaged	13.00	13.00
	Exploratory	5.09 - 12.29	11.47 - 12.99
	Feeding	3.44 - 12.01	10.14 - 12.94
	Nesting	2.72 - 11.84	8.33 - 12.82

Appendix C: Specimen Data

Table 42. - New specimen failure data.

Specimen	Damage	$M_{failure}$ (kN·m)	$V_{failure}$ (kN)	$\emptyset_{failure}$ (mm)*	Failure Mode
45-1-1	Neutral Axis Feeding	50.36	25.18	276.93	Bending
45-1-2	Control	82.16	41.08	306.53	Bending
45-1-3	Tension Exploratory	80.46	9.23	329.77	Bending
45-2-1	Compression Nesting	36.98	4.24	268.97	Bending
45-2-2	Control	96.71	48.36	293.48	Bending
45-2-3	Tension Exploratory	82.78	9.49	319.90	Bending
50-1-1	Control	42.96	25.27	240.93	Bending
50-1-2	Control	79.83	39.92	271.20	Bending
50-1-3	Tension Nesting	73.74	8.46	313.54	Bending
50-2-1	Compression Exploratory	29.92	3.43	236.19	Bending
50-2-2	Control	61.32	30.66	282.34	Bending
50-2-3	Control	106.10	62.41	326.38	Bending
50-3-1	Neutral Axis Nesting	24.49	12.25	214.86	Shear
50-3-2	Control	37.44	18.72	263.24	Bending
50-3-3	Compression Nesting	62.64	7.18	313.22	Bending
55-1-1	Tension Nesting	32.44	3.72	257.51	Bending
55-1-2	Control	93.96	46.98	301.76	Bending
55-1-3	Compression Feeding	92.91	10.65	342.50	Bending
55-2-1	Control	86.09	50.64	268.64	Bending
55-2-2	Control	142.97	71.49	317.35	Bending
55-2-3	Neutral Axis Nesting	143.37	71.68	355.23	Shear
55-3-1	Neutral Axis Nesting	39.06	19.53	247.96	Shear
55-3-2	Control	90.51	45.26	299.85	Bending
55-3-3	Control	138.50	69.25	346.00	Bending
60-1-1	Compression Feeding	38.59	4.43	250.51	Bending
60-1-2	Control	93.57	46.79	299.21	Bending
60-1-3	Tension Feeding	97.78	11.21	330.72	Bending
60-1-4	Compression Exploratory	166.04	19.04	366.06	Bending
60-2-1	Tension Feeding	31.54	3.62	244.78	Bending
60-2-2	Control	72.20	36.10	280.75	Bending
60-2-3	Compression Exploratory	97.19	11.15	314.17	Bending
60-2-4	Compression Nesting	108.93	12.49	358.74	Bending
60-3-2	Control	128.37	64.19	334.23	Bending

Table 43. - New specimen failure data (cont.).

Specimen	Damage	M_{failure} (kN·m)	V_{failure} (kN)	Ø_{failure} (mm)*	Failure Mode
60-3-3	Neutral Axis Feeding	181.68	90.84	396.30	Bending
60-3-extra	Compression Nesting	29.19	3.67	259.42	Bending
60-4-1	Neutral Axis Feeding	41.21	20.61	237.14	Bending
60-4-2	Control	71.22	35.61	272.15	Bending
60-4-3	Neutral Axis Exploratory	102.25	51.13	305.58	Bending
60-4-4	Neutral Axis Nesting	147.20	73.60	369.24	Shear
B-1-2	Control	125.98	62.99	332.63	Bending
B-1-3	Tension Feeding	143.27	16.43	374.02	Bending
B-2-2	Control	72.78	36.39	296.03	Bending
B-2-3	Tension Nesting	66.50	7.63	337.41	Bending

Table 44. - In-service specimen failure data.

Specimen	M_{failure} (kN·m)	V_{failure} (kN)	Ø_{failure bending} (mm)*	Ø_{failure shear} (mm)*	t_{shell} (mm)	Failure Mode
D-1-1 (Control)	7.70	5.13	-	224.29	40.00	Shear
D-1-2 (Control)	8.88	11.03	-	249.78	35.00	Shear
D-2-1	18.25	2.09	193.21	-	-	Bending
D-2-2 (Control)	51.73	25.87	-	221.86	-	Shear
D-3-1	23.45	2.69	219.63	-	-	Bending
D-3-2 (Control)	41.18	20.59	249.87	-	-	Bending
D-4-1 (Control)	14.84	8.71	-	224.73	45.00	Shear
D-4-2 (Control)	36.31	18.16	-	236.63	40.00	Shear
D-4-3 (Control)	46.24	30.83	280.02	-	37.50	Bending
RP-1-1	52.38	26.19	265.79	-	-	Bending
RP-1-2 (Control)	95.48	47.74	300.80	-	-	Bending
RP-2-1 (Control)	32.61	17.92	231.22	-	-	Bending
RP-2-2 (Control)	43.70	24.28	253.53	-	-	Bending
RP-3-1	40.40	4.63	288.07	-	-	Bending
RP-3-2 (Control)	147.76	73.88	335.82	-	-	Bending
C-1-1	78.96	39.48	309.08	-	-	Bending
C-1-2	83.79	167.58	349.96	-	-	Bending
C-1-3 (Control)	225.11	112.56	385.15	-	-	Bending
60-3-1	68.91	7.90	298.26	-	-	Bending
60-3-2 (Control)	128.37	64.19	334.23	-	-	Bending

Table 45. - In-service specimen failure data (cont.).

Specimen	M _{failure} (kN·m)	V _{failure} (kN)	Ø _{failure bending} (mm)*	Ø _{failure shear} (mm)*	t _{shell} (mm)	Failure Mode
B-1-1	36.90	4.23	288.07			Bending
B-1-2 (Control)	125.98	62.99	332.63	-	-	Bending
B-2-1	34.45	3.95	264.2	-	-	Bending
B-2-2 (Control)	72.78	36.39	296.03	-	-	Bending

*Note: Ø represents diameter of specimen cross-section.

Table 46. - In-service pole woodpecker damage dimensions.

Pole	Hole #	Width (mm)	Depth (mm)
D-1	1	40	53
	2	40	53
	3	30	82
	4	60	130
	5	35	130
	6	50	130
	7	35	130
	8	35	130
	9	70	130
D-2	1	50	86
	2	50	86
	3	30	75
D-3	1	50	110
D-4	1	30	45
	2	70	155
C-1	1	80	125
	2	80	170
	3	80	145
	4	70	90
	5	80	155
	6	70	125
	7	75	135
	8	80	135
	9	80	165
	10	80	155
	11	70	145
	12	70	95
	13	75	140

Table 47. - In-service pole woodpecker damage dimensions (cont.).

Pole	Hole #	Width (mm)	Depth (mm)
60-3	1	70	130
	2	80	175
	3	50	115
	4	90	155
	5	30	50
RP-1	1	80	195
RP-2	1	85	190
RP-3	1	100	240
	2	80	190
B-1	1	90	240
B-2	1	80	185